ACTA UNIVERSITATIS SZEGEDIENSIS

ACTA PHYSICA ET CHEMICA

NOVA SERIES

TOMUS XXVI FASCICULI 3—4

AUSHAF 26 (3—4) (111—220) (1980)

HU ISSN 0324—6523 Acta Univ. Szeged
HU ISSN 0001—6721 Acta Phys. et Chem.

SZEGED, HUNGARIA
1980

ACTA UNIVERSITATIS SZEGEDIENSIS

ACTA PHYSICA ET CHEMICA

NOVA SERIES

TOMUS XXVI FASCICULI 3—4

AUSHAF 26 (3—4) (1980)
HU ISSN 0324—6523 Acta Univ. Szeged
HU ISSN 0001—6721 Acta Phys. et Chem.

SZEGED, HUNGARIA
1980

Kiadja

a József Attila Tudományegyetem Természettudományi Kara
(Szeged, Aradi vértanúk tere 1.)

Kiadványunk rövidítése:

Acta Phys. et Chem. Szeged

A POLARIZATION SPECTROFLUORIMETER WITH ON-LINE DATA PROCESSING*

By

I. VASS, N. MAREK** and J. HEVESI***

Department of Theoretical Physics, József Attila University, Szeged

(Received November 1. 1980)

Semi-automatic set up adaptable for series measurements is described for determination of polarization of fluorescence emission with high precision. Measurements of fluorescence intensities are carried out in a spectrofluorimeter equipped with polarizers. The control of the measurements and on-line data processing is made by a minicomputer WANG-600-14.

Examination of fluorescence polarization is a useful tool for studying the nature of electric transitions associated with absorption and emission of fluorescing molecules [1]. Fluorescence polarization technique is often used for the investigation of intermolecular energy transfer [2], molecular motions in solutions, microviscosity of solvents [3], and for a number of biological problems [4].

The degree of fluorescence polarization p is defined by the following relationship:

$$p = \frac{I_{\parallel} - I_{\perp}}{I_{\parallel} + I_{\perp}}, \tag{1}$$

where $I_{\parallel}$ is the fluorescence intensity polarized in the same plane as the exciting beam, and $I_{\perp}$ is the fluorescence intensity polarized at right angels thereto. Although several methods were elaborated for determination of p [5—11], computer data handling offers new possibilities for fast and very precise determination of luminescence polarization. A usual method is to measure the fluorescence intensities $I_{\parallel}$ and $I_{\perp}$ either subsequently or simultaneously [6, 8, 10, 12]. By this simple method, however, due to instability in the intensity of exciting light and fluctuations in photomultiplier dark current confident results can only be obtained by statistical data evaluation from a great number of repetitions of the measurement. Especially at low fluorescence intensities this makes the measurements rather tedious.

The aim of the present work was to construct an equipment which connects the simplicity of the direct method with the controlling and on-line data processing facilities of computers.

* Presented at the 3rd Summer School on Luminescence, Budapest, August 25—26, 1980.

** Department of Medical Chemistry, Medical University, Szeged.

*** Department of Biophysics, József Attila University, Szeged.

Fig. 1 shows the block diagram of the instrument. Exciting light is provided by an 500 W Xe arc lamp *L*. The polarized monochromatic light incident on the sample, located in a termostated cuvette *C*, is obtained by a Hilger double grating monochromator *M* (Typ. D331), and by polarizer P_1, mounted on a hand rotating disc. Before collection at the photomultiplier PM (EMI 9558 QB), the fluorescence light passes through a filter *F*, to block the scattered light, and polarizer P_2, with

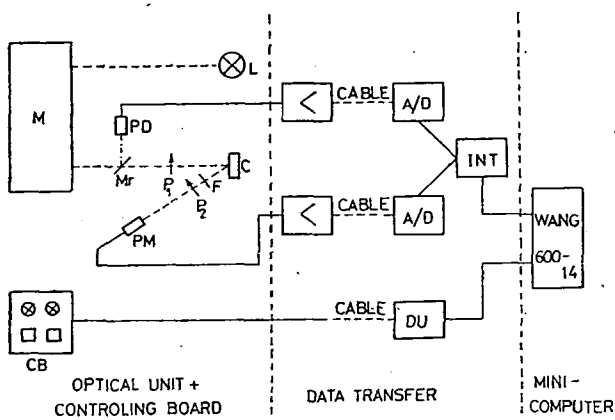

Fig. 1. Block diagram of the equipment

fixed position. Arrows on Fig. 1 indicate the electric vectors of the polarizers P_1 and P_2, respectively. For measuring the intensity of the exciting light a mirror *Mr*, and a photodiode *PD* is used. After suitable amplification the signals of photomultiplier and photodiode are transferred separatly to two analog-to-digital converters *A/D*, which are synchronized to each other with a maximal sampling rate of 50 s^{-1}.

The digital data proportional to the exciting and the fluorescent light enter simultaneously the minicomputer WANG—600—14, across a digital microinterface INT.

The semi-automatic measurement is processed by a laboratory-built unit *DU*, constructed from digital integrated circuits. This unit makes possible to start the computer program at the optical unit — located in about 50 m distance from the minicomputer — and gives information about the run of the program by a controlling board *CB*.

During the measurement the electric vector of the exciting light passing through the polarizer P_1 was brought first into parallel, then into perpendicular position with respect to the electric vector of fluorescence light passing through the fixed polarizer P_2. The partially polarized light from monochromator *M*, that also depends on the wavelength λ, has generally different intensity in the two positions of P_1. Taking into consideration this fact in determining *p*, the quotient $c(\lambda)=I_{\perp,e}(\lambda)/I_{\parallel,e}(\lambda)$ has to be measured. To carry out this, a scrambler was put into the sample holder and in this way P_2 obtained always depolarized light.

Taking into account the dark current of the photomultiplier I_d, the following formula was used for the calculation of p

$$p = \frac{(I_{\parallel} - I_d)c(\lambda) - (I_{\perp} - I_d)}{(I_{\parallel} - I_d)c(\lambda) + (I_{\perp} - I_d)}. \tag{2}$$

The flow diagram of the measurement is shown in Fig. 2. The random errors of this method originate mainly from two sources. The first is the fluctuation of the dark current and the electric noise of the whole equipment. The distribution of a great number of intensities was found to be Gaussian-type, so the relative error of the mean value is $\Delta I_{rel} = \sigma_n / \bar{I} \sqrt{n}$, where n is the number of the measurements, σ_n is the

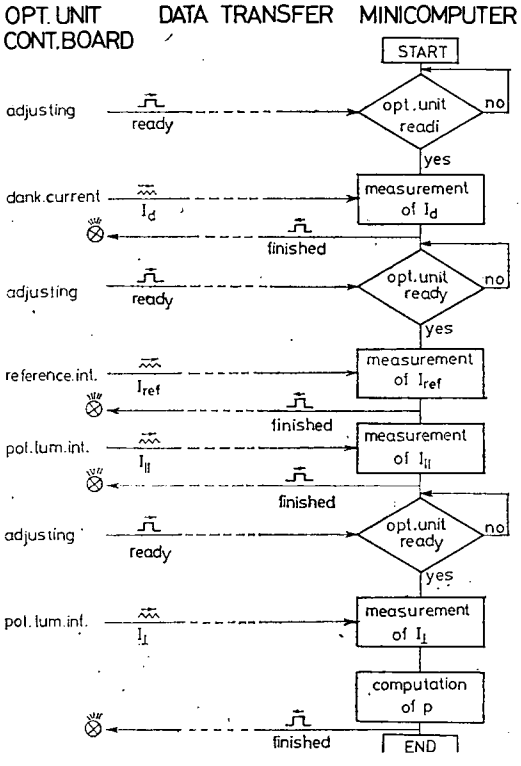

Fig. 2. Flow diagram of the measurement

standard deviation and $\bar{I}$ is the mean value. To reduce the error due to the fluctuation of the dark current, the computer program continously makes the sampling and compute ΔI_{rel}. When ΔI_{rel} is less than a given error limit, δ, the sampling stops. The great advantage of this sampling method is that the sampling number is not fixed, but is always optimal for the given error limit δ. The other source of the errors is the instability of the exciting lamp. To avoid this difficulty, before the measurement of $I_{\parallel}$ and $I_{\perp}$, we determine the intensity of the exciting light and this value is consi-

dered as reference I_{ref}, in the following. In determination of $I_{\parallel}$ and $I_{\perp}$ the sampling procedure is similar to that of the dark current. Except that in this case, together with the intensity of the polarized fluorescence, the intensity of the exciting light I_g is measured, too. If $|I_g - I_{ref}| < \varepsilon$, where ε is programmed error limit, the measured $I_{\parallel}$ or $I_{\perp}$ value is accepted, if $|I_g - I_{ref}| > \varepsilon$ the measurement is repeated. The sampling continues until $\sigma_n / \bar{I} \sqrt{n} < \delta$.

Because of the continuous computations during the measurement the maximal sampling rate was reduced from $50\,s^{-1}$ to $12.5\,s^{-1}$. Fig 3 shows the absolute and relative error of p calculated from ten test measurements at $\delta = \varepsilon = 1\%$. It can be seen that the absolute error Δp is nearly constant independently on the value of p, and so the relative error $\Delta p/p$ is steeply rising at low values of p. With appropriate choice of the error limits δ and ε, the desired absolute or relative error for a certain p can be obtained even at low fluorescence intensities. Setting low error levels the time necessary for the measurement considerably increases. For the degree of polarization of $10^{-4}\,M$ Na-fluorescein solution we obtain $p = 0.0016 \pm 0.0012$, which is similar to earlier results [8].

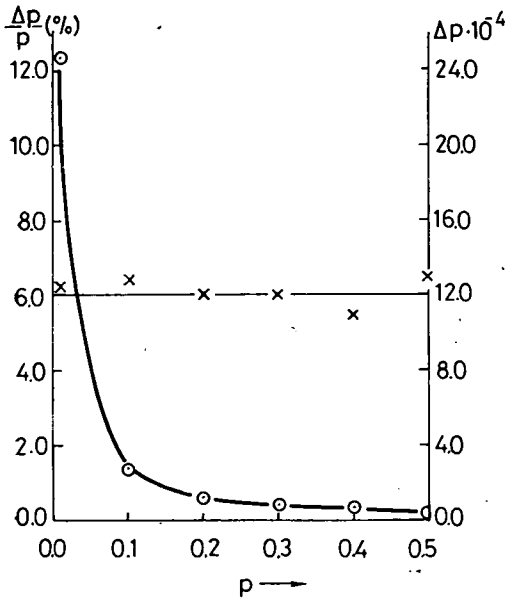

Fig. 3. Absolute and relative error of 10 p values as a result of test measurements $\delta = \varepsilon = 1\%$, ⊙ $-\Delta p$ (absolute error), —x— $\Delta p/p$ (relative error)

In conclusion, we may say that our set up connecting the direct determination of p with an up-to-date data processing method makes possible the fast determination of fluorescence polarization with high precision. The errors due to the instability of the exciting light and fluctuations of the dark current can be pushed under a given level by the optimal choice of the number of measurements to these error limits. The p values obtained can be saved on magnetic casette for later evaluation.

References

[1] *Vavilov, Sz. I.:* ZhETF **10**, 1363 (1940).
[2] *Förster, Th.:* Ann. Physik **2**, 55 (1948).
[3] *Nishijama, Y., G. Oster:* Bull. Chem. Soc. Japan **33**, 1649 (1960).
[4] *Goedheer, J. C., J. C. van der Commen:* Polarized Light Spectroscopy of Biological Systems. Proceedings of Spring School, Kolobrzeg, (1980).
[5] *Wille, H.:* Optik **9**, 84 (1952).
[6] *Ketskeméty, I., L. Gargya, E. Salkovits:* Acta Phys. et Chem. Szeged **3**, 16 (1957).
[7] *Dehler, J., F. Dörr:* Z. angew. Phys. **19**, 147 (1965).

[8] *Vize, L.:* Acta Phys. et Chem. Szeged **15**, 27 (1969).
[9] *Bauer, R. K.:* J. of Phys. E: Sci. Inst. **3**, 965 (1970).
[10] *Teale, F. W.:* J. of Phys. E: Sci. Inst. **3**, 555 (1970).
[11] *Clout, P. N., M. A. Haque, D. W. O. Heddle:* J. of Phys. E: Sci. Inst. **4**, 893 (1971).
[12] *Teissié, J., B. Valeur, L. Monnerie:* J. of Phys. E.: Sci. Inst. **8**, 700 (1975).

ПОЛЯРИЗАЦИОННЫЙ СПЕКТРОФЛУОРИМЕТР С НЕПОСРЕДСТВЕННОЙ ОБРАБОТКОЙ ДАННЫХ

И. Ваши, Н. Марек и Й. Хевеши

Описан полуавтоматический аппарат применимый к серийным измеремиям поляризации флуоресценции с большой точностю. Проведены измерения интенсивности флуоресценции в спектрофлуориметре с поляризаторами. Контроль измерения и непосредственную обработку данных проводили на настольном вычислителе типа WANG—600—14.

GENERATION OF SUBNANOSECOND PULSES IN NITROGEN LASER-PUMPED TUNABLE DYE LASERS

By

B. RÁCZ, ZS. BOR, G. SZABÓ and S. SZATMÁRI

Institute of Experimental Physics, Attila József University, Szeged, Hungary

(Received 30. October, 1980)

The temporal behaviour of nitrogen laser-pumped dye lasers was investigated experimentally in order to generate short, subnanosecond, narrow-linewidth pulses. The change of the time position of dye laser pulses was measured by the change of laser wavelength and cavity length. A new type oscillation in dye lasers was studied. This oscillation had cavity round-trip time modulation. By using high-cavity length, tunable subnanosecond pulses were obtained. The intensity competition in two-wavelength lasers can produce subnanosecond pulses with very short fall time.

Introduction

The dynamical investigation of photophysical and photochemical processes demands tunable, narrowband, and very short light pulses. Q switched solid-state lasers, nitrogen laser-pumped dye lasers produce several nanosecond long pulses. Mode-locked dye lasers generate 5—0.2 ps pulses, but they are too expensive. The gap between nanosecond and picosecond pulses could be covered by nitrogen laser-pumped subnanosecond dye lasers.

A great number of methods for producing subnanosecond light pulses have been reported. One of them described in [1—3] is based on relaxation oscillations. In that case, cavities with extremely low decay times are used and, by proper control of pumping level, 0.5—1 ns pulses with 50—500 W peak power were generated. An important disadvantage of this method is that: because of the short cavity no high wavelength selection can be used. 1—1.5 nm spectral linewidths were reported, these are too broad for most applications. Another method for subnanosecond pulse generation using relatively long cavity $L=300$ mm, and high spectral selection has been presented in [4, 5].

Though, to tell the truth, these autors did not distinguish their method from the relaxation oscillations. For a certain spectral range and pumping power, single pulses have been generated, with a pulse duration of 450 ps (fwhm) and 0.002 nm linewidth.

In this paper, we are presenting the results of a systematic investigation of temporal behaviour of nitrogen laser pumped dye lasers. Using these results the conditions for production of single subnanosecond pulses in a long cavity dye laser, and a qualitative explanation of short pulse generation is proposed. A simple and new resonator configuration is presented for very long-cavity dye lasers. As a result of the comprehensive study of the temporal behaviour of two wavelength dye lasers, another simple method is developed for producting short dye-laser pulses.

Experimental arrangement

The most used experimental arrangement can be seen in Fig. 1. Pumping pulses were provided by a nitrogen laser having 200 kW peak power, 7 ns pulse duration (fwhm) operating at 25 pps. A $5 \cdot 10^{-3}$ M/l ethanol solution of Rhodamine 6G and $5 \cdot 10^{-3}$ M/l 7-diethylamino-4-methylcoumarin were used as active material. The dyes were in a 1 cm long flowing dye cell. Five different dye laser configurations were investigated; Fig. 1 shows the most complicated double-wavelength dye laser, and Fig. 2 shows the other four dye laser configurations. In each case, the grating was a 1800 lines/mm ruled grating, and the output coupler was an uncoated flat mirror substrate. The two-wavelength laser had a grating as beam expander [6], and its 0-th order was fed back by another autocollimation grating. DL. 1 is a simple, transversally pumped configuration, DL. 2 uses a grating beam expander; DL. 3 and DL. 4 have an intracavity lens.

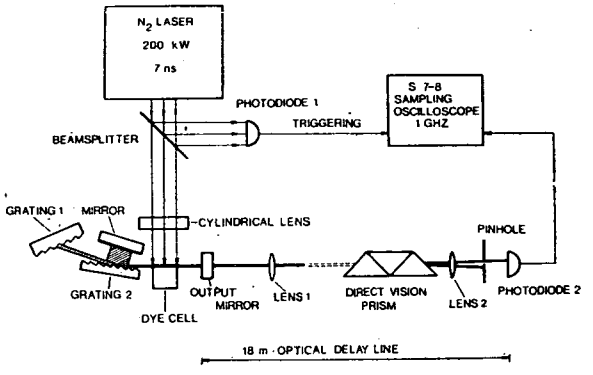

Fig. 1. Experimental arrangement for measuring time position and pulse shape of dye lasers.
Two wavelength dye laser configuration

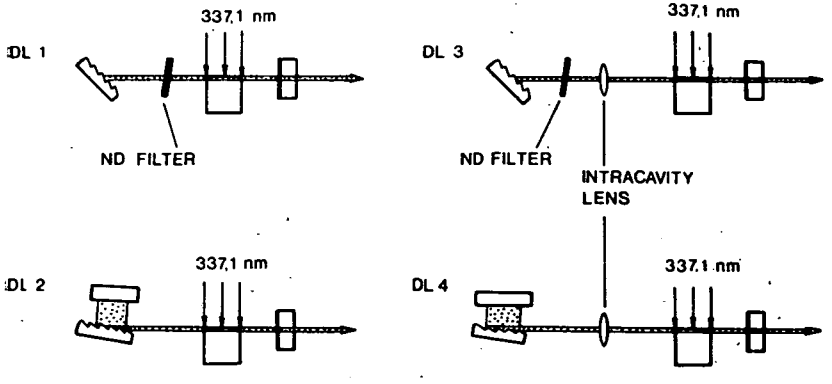

Fig. 2. The used resonator configurations

The intracavity lens was so installed, that the focal plane of the lens coincided with the dye cell side-window; consequently, the grating and the intracavity lens formed a monochromator with the excited region as an entrance and exit "slit". The use of intracavity lens results in higher spectral selectivity and higher efficiency of feedback. With such an intracavity lens DL. 3 and DL. 4 were unstable resonators, but the "walk off" losses were much lower than the other losses of the cavity.

The light emerging from the dye lasers was passed through a lens and a direct vision prism, so that amplified spontaneous emission (ASE), or the outputs of the double-wavelength laser could be selected. At the same time, this spectral selector served as an 18 m long optical delay line. The light was detected by an ITL HSD 1850 biplanar photodiode. A small fraction of nitrogen laser ligth with a TF 50 photodiode triggered the S 7—8 sampling oscilloscope. The rise time of the whole system was 300 ps. The wavelength and linewidth of the dye lasers were measured by a DFS—8 spectrograph and a IT—51 Fabry—Perot interferometer.

Results

Wavelength dependence of the time position of dye-laser pulses

It is well known that the dye-laser pulse apart from some delay, closely follows the shape of the exciting nitrogen laser pulse shape. The delay between the two depends on the pumping power and on the decay time of the cavity. Supposing constant pumping power and constant resonator configuration, there is another important parameter *Viz:* the laser wavelength. The gain curve of the dye depends on the wavelength; with lower gain, the laser is delayed in reaching the threshold and with the maximum gain curve, the laser rises sharply. These dye-laser properties can be predicted by the simple rate equation model [3]. Fig. 3 shows the delay of the dye-laser pulses to be as we calculated, with 100 kW pumping power and $\tau = 10$ ps cavity decay time.

To verify this calculation, the delay have been measured by the use of the DL. 2 resonator configuration. Fig. 4 shows the relative time position of the dye laser

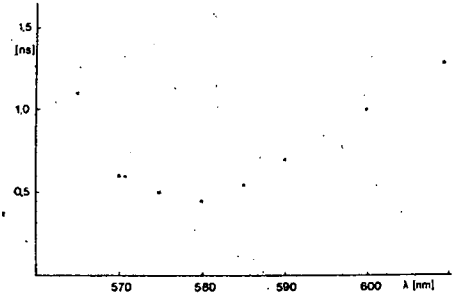

Fig. 3. Calculated time position of dye laser pulses. Parameters: active material Rhodamine 6G, pumping power 100 kW, resonator decay time 10 ps

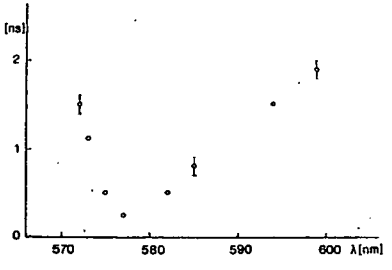

Fig. 4. Measured time position of dye laser pulses. Parameters: as before

pulses. The active material was a Rhodamine 6G solution in ethanol, similar results were obtained for a 7-diethylamino-4-methylcoumarin solution. The qualitative agreement of experimental and theoretical results is satisfactory, because of the simplicity of the model.

The effect of resonator length on the time position of the dye laser pulses

The development of a dye laser pulse begins when the ASE emerging from the dye cell enters the sepctral selector, and a small part of it is fed back to the active region. Using higher spectral selection (*i.e.* beam expander), the distance between the dye cell and the spectral selector could be as much as 10—15 cm, and the above-mentioned round trip takes about 0.8—1 ns. Therefore the time position of the dye laser pulses must depend on cavity length.

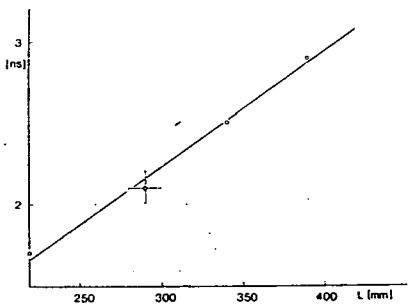

Fig. 5. The relative change of time position of dye laser pulses. Resonator configuration: DL. 2

Experimental measurements with DL. 2 confirmed this assumption as shown, in Fig. 5. In the course of measurements, the distance between the dye cell and the output coupler was fixed and the cavity length was altered by the movement of the grating. These results show the limits of the simple rate equation model, because when increasing the resonator length the decay time also increases in terms of the model. When substituting increasing decay times for rate equations, the delay decreases contrary to experience.

Oscillations in long cavities

In many cases the shape of the dye laser pulses showed irregular pulsations. These pulsations are not relaxation oscillations, because they could be observed far above the threshold and in a relatively long cavity (30 cm). A typical oscillation is displayed in Fig. 6. The systematic study of such pulses showed that the time separation (t) between subpulses was equal to the cavity round-trip time, and was independent of the pumping power laser wavelength and resonator configuration (see Fig. 7).

The measured points with $L=250$ mm and 400 mm represent different cavity configurations. The measurements described above prove that these oscillations differ essentially from the relaxation oscillations described in [1—3].

To find the origin of this pulsation, the temporal development of the pulses was analised. The temporal development of laser pulses begins with the ASE as previously mentioned. The temporal behaviour of ASE was observed through the output coupler, when the grating from DL. 1 was removed. Fig. 8 shows the ASE pulse as having a short rising half in accordance with the increase of excited-state population. The moment, when the ASE is fed back from the output mirror to the dye cell, the excited state population sharply decreases, and consequently, the level

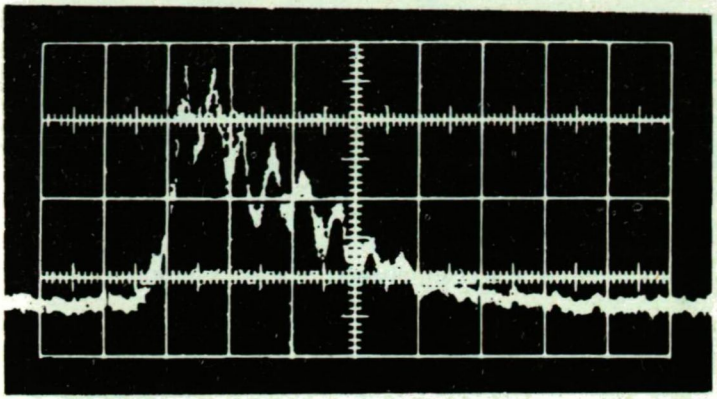

Fig. 6. Oscillations in nitrogen laser pumped dye laser.
Horizontal scale: 2 ns/div

of ASE propagating into the direction of the output coupler also decreases. Since the dye pumped strongly, the system would reach the steady state quickly and, therefore, the ASE level would continue to be constant during the remaining part of the pulse. This overshot in the ASE is responsable for the oscillation.

Whether this overshot causes oscillations or not, depends on the efficiency of the feedback of the grating. Here the efficiency of feedback is defined as the photon flux entering the active region from the direction of the grating divided by the photon flux emerging from the active region towards the grating

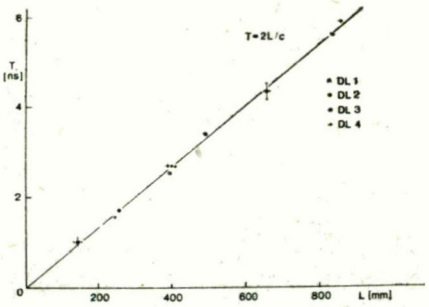

Fig. 7. The time separation between subpulses as a function of resonator length

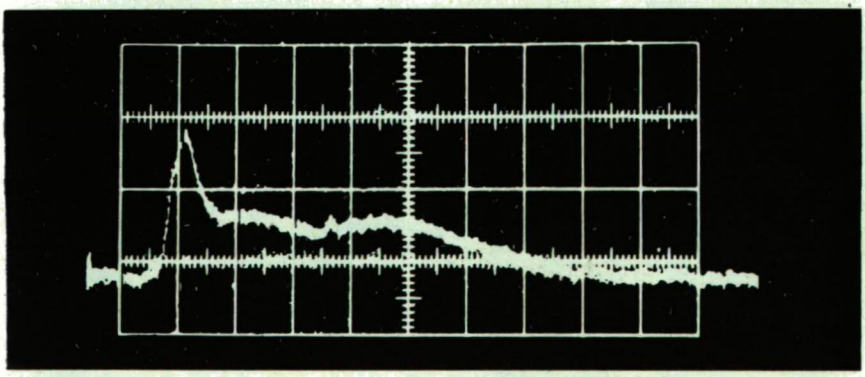

Fig. 8. Temporal behaviour of amplified spontaneous emission in case of one mirror resonator. Horizontal scale 2 ns/div

(*i.e.* spectral selection, transmission of ND filters and the beam expander, reflectivity of the grating and losses due to the divergence of the ASE beam are taken into account). If the intensity of the beam fed back from the grating to the dye cell is so high as to cause deep saturation, no oscillation occurs. (It is well known that the output power of a deeply saturated amplifier depends on the pumping rate alone, and is independent of the input power.)

If the intensity fed back from the grating is so high as to cause partial saturation, the leading part of the pulse will be more strongly amplified than its tail. As a result of subsequent transits through the active region, the initial overshot of ASE gained more, and the tail of the pulse was suppressed. These assumptions were verified experimentally, and as well as theoretically. (See theoretical part.)

Experimentally we changed the feedback in the lasers DL. 1 and DL. 3, inserting a set of ND filters between the grating and the dye cell. With the decrease of feedback, the modulation depth in the dye-laser pulse will grow, and the relative intensity of the pulses follows it by changing (see Fig. 9). Note that the time position of the peaks of subpulses is unchanged. According to our measurements and calculations, the condition of the oscillations is an about 10^{-5}—10^{-6} feedback efficiency. This is why, as a rule in a Hänsch-type laser no oscillations of such kind-were ob-

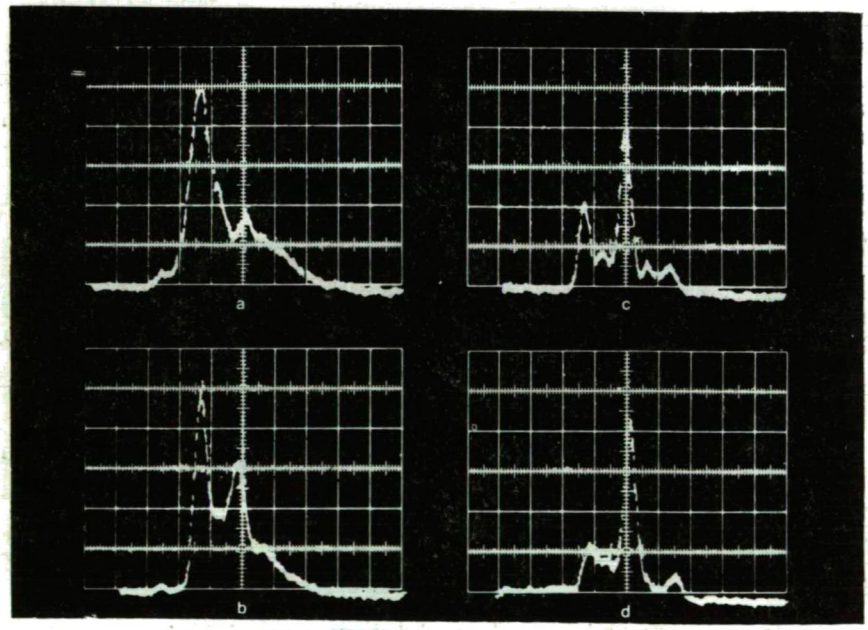

Fig. 9. Pulse shape of dye laser pulses with decreased feedback efficiency

served, since this laser has usually the feedback efficiency of 10^{-3}. A convenient method of the continuous variation of feedback efficiency is the application of a grazing incidence grating. By changing the angle of incidence to the grating, the efficiency of the feedback can be adjusted to such a low value as necessary for the production of the oscillations.

The number of generated subpulses depends on the cavity round-trip time and on the time during which the active medium has a proper gain. With the increase of the cavity length, the number of subpulses may be decreased, and it is possible to generate a single pulse. If the cavity length is increased up to 700 mm for DL. 1 and DL. 2, the laser is about to come up to the threshold. In order to improve the feedback, an intracavity lens was used.

The effect of intracavity lens

The laser arrangement is shown in Fig. 2 DL. 3 and DL. 4. The intracavity lens, as described in the experimental arrangement, formed a monochromator with the active region as an entrance and exit slit. The effectivity of feedback is defined previously. Since both systems, with and without intracavity lens, have the same linear dispersion in the dye cell, it is obvious that the ratio of the effectivities is nearly equal to the ratio of the vertical dimension of the back-reflected of ASE spots *i.e.*:

$$\frac{\eta_{IL}}{\eta} = \frac{2L\theta}{a}.$$

Where η and η_{IL} are the effectivities of feedback for the simple cavity and cavity with lens, θ is the divergence of the beam emerging from the dye cell and a is the diameter of the active region, L is the distance between the grating and dye cell. Fig. 10 shows the output energies versus cavity length with and without intracavity lens. For longer cavities, the output with intracavity lens is much higher than without lens. It can be seen that the resonator length could be as much as 1 m.

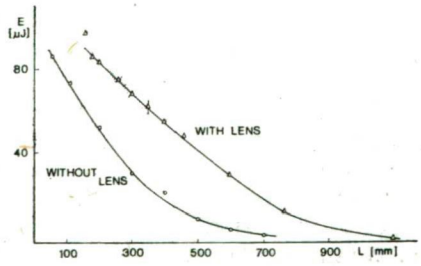

Fig. 10. The effect of intracavity lens on the output energy of dye lasers

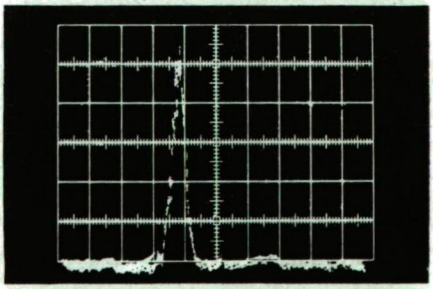

Fig. 11. Subnanosecond output pulse of a 90 cm long cavity dye laser (DL. 4.). Horizontal scale 2 ns/div

By using a 90 cm long cavity with a grazing incidence grating (6 ns round-trip time!) and an intracavity lens, stable single pulses can be obtained. The halfwidth of pulses was 0.55 ns (deconvoluted value), the time bandwidth product was 1.3, and the peak power 8 kW. The shot-to-shot stability was higher than 5 p.c. as seen in Fig. 11.

Temporal behaviour of two-wavelength dye lasers

The two-wavelength operation was achieved by several authors using a double cavity of different type. The relative intensity of the different wavelengths depends on the decay time of resonators and the relative position of wavelegths on the gain curve of the dye. This phenomenon was described by FRIESEM et al [7]. The competition between the independent cavities determines not only the relative intensities but also the temporal characteristics of the two-dye lasers. This temporal behaviour has not been investigated so far.

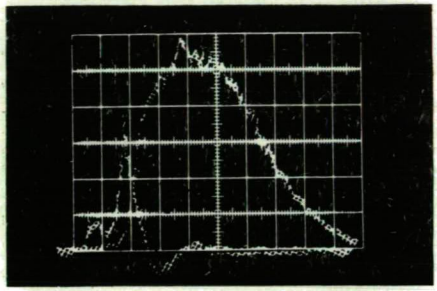

Fig. 12. Time behaviour of a two wavelength dye laser (The outputs were measured separately! 1 ns/div)

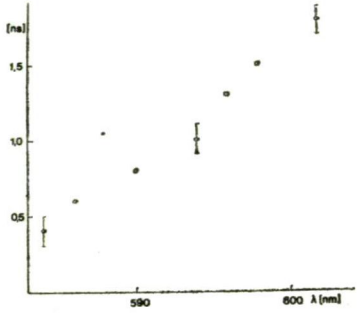

Fig. 13. The halfwidth of the first dye laser pulse as a function of wavelength of second dye laser

A typical pair of dye-laser pulses can be seen in Fig. 12 using the experimental arrangement of Fig. 1. The active material was Rhodamine 6G, and the wavelengths $\lambda_1 = 574$ nm and $\lambda_2 = 584$ nm. The most important information of Fig. 11 is that the two lasers do not operate simultaneously. According to the results of the previous section, the shorter cavity operates first. The length of cavities is: grazing incidence grating + mirror: 15 cm, autocollimation grating: 25 cm. A further important characteristic of this system is that the pulsewidth of the first laser pulse depends on the wavelength of the second laser. Fig. 13 shows the pulsewidth of the fixedwavelength first laser for different wavelengths of the second laser. It can be seen that,

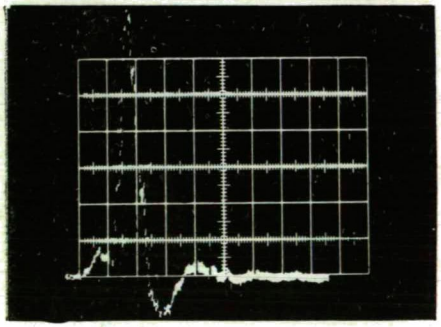

Fig. 14. Subnanosecond pulse of a two wavelength dye laser. Horizontal scale 1 ns/div

as the laser wavelength comes near to the maximum gain curve, the second laser-ises more rapidly, so the halfwidth of the first pulse decreases. Besides the two-wavelength operation, this method allows us to change the pulsewidth continuously and produces subnanosecond operation.

Fig. 14 shows a subnanosecond pulse in case $\lambda_1 = 574$ nm, $\lambda_2 = 584$ nm. It is interesting to note that this pulse has not only a sharp rising part but also a sharp fall indicated by the overshot of the oscilloscope.

Conclusions

We have investigated the time behaviour of nitrogen laser-pumped dye lasers. The time position of dye-laser pulses has a strong wavelength dependence. The delay between exciting and dye-laser pulse increases with the increase of cavity length. The origin and most important properties of an oscillation of a new type were investigated. The oscillation has a cavity round-trip modulation time. Using a resonator configuration of a new type and a very long cavity, single 0.55 ns long pulses were generated. It was demonstrated that two-wavelength dye lasers can produce subnanosecond pulses as well.

References

[1] *Lin Ch.:* Journal of Appl. Phys. **46,** 4076 (1975).
[2] *Lin Ch.:* IEEE J. Quant. Electron. **QE—11,** 602 (1975).
[3] *Rácz, B., Zs. Bor, G. Szabó, Cs. Zoltán:* Acta Phys. et Chem. Szeged **23,** 367 (1977).
[4] *Borgström S. A.:* Physica Scripty **14,** 92 (1976).
[5] *Wyatt R.:* Opt. Commun. **26,** 429 (1978).
[6] *Shoshan I., U. P. Oppenheim:* Opt. Commun. **25,** 375 (1978).
[7] *Friesem A. A., U. Ganiel, G. Neumann:* Appl. Phys. Letters **23,** 249 (1973).

ГЕНЕРАЦИЯ СУБНАНОСЕКУНДНЫХ ИМПУЛЬСОВ В ЛАЗЕРАХ, ПЕРЕСТРАИВАЕМЫХ НА КРАСИТЕЛЯХ, ВОЗБУЖДЕННЫХ АЗОТНЫМ ЛАЗЕРОМ

Б. Рац, Ж. Бор, Г. Сабо и Ш. Саттмари

Временная характеристика лазеров на красителях, возбужденных азотным лазером, была исследована для того, чтобы генерировать короткие, субнаносекундные узко-полосные импульсы. Изменение временной задержки импульсов лазера на красителе было измерено изменением длины волны и длины резонатора лазера. Был испытан новый тип осцилляции в лазерах на красителе. Эта осцилляция вероятно модулирована возвратно-поступательным временем резонатора. Получены перестраиваемые, субнаносекундные импульсы, используя длинный резонатор. В лазерах, имеющих две длины волн, конкуренция интенсивностей может привести к образованию субнаносекундных импульсов, именяющих короткие фронты.

IMPROVED MODEL OF NITROGEN LASER-PUMPED DYE LASERS

By

B. RÁCZ and G. SZABÓ

Institute of Experimental Physics, Attila József University, Szeged, Hungary

(Received November 1, 1980)

The time behaviour of nitrogen laser-pumped dye lasers was investigated theoretically. The time-space dependent rate equation model of dye lasers was improved. A numerical solution of these equations proved very time consuming. Therefore a simplification of equations was performed. The simplified equations were solved numerically, the delay of dye laser pulses, the oscillation having cavity round-trip time modulation, and the modulation depth were investigated. The production of subnanosecond pulses by long cavity dye lasers, and by two wavelength dye lasers, were demonstrated by the model.

Introduction

The temporal behaviour of laser-pumped dye lasers has been investigated for a long time. One of the first papers of P. P. SOROKIN et al. [1] gave a simple rate equation model of dye lasers, describing the fundamental properties of the dye laser produced by them. J. B. ATKINSON and F. P. PACE investigated this model more precisely [2]. The small signal approximation, and computer solution of rate equations [3, 4] predicted relaxation oscillations, and this phenomenon was found experimentally as well. Moreover, this model proved successful in the investigation of spectral properties of pulsed dye lasers [5].

The most important disadvantage of these models is that, the real resonator configuration cannot be taken into account directly, the cavity decay time alone depends on the cavity length, but this parameter is not affected by the place of the dye cell. A rigorous analysis shows a further problem of these equations, when the change in the photon number, and in the populations is considerable during a round trip time. U. GANIEL et al. eliminated these problems by using time and space dependent rate equations for ring lasers and injection. The validity of their solution is limited by the simplifications used [6]. A more general situation was treated by R. WYATT by using real dye, resonator, and pumping parameters. The solutions showed the possibility of production of subnanosecond dye laser pulses [7].

The aim of this paper is to show a calculation method which has the simplicity of time dependent rate equations but also allows the real resonator construction to be taken into account. By using this method, the most important properties of long cavity dye lasers can be explained.

The dye laser model

For the sake of simplicity let us suppose that:
— the effect of triplet states is negligible
— the excited state absorption is negligible
— the time duration of the thermalization of higher excited state is very short compared to other processes
— photochemical processes are not taken into account
— a two-level system of states is taken into consideration
— the active volume has a square cross section
— the excitation light intensity is constant along the optical axis
— the photon flux and populations perpendicular to the optical axis are constant
— the reflections in the boundary of active volume are not considered
— the divergence of the laser photon flux is equal to the experimental value
— the effect of scattering is negligible
— the reflectivity of the output mirror does not depend on the wavelength
— the divergence of amplified spontaneous emission (ASE) is equal to the angle between the diagonals of the excited volume.

The geometry of the dye laser can be seen in Fig. 1. Therefore, the time and space dependent rate equations are:

$$\frac{\partial N_1(x,t)}{\partial t} = I_p(t)\sigma_a(\lambda_p)N_0(x,t) - N_1(x,t)\int_0^\infty \sigma_e(\lambda)[I_L^+(x,t,\lambda)+I_A^+(x,t,\lambda)+$$
$$+ I_L^-(x,t,\lambda)+I_A^-(x,t,\lambda)]\,d\lambda$$

$$\pm\frac{dI_L^\pm(x,t,\lambda)}{dx} = N_1(x,t)\sigma_e(\lambda)I_L^\pm(x,t,\lambda)+\tau^{-1}N_1(x,t)E(\lambda)g_L^\pm(x)$$

$$\pm\frac{dI_A^\pm(x,t,\lambda)}{dx} = N_1(x,t)\sigma_e(\lambda)I_A^\pm(x,t,\lambda)+\tau^{-1}N_1(x,t)E(\lambda)g_A^\pm(x)$$

$$N_0(x,t)+N_1(x,t) = N = \text{const.}$$

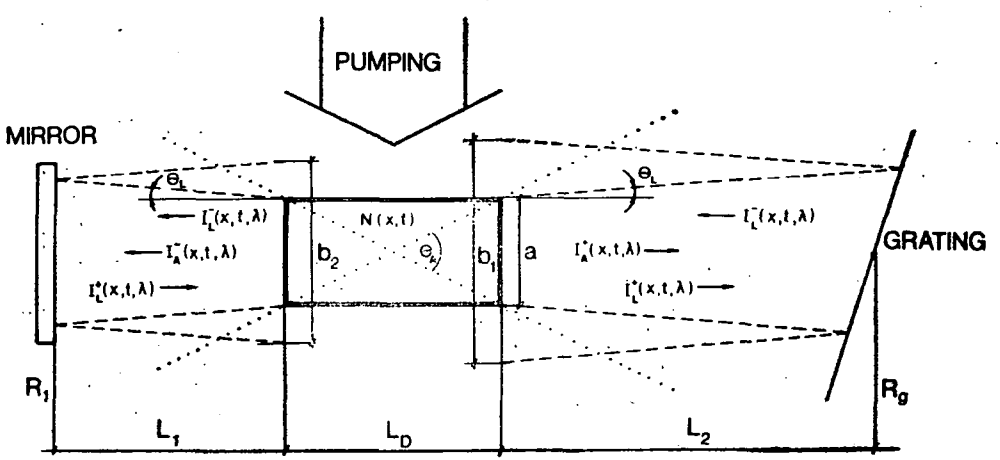

Fig. 1. The dye laser model

where:

$$\frac{d(I^{\pm})}{dx} = \frac{\partial(I^{\pm})}{\partial x} \pm \frac{n}{c} \cdot \frac{\partial(I^{\pm})}{\partial t}$$

supposing:

$$\frac{d\lambda}{dx} = 0.$$

The symbols are the following:
N the density of active molecules,
$N_0(x,t)$, $N_1(x,t)$ the population of ground and excited states,
$I_p(t)$ the pumping power density,
$\sigma_a(\lambda)$, $\sigma_e(\lambda)$ absorption and emission cross sections of the dye,
τ fluorescence lifetime,
$I_L^{\pm}(x, t, \lambda)$ laser photon flux per unit wavelength propagating in the $\pm x$ direction,
$I_A^{\pm}(x, t, \lambda)$ ASE photon flux per unit wavelength propagating in the $\pm x$ direction,
$E(\lambda)$ fluorescence emission spectrum normalized to quantum yield,
$g_L^{\pm}(x) \cdot g_A^{\pm}(x)$ geometrical factor for spontaneous emission,
n the refractive index of solution,
c the velocity of light.
Boundary and initial conditions are the following:

$$I_L^{\pm}(x, 0, \lambda) = 0, \quad I_A^{\pm}(x, 0, \lambda) = 0, \quad N_1(x, 0) = 0,$$

$$I_L^{-}\left(0, t + \frac{L_1}{c}\right) = \frac{a^2}{(a + L_1\theta_L)^2} I_L^{-}(L_1, t),$$

$$I_L^{+}(0, t) = R_1 I_L^{-}(0, t),$$

$$I_L^{+}\left(L_1, t + \frac{2L_1}{c}\right) = \frac{a^2}{b_2^2} R_1 I_L^{-}(L_1, t),$$

$$I_L^{+}\left(L_1 + L_0 + L_2, t + \frac{L_2}{c}\right) = \frac{a^2}{(a + \theta_L L_2)^2} I_L^{+}(L_1 + L_D, t),$$

$$I_L^{-}(L_1 + L_D + L_2, t) = R_g I_L^{+}(L_1 + L_D + L_2, t), \quad I_A^{+}(L_1', t) = I_A^{-}(L_1 + L_D, t) = 0,$$

$$I_L^{-}\left(L_1 + L_D, t + \frac{2L_2}{c}\right) = \frac{a^2}{b_1^2} R_g I_L^{+}(L_1 + L_D, t), \quad I_A^{-}(L_1, t) = I_A^{+}(L_1 + L_D, t).$$

The output of the laser can be calculated as:

$$I_L(0, t) = I_L^{-}(0, t)(1 - R_1).$$

The coupled rate equations were solved numerically by a PET2001 computer using finit difference method, supposing:

$$N_1(x, t) \int_0^{\infty} \sigma_e(\lambda)[I_L^{+}(x, t, \lambda) + I_A^{+}(x, t, \lambda) + I_L^{-}(x, t, \lambda) + I_A^{-}(x, t, \lambda)]\, d\lambda =$$

$$= N_1(x, t)\bar{\sigma}_{eL}[I_L^{+}(x, t) + I_L^{-}(x, t)]\, \Delta\lambda_L + N_1(x, t)\bar{\sigma}_{eA}[I_A^{+}(x, t) + I^{-}(x, t)]\, \Delta\lambda_A$$

meaning that spectral changes were not taken into consideration. The parameters were the following: $I_p(t)=5.07\cdot 10^{23}t^4e^{-0.75t}\,\frac{\text{photon}}{\text{cm}^2\,\text{s}}$ $\sigma_a(\lambda_p)=2.4\cdot 10^{-17}\,\text{cm}^2$, $R_1=0.04$, $R_g=0.6$, $a=0.2$ mm, $\theta_L=3$ mrad, $\theta_A=20$ mrad, $L_1=6$ cm, $L_D=1$ cm, $L_2=15.5$ cm, $\tau=5.5$ ns, $\Delta\lambda_L=1$ nm, $\Delta\lambda_A=10$ nm, $N=3\cdot 10^{18}\,\frac{1}{\text{cm}^3}$.

The numerically stable convergent solution can be seen in Fig. 2. The most important informations about this figure:

— the dye laser output has oscillations,

— the amplitude and modulation of pulses change,

— the modulation with $2L/c$ period is due to a group of subpulses going forth and back between the mirror and the grating. Unfortunately, the calculation of this pulse was very time consuming, and for this reason, further simplifications were made. It is obvious that this model has two important parts, the amplifier cell, and a storage and delay system of the photon flux. The amplifier can be simplified without modifying the storage and delay system.

Let us assume that:

$$\int_0^{L_D} N_1(x,t)\,dx = N_1(t)L_D$$

and the spontaneous emission is negligible compared to the laser photon flux *i.e.*:

$$\pm\frac{dI_L^{\pm}(x,t)}{dx} = N_1(t)\bar{\sigma}_{eL}I_L^{\pm}(x,t).$$

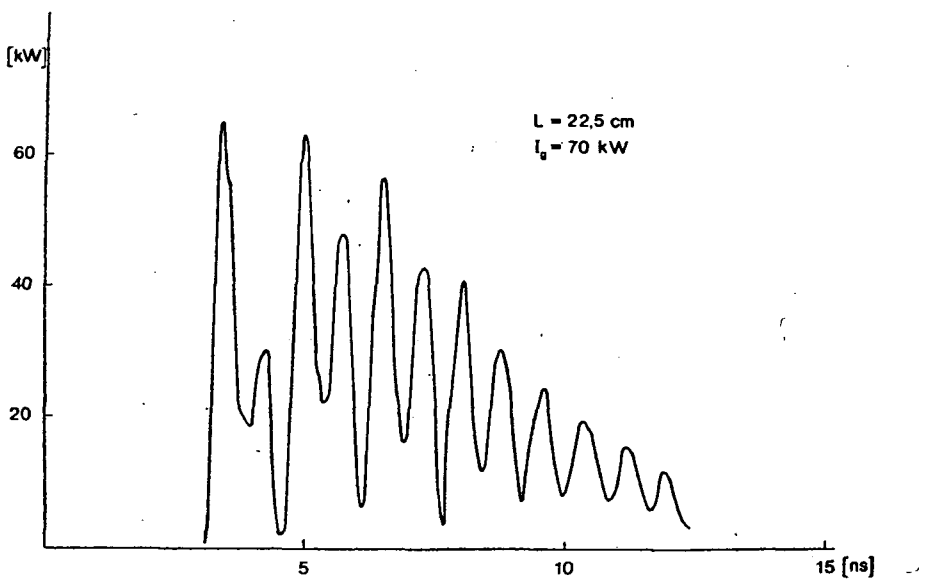

Fig. 2. The numerical solution of time and space dependent rate equations

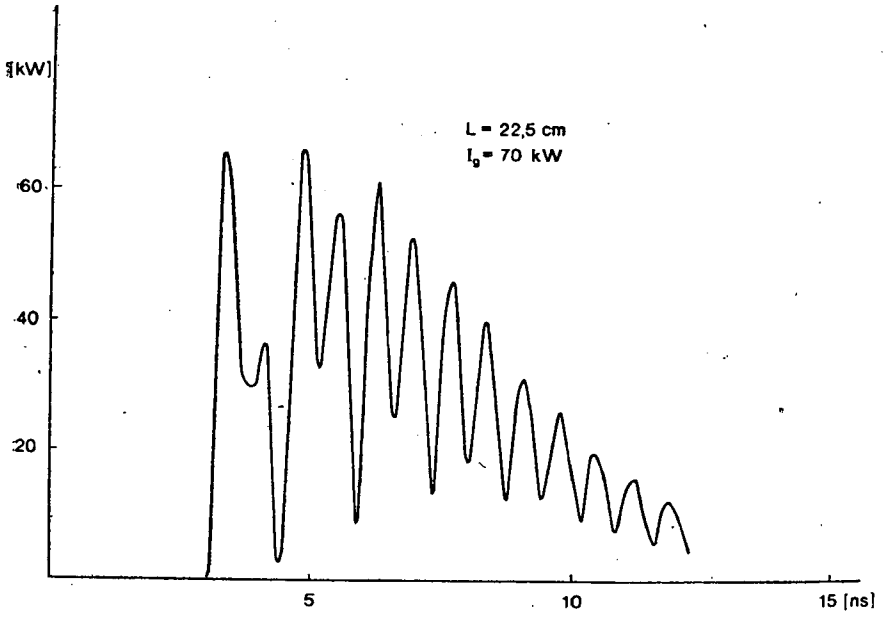

Fig. 3. The numerical solution of simplified equations

The solution of this equation is the following:

$$I_L^+(L_1+L_D, t) = I_L^+(L_1, t)e^{N_1(t)\sigma_{eL}L_D}.$$

The ASE photon flux is:

$$I_A^+(t) = \int_0^{L_D} E(\lambda)\frac{N_1(t)}{\tau} g_A^+ e^{N_1(t)\bar{\sigma}_{eA}(L_D-x)}\,dx = \frac{E(\lambda)}{\bar{\sigma}_{eA}\tau}[e^{N_1(t)\bar{\sigma}_{eA}L_D}-1].$$

Therefore, the equations to be solved are:

$$\frac{\partial N_1(t)}{\partial t} = I_p(t)\sigma_a(\lambda_p)N_0(t) - \frac{N_1(t)}{\tau} - N_1(t)\bar{\sigma}_{eL}[I_L^+(t)+I_L^-(t)]\,\Delta\lambda_L - N_1(t)\bar{\sigma}_{eA}[2I_A^+]\Delta\lambda_A,$$

$$I_L^+(L_1+L_D, t) = I_L^+(L_1, t)e^{N_1(t)\bar{\sigma}_{eL}L_D} + sI_A^+(L_1+L_D, t),$$

$$I_L^-(L_1, t) = I_L^-(L_1+L_D, t)e^{N_1(t)\bar{\sigma}_{eL}L_D} + sI_A^-(L_1, t),$$

$$I_A^-(L_1, t) = \frac{E(\lambda)}{\bar{\sigma}_{eA}\tau}[e^{N_1(t)\bar{\sigma}_{eA}L_D}-1],$$

$$I_A^+(L_1+L_D, t) = \frac{E(\lambda)}{\bar{\sigma}_{eA}\tau}[e^{N_1(t)\bar{\sigma}_{eA}L_D}-1],$$

where s is the portion of ASE propagating along the laser photon flux, the initial and boundary conditions are the same as before. When the same parameters are used as for the original equations, the solution can be seen in Fig. 3. The curves of Fig. 2 and Fig. 3 are equal better than 5%. The simplified equations were solved by using a set of different parameters.

Results

The time position of the rise of dye lasers was investigated experimentally in [9]. These measurements showed that: when the cavity length was increased, the delay between exciting and the dye laser pulse also increased. In contrast to this fact, the numerical solution of time dependent rate equations showed the decrease of the delay when the cavity length was increased. This discrepancy disappears in the solution of time and space dependent equations. Fig. 4 shows the calculated time delay as a function of the resonator length. The agreement between theoretical and experimental results is satisfactory, the slope of the curves is equal.

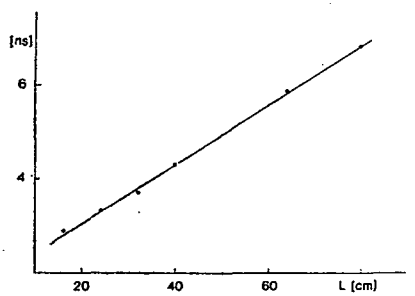

Fig. 4. The calculated delay of dye laser pulses as a function of resonator length

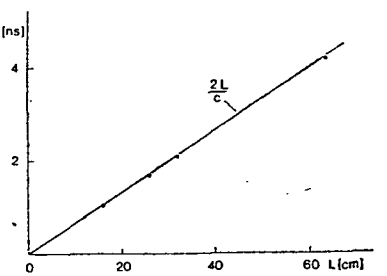

Fig. 5. The calculated time between pulse groups as a function of cavity length

The oscillations of long cavity dye lasers with cavity round trip modulation were discovered and investigated experimentally [8, 9]. The solutions of the time and space dependent equations can describe these important properties of nitrogen laser pumped dye lasers well. The pulsations of Fig. 2, 3 seem to be irregular just as experimental time behaviours do. The detailed study of these pulses showed the cavity round trip time modulation in every case. The number and amplitude of subpulses in Fig. 2, 3 depend on the resonator parameters, *i.e.* front mirror-dye cell distance, and the reflectivity of front mirror and the grating. Fig. 5 shows the time between pulse groups as a function of resonator length. The agreement with experimental results is apparent.

The modulation depth of oscillations of this type increases with the decrease in feedback efficiency. Fig. 6 (a), (b), (c) show the time behaviour of a 16 cm long cavity dye laser as increasing the reflectivity of the grating. The decrease of modulation depth can also be seen very well. Similar results obtained for 32 cm long cavities.

The investigated properties of dye lasers allowed us to give the condition for generation of single subnanosecond pulses. The condition is the following: cavity round trip time must be high enough in comparison with the duration of the exciting pulse. According to experimental conditions, the resonator length was increased to 1 m and the calculated solution can be seen in Fig. 7.

The application of this model to investigating the optimum conditions for subnanosecond pulses, and two-wavelength dye lasers is in progress.

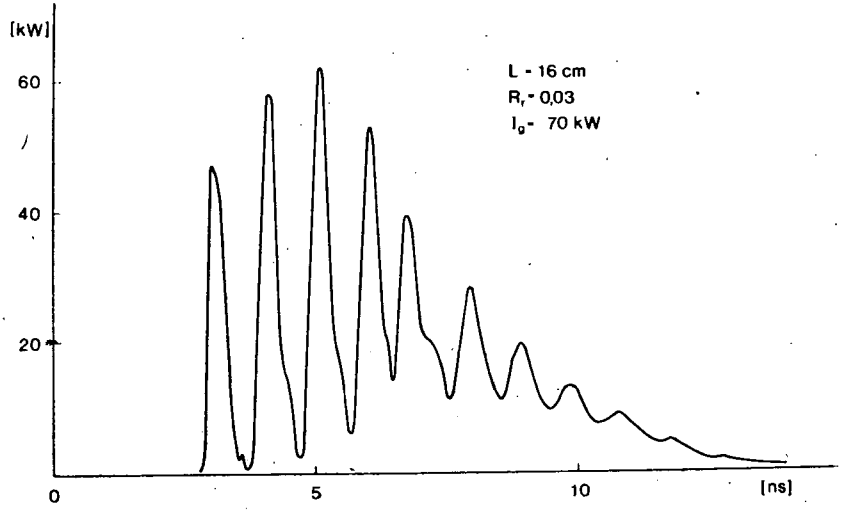

Fig. 6. (a)

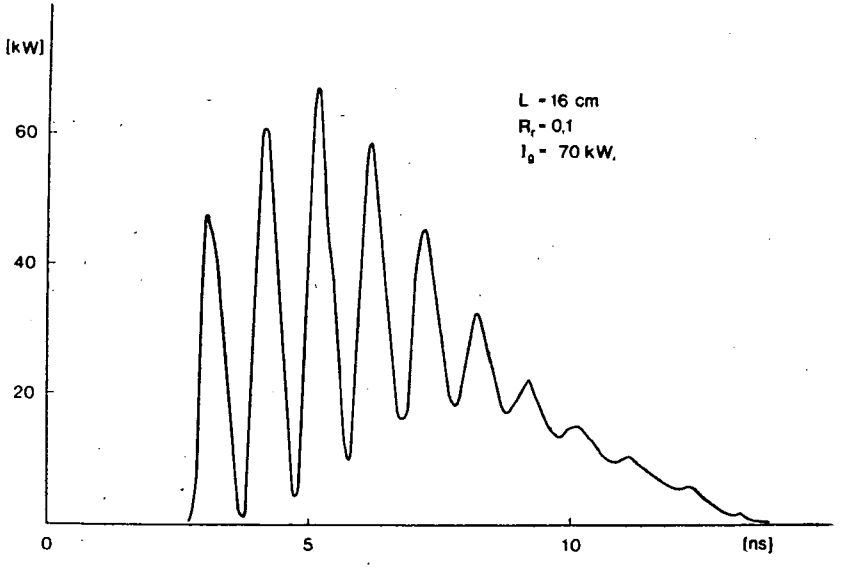

Fig. 6. (b)

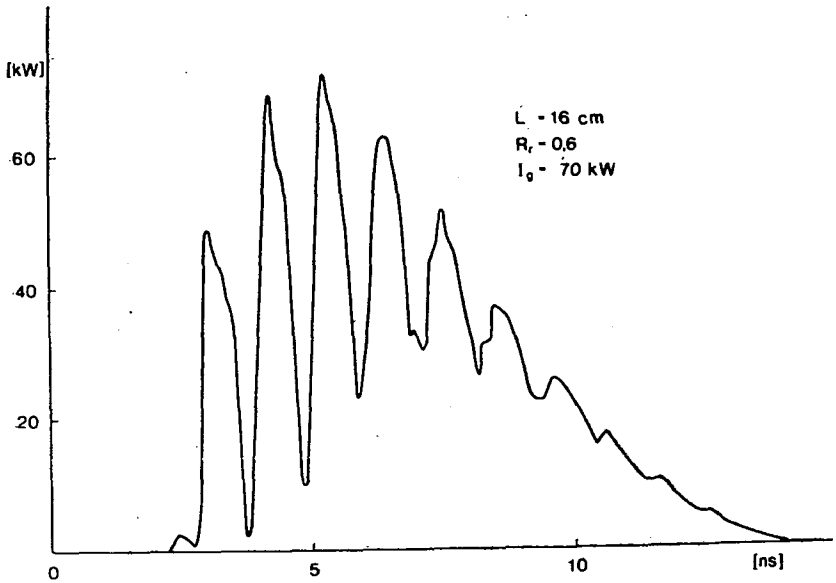

Fig. 6. (c). The modulation depth of subpulses as a function of feedback efficiency ($R_p = R_g$)

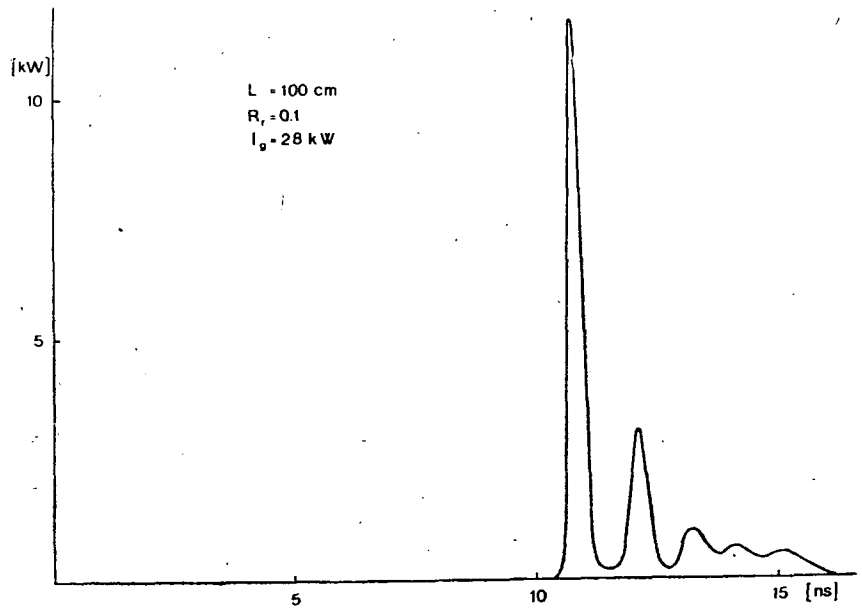

Fig. 7. Single subnanosecond pulse

References

[1] *Sorokin, P. P., J. R. Lankard, E. C. Hammond, V. L. Moruzzi:* IBM J. Res. Develop., **II.** 130 (1967).
[2] *Atkinson, J. B., F. P. Pace:* IEEE J. Quantum Electron. **QE—9,** 569 (1973).
[3] *Lin, Ch.:* IEEE J. Quantum Electron. **QE—11,** 602 (1975).
[4] *Rácz, B., Zs. Bor, G. Szabó, Cs. Zoltán:* Acta Phys. et Chem. Szeged **23,** 367 (1977).
[5] *Juramy, P., P. Flamant, Y. H. Meyer:* IEEE J. Quantum Electron. **QE—13,** 855 (1977).
[6] *Ganiel, U., A. Hardy, D. Treves:* IEEE J. Quantum Electron. **QE—12,** 704 (1976).
[7] *Wyatt, R.:* Applied Physics **21,** 353 (1980).
[8] *Wyatt, R.:* Opt. Comm. **25,** 375 (1978).
[9] *Rácz, B., Zs. Bor, G. Szabó, S. Szatmári:* this volume.

УЛУЧШЕНИЕ МОДЕЛИ ЛАЗЕРОВ НА КРАСИТЕЛЕ, ВОЗБУЖДЕННЫХ АЗОТНЫМ ЛАЗЕРОМ

Б. Рац и Г. Сабо

Теоретически исследована временная характеристика лазеров на красителях, возбужденных азотным лазером. Развиты кинетические уравнения зависящие от пространства и времени. Числовое решение этих уравнений требует много времени, поэтому было осуществлено упрощение уравнений. Было проведено числовое решение упрощеных уравнений. Проведено исследование задержки импульсов лазера на красителе, осцилляции, имеющей модуляцию возвратно-поступательного времени резонатора, и глубина модулации. Были показаны на модели субнаносекундные импульсы из длинного резонатора и лазера на красителе с двумя длиннами волн.

GENERATION OF NEARLY TRANSFORM-LIMITED SUBNANOSECOND LIGHT PULSES BY LONG CAVITY DYE LASER

By

J. HEBLING, ZS. BOR, B. RÁCZ, B. NÉMET and I. SÁNTA

Institute of Experimental Physics, Attila József University, Szeged

(Received November 1. 1980)

A long cavity dye-laser-amplifier system for generating single subnanosecond light pulses was investigated. The pumping light source was a TEA nitrogen laser with duration of 1 ns. The duration of the pulses obtained of the dye-laser-amplifier system was 155 ps. The spectral bandwidth was narrower than 0.01 nm. The spectrum band was modulated with a period equal to the FSR of a Fabry—Perot interferometer of 3.8 cm spacing. In the dye laser the optical pathlength between the wall of the oscillator cell and the output coupler was equal to this spacing.

From the point of view of spectroscopic applicability, lasers producing light pulses with short duration and narrow bandwidth are preferable. The simultaneous reduction of duration and bandwidth are limited by the Fourier-transform-limit. Up to now, subnanosecond transform-limited light pulses were generated only by mode-locked lasers and distributed feedback lasers. Recently, it has been reported by several authors [1, 2, 3] that nitrogen-laser-pumped dye lasers can generate subnanosecond transform-limited light pulse. The time behaviour of these long-cavity dye lasers are also described [4, 5] by a time-space dependent model. It is interesting to note that in [1, 2, 6] the authors did not distinguish their method from relaxation oscillations, and they used long cavity in order to get narrow linewidth. The effect of cavity length was made clear in [3]. Table I lists the results achieved by long cavity dye lasers.

Fig. 1 shows the experimental arrangement. The pumping source was a TEA nitrogen laser with 250 kW output power and 1 ns pulse-duration. The UV light was divided by a beamsplitter and focussed on to the oscillator and amplifier cell by cylindrical lenses. The application of an amplifier was necessary, because we were not able to produce single pulses with the dye laser. Therefore, with the aid of the amplifier a single pulse was selected from the cavity round-trip-time modulated pulse train. The pumping of the amplifier cell was delayed so (with 2 ns) that the amplifier amplified only the first pulse of the pulse train. The oscillator and amplifier cell was a 1 cm long silica cell, tilted by about 15°. The laser and amplifier dye was Rhodamin 6G $3 \cdot 10^{-3}$ mol/l in ethanol. The output coupler was a 2 mm thick uncoated planparallel glass flat. The distance between the output coupler and the centre of the oscillator cell was 2.7 cm. Lens 1 with a 25 cm focal length was at a distance of 25 cm from the dye cell, and so it reduced the divergence of the light

Table I

Generation of subnanosecond narrow-band laser pulses in nitrogen-laser-pumped dye lesers (The values in brackets are valid in case of single shot)

Authors	Pump pulse duration (*ns*)	Dye laser pulse duration (*ns*)	Time-bandwidth product / Transform limit
S. A. Borgström [6]	4	1	20
R. Wyatt [1]	3	0,6	6 (2,4)
G. Veith—A. J. Schmidt [2]	0,6	0,04	3,6*
B. Rácz et al. [3]	7	0,55	3
The present work	1	0,15	3 (1)

* The above value was calculated by us from the described pulse-duration and linewidth data in [2], but these data may probably not been obtained simultaneously because from Fig. 2 of [2] a larger product than 5 can be calculated for this value.

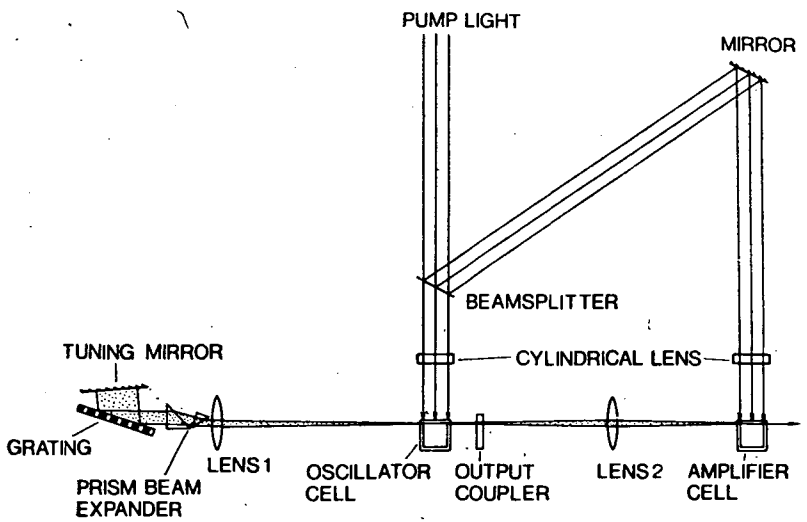

Fig. 1. The long cavity dye laser-amplifier arrangement

coming from the oscillator cell output coupler system to

$$\delta\theta = \frac{a}{f} = \frac{0.02\ \text{cm}}{25\ \text{cm}} = 8 \cdot 10^{-4}\ \text{rad},$$

where $a = 0.02$ cm is the absorption depth of the dye.

Two prism were used as beam expander ($\times 10$). The diffraction grating was 1300 lines/mm operating as grating expander with the angle of incidence $\alpha = 67.5°$ and $\alpha = 78°$, respectively. With the above data from the Eq. (7) of [7] the resultant

passive bandwidth $\delta\lambda=0.012$ nm and $\delta\lambda=0.006$ nm, respectively. The light of the dye laser was focussed by lens 2 ($f=10$ cm) on the amplifier cell.

The duration of the amplified pulses was measured by one of the usual nonlinear optical correlation techniques, using SHG with collinear, identically polarized beams [8] in a phase-matched ADP-crystal. The SH signal was measured and averaged by a LP—20 laser photometer. Assuming a Gaussian pulse shape, a pulse duration of (155 ±25) ps and (228 ±16) ps could be deduced from the measurements of the autocorrelation function if $\alpha=67.5°$ and $\alpha=78°$, respectively.

The linewidth of the pulses was measured by a Fabry—Perot etalon of 8 mm spacing. $\delta\lambda=0.010$ nm and $\delta\lambda=0.006$ nm linewidths were obtained by taking photographs from an interference pattern of 20 pulses if $\alpha=67.5°$ and $\alpha=78°$, respectively. These linewidths well correspond to the above-calculated passive linewidths. The measured time-bandwidth product is 3.1 and 2.9 times the Fourier-transform-limit for a Gaussian pulse. Some of the interference pattern of a single pulse showed a single narrow spectrum line, and the other part of the interference pattern showed a double spectrum line. The linewidth of the single spectrum line was 0.003 nm if both $\alpha=67.5°$ and $\alpha=78°$. This linewidth value was the transform-limit-pair of 155 ps, and 1.4 times the transform-limit-pair of 228 ps. The frequency difference of the two lines of the double spectrum line was equal to the FSR of a Fabry—Perot interferometer of 3.8 cm spacing. In the dye laser the optical pathlength between the left wall of the oscillator cell and the output coupler was equal to this spacing.

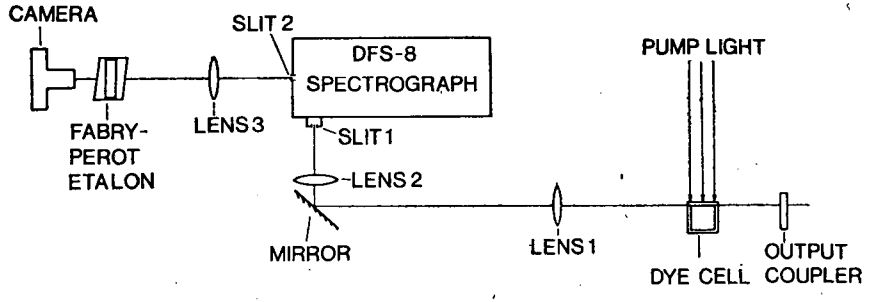

Fig. 2. Experimental arrangement for the measurement of the spectral modulation of the light of the dye cell-output coupler system

We demonstrated that this agreement is no accident using the arrangement shown in Fig. 2. The grating and prism were removed and the light of the dye-cell output-coupler system was focussed by lens 1 ($f_1=25$ cm) and lens 2 ($f_2=10$ cm) on the entrance slit of DFS—8 spectrograph. The DFS—8 spectrograph had 0.6 nm/mm reciprocal linear dispersion, and was used as a monochromator. The entrance and exit slitwidths were 100 μm. The output of the monochromator was analysed by a Fabry—Perot etalon having a 5 mm spacer. The interference pattern of 800 shots was photographed by a camera having an objective with a focal length of 250 mm. Fig. 3 shows the results of the measurements, where d_{FP} is the spacing of such a Fabry—Perot interferometer, having an FSR equal to that calculated from the interference pattern, and d_G is the — geometrically determined — optical

pathlength between the left wall of the dye cell and the right side of the output coupler. Fig. 3 demonstrates that the difference of measured results from the solid line, expressing that d_{FP} and d_G are equal, is smaller than the limit of error. Consequently, the light of the long-cavity dye-laser observed spectrum-line structure is attributable to interference phenomena produced between the wall of the dye cell and the output coupler. On the basis of this, the spectral evolution of our dye laser can be explained as follows: In consequence of the interference phenomena, the Fabry—Perot lines modulated light beam is propagated into the direction of the spectral selective system. From these lines several are selected and fed back to the spectral selective system. Between the FSR of Fabry—Perot "interferometer" $\Delta\nu_{FSR}$ and the selectivity of the spectral selective system $\Delta\nu_{SS}$, obtained the following relation: $\Delta\nu_{FSR} < \Delta\nu_{SS} < 3 \cdot \Delta\nu_{FSR}$. This inequality is valid for the measured value, too.

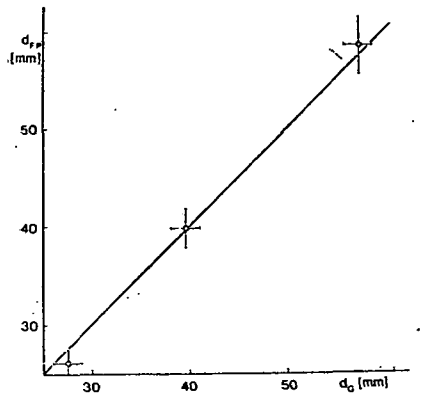

Fig. 3. The distance between the left wall of the cell and the right side of the output coupler measured by Fabry—Perot analyser versus calculated distance

References

[1] *Wyatt, R.:* Opt. Commun. **26,** 429 (1978).
[2] *Veith, G., A. J. Schmidt:* Opt. Commun. **30,** 437 (1979).
[3] *Rácz, B., Zs. Bor, G. Szabó, S. Szatmári:* Acta Phys. et Chem Szeged (to be published).
[4] *Wyatt, R.:* Appl. Phys. **21,** 353 (1980).
[5] *Rácz, B., G. Szabó:* Acta Phys. et Chem. Szeged (to be published).
[6] *Borgström, S. A.:* Phys. Scripta **14,** 92 (1976).
[7] *Shoshan, I., U. P. Oppenheim:* Opt. Commun. **25,** 375 (1978).
[8] *Gloge, D., T. P. Lee:* Appl. Phys. **42,** 307 (1971).

ГЕНЕРАЦИЯ ТРАНСФОРМ-ЛИМИТАЦИОННЫХ ИМПУЛЬСОВ С СУБНАНОСЕКУНДНОЙ ДЛИТЕЛЬНОСТЬЮ ИЗЛУЧЕНИЯ ДЛИНОРЕЗОНАТОРНОГО ЛАЗЕРА НА КРАСИТЕЛЕ

Й. Хеблинг, Ж. Бор, Б. Рац, Б. Немет и И. Шанта

Исследован длинорезонаторный лазер-усилитель на красителе с целью генерации импульсов с субнаносекундной длительностью. Возбуждающий свет был получен из лазера на атмосферном азоте с поперечным разрядом длительностью 1 нс. Длительность импульсов генерированнихся из лазер-усилителя на красителе был 155 пс. Спектральное уширение импульсов было меньше чем 0,01 нм. Спектр был модулирован периодом постоянной эталона Фабри—Перо, толщиной 3,8 см. Длительность оптического пути в лазере на красителе между стеной и окном осциллятора выла равна этой толщине.

DIELECTRIC ABSORPTION STUDIES IN CHLORO AND NITRO SUBSTITUTED ANILINES IN BENZENE*

By

S. K. SAXENA[1], C. L. GUPTA[2], M. N. SHARMA and M. C. SAXENA

Microwave and E.P.R. Research Laboratory
Department of Physics, Lucknow University, Lucknow, India

(Received July 4, 1980)

Dielectric absorption studies on four substituted anilines *viz.* 3-chloro aniline (A), 4-chloro-3-nitro aniline (B), 4-chloro-2-nitro aniline (C), 2-chloro-4-nitro aniline (D) have been made in the dilute solution of benzene and over a range of temperature in the microwave region of wave length 3.11 cm. The distribution parameter has been found to be low in the case of 3-chloro aniline, and for the other three molecules it is slightly high. The dielectric absorption was therefore, resolved by Higasi, Koga and Nakamura method which yielded two relaxation times $\tau_{(1)}$ and $\tau_{(2)}$. The $\tau_{(1)}$ and $\tau_{(2)}$ are widely different in the case of molecules **B** and **C**, showing the flexible nature of these molecules in the microwave field. The flexibility of the molecules increases as the relaxation time decreases. This is in agreement with our previous observations. The relaxation time has been found to be the highest in the case of 2-chloro-4-nitro aniline. The higher relaxation time is explained on the basis of hydrogen bonding taking place in case anilines in ortho position. These results are in agreement with the observations of Smyth et al.

Introduction

FISCHER [1] suggested that non rigidity was an important feature of anilines and predicted the rotation of $—NH_2$ group around C—N bond. Since then measurements have been made by many workers [2—7] to investigate the non rigidity of anilines. GRUBB and SMYTH [8] studied primary and secondary amines and diamines in viscous medium and in dilute solutions and have resolved the dielectric data in terms of two relaxation times. WILLIAM [9] has given a theoretical treatment and discussed that internal reorientation is feasible in amines. STOCKHAUSEN [10] and KLAGES [11] studied anilines and attributed the short group relaxation time to the inversion of non polar configuration of $—NH_2$ group through the plane of phenyl ring. FLORANTA and KADABA [6] studied the *o*-, *m*- and *para* chloro aniline both in pure liquid and in dilute solution and analyzed their results in terms of two relaxation times attributed to the rotation of molecule and the inversion of $—NH_2$ group. CHITOKU and HIGASI [12] studied anilines, methyl anilines, dimethyl anilines and *p*-nitro aniline and have reported very small values of distribution parameter for these compounds. According to the existing literature [1—12] amines behave as

* The work supported by U.G.C. (India).

[1] (On leave) Department of Physics, D.B.S. College, Kanpur.

[2] (On leave) Department of Physics, K.S. Saket P.G. College, Faizabad.

feebly flexible molecules, though not much work has been reported on trisubstituted anilines. Therefore, it was considered worthwhile to carry out dielectric measurements on *X*-band in the dilute solution of benzene and over the range of temperature (297—321 K) on 3-chloroaniline (**A**), 4-chloro-3-nitroaniline (**B**), 2-chloro-4-nitroaniline (**C**) and 4-chloro-2-nitroaniline (**D**). The effect of chloro and nitro group on the group relaxation process of $-NH_2$ group have been examined and the energy barriers associated with the different modes of relaxation have been evaluated. 3-chloroaniline has been used to compare and verify the results obtained by Higasi method and to study the systematic variation of chloro and nitro group in the *o*, *m*, and *para* position in the studied anilines.

Chemicals

The chemicals used were of purest quality available, obtained from B.D.H. England. The physical properties have been checked against the literature values. The solvent used in the measurements was benzene of the A.R. grade, obtained from B.D.H., England, and was distilled twice before use.

Experimental

The dielectric constant ε' and dielectric loss ε'' have been measured at *X*-band by the technique of ROBERTS and VON HIPPEL [13] latter modified by DAKIN and WORKS [14]. The static dielectric constant ε_0 was measured at 300 KHz by dipolemeter based on the principle of heterodyne beat method. The refractive indices of the different solutions were measured by Abbe's refractometer, the density and viscosity by pyknometer and Oswald's viscometer respectively. The measurements of ε' and ε'' are accurate up to $\pm 2\%$ and $\pm 5\%$ respectively.

The most probable relaxation time τ_{OH} and distribution parameter α have been evaluated by Higasi method [15], using equations (1) and (2)

$$\tau_{OH} = \frac{1}{\omega}\left[\frac{A^2+B^2}{C^2}\right]^{\frac{1}{2(1-\alpha)}} \tag{1}$$

$$1-\alpha = \frac{2}{\pi}\tan^{-1}\left(\frac{A}{B}\right) \tag{2}$$

where

$$A = a''(a_0-a_\infty)$$

$$B = (a_0-a')(a'-a_\infty)-a''^2$$

$$C = (a'-a_\infty)^2+a''^2.$$

The slopes a_0, a', a'' and a_∞ are defined earlier [16] obtained by plotting weight fractions *versus* ε_0, ε', ε'' and ε_∞ and ω is the angular frequency selected for the measurements.

In the absence of multifrequency data being available Higasi, Koga and Nakamura method [17] has been utilized. It has been observed [18—20] in previous studies that $\tau_{(2)}$ stands for the molecular relaxation time τ_1 and the relaxation time $\tau_{(1)}$ associated with group process is a implicit function of τ_1, τ_2 and C_2 defined by equation (3) and (4)

$$\tau_{(1)} = \frac{1}{\omega} \frac{a''}{(a'-a_\infty)}, \tag{3}$$

$$\tau_{(2)} = \frac{1}{\omega} \frac{(a_0-a')}{a''}. \tag{4}$$

With no elaborate and accurate method being available for the measurement of a_∞, the most general approximation $a_\infty = a_D$ has been applied to calculate the slope at infinite frequencies. The equations (3) and (4) are employed when the measurements of the slopes have been made very accurately. If $\tau_{(1)}$ and $\tau_{(2)}$ come out widely separated, it is a clear indication of more than a single relaxation process occurring in the system. Contrary to this, $\tau_{(1)} \approx \tau_{(2)}$ may be treated as a criterion [18] for the pure Debye type of dispersion and is indicative of a single relaxation time. The average relaxation time $\tau_{(0)}(=\sqrt{\tau_{(1)}, \tau_{(2)}})$ is the square root of the product of $\tau_{(1)}$ and $\tau_{(2)}$.

The enthalpy of activation $\Delta H\tau_{(2)}$, $\Delta H\tau_{(0)}$ and $\Delta H\tau_{OH}$ have been determined from the straight line plots of $\log \tau_{(2)} \cdot T$, $\log \tau_{(0)} \cdot T$ and $\log \tau_{OH} \cdot T$ against $\frac{1}{T}$, wherever possible. The free energy of activation and the entropy of activation have been calculated by employing Eyring theory [21] of rate process.

Results

The value of the slopes a_0, a', a'' and a_∞ for all the four molecules in dilute solution of benzene and at varying temperatures have been reported in Table I. The most probable relaxation time together with the distribution parameter α are given in Table II. The value of dielectric relaxation time $\tau_{(1)}$, $\tau_{(2)}$ and $\tau_{(0)}$ and the enthalpies of activation $\Delta H\tau_{(2)}$ and $\Delta H\tau_{(0)}$ and $\Delta H\eta$ have been reported in Table III.

Discussion

(A) *3-Chloroaniline*

The distribution parameter α for this molecule has been found to be sufficiently low (0.0—0.8) in the range of temperature 297—321 K. The most probable relaxation time at 297 K has been found to be 16.3 ps. This value agrees well with the relaxation time τ_0(=15.5 ps) by ELORANTA and KADABA [6] on *meta* chloro aniline using COLE—COLE [22] method. The small value of α indicates the rigid nature of molecule in the microwave field under investigation. In order to analyze, the dielectric dispersion data has been further analyzed by Higasi, Koga and Nakamura method [17], which yielded two relaxation time $\tau_{(1)}$(=14.2 ps) and $\tau_{(2)}$(=18.3 ps)

Table I

Value of slopes a_0, a', a'', a_∞ for the samples in benzene at different temperature

Compound	Temp. K	a_0	a'	a''	a_∞
(A) 3-chloro aniline	297	8.00	4.44	3.00	0.68
	305	7.00	4.20	2.95	0.49
	313	6.20	4.00	2.90	0.32
	321	5.06	3.25	2.20	0.27
(B) 4-chloro-3-nitro aniline	297	24.2	9.1	8.0	−1.25
	305	13.3	5.0	4.3	−0.66
	313	10.0	4.12	4.0	−0.40
	321	6.15	2.75	3.0	−0.30
(C) 4-chloro-2-nitro aniline	297	30.0	9.0	10.6	0.71
	305	25.0	7.4	9.1	0.48
	313	18.2	6.1	7.5	0.33
	321	13.8	6.0	5.71	0.31
(D) 2-chloro-4-nitro aniline	297	50.0	12.0	16.7	0.37
	305	40.1	10.5	14.3	0.38
	313	32.0	10.0	10.8	0.35
	321	26.2	9.5	9.5	0.32

at 297 K. The $\tau_{(1)}$ and $\tau_{(2)}$ values are quite close to each other, which indicates a single Debye type of dispersion occurring in the molecule. The results are in agreement with the observation of [6]. The smaller value group relaxation in the case of aniline was explained on the basis of high value of critical wavelength selected for the measurements. The dispersion in aniline occurs in the mm region and hence the absence of group relaxation time and distribution parameter in the higher wavelength region.

The equality in the values of $\tau_{(1)}$ and $\tau_{(2)}$ and very small value of distribution parameter α indicates that the dispersion is only feebly occurring in the 3.11 cm wavelength region.

The average relaxation time $\tau_{(0)}$ (=16.1 ps) agrees very well with τ_{OH} (=16.3 ps) at 297 K. These results are in agreement with our earlier studies on N-substituted amides [20], α-substituted benzyl cyanides [16] and the observation of HIGASI et al. on alkyl acetate [23].

Enthalpies associated with different processes involved in the dielectric absorption have been evaluated and found to be $\Delta H\tau_{OH}$ (=6.5 kJ mol^{-1}), $\Delta H\tau_{(2)}$ (=8.4 kJ mol^{-1}), $\Delta H\tau_{(0)}$ (=6.1 kJ mol^{-1}) and ΔH_η (=10.5 kJ mol^{-1}). The enthalpy $\Delta H\tau_{(1)}$ is not very accurate due to the irregular variation of $\tau_{(1)}$. The enthalpy 6.5 kJ mol^{-1} associated with most probable relaxation time τ_{OH} can be compared with the enthalpy of average relaxation time (=6.1 kJ mol^{-1}). The most probable enthalpies of activation are less than the corresponding free energies and so the entropies are usually negative. According to BRANIN and SMYTH [24] a negative entropy of activation indicates that there are fewer configurations possible in the activated state and for these configurations the activated state is more ordered than the normal state, which is in agreement with our previous studies [4, 5, 16]. The

enthalpy of viscous flow is highest because the process of viscous flow involves both rotation and translation, while the process of dipole orientation involves only the rotation of the molecules. Similar conclusion has been derived by HOLLAND and SMYTH [25].

(B) *4-Chloro-3-nitroaniline*

The distibution parameter for this compound has been found to be (0.05—0.27) in the range of temperature 297—321 K. The most probable relaxation has been found to be $\tau_{OH} = 23.7$ ps at 297 K. This relaxation time can be compared with the relaxation time of 4-chloro aniline [6] (=21.5 ps) in benzene. The presence of $-NO_2$ group at the position 3 slightly increases the relaxation time of the molecule. Due to the high value of α the dielectric absorption was resolved, which gave two relaxation times $\tau_{(1)}$ (=12.7 ps) and $\tau_{(2)}$ (=31.1 ps). The $\tau_{(1)}$ and $\tau_{(2)}$ are widely different from each other, suggesting the flexibility of the molecule under the microwave field. The relaxation time $\tau_{(1)}$ associated with group process has been found to be irregular with temperature where as $\tau_{(2)}$, representing the molecular process is decreasing with the temperature. These observations are in agreement with the observation of SRIVASTAVA et al. [26] in N, N-dimethyl aniline and N, N-diethyl aniline.

The average relaxation time $\tau_{(0)}$ has been found to be 19.9 ps which is slightly less than τ_{OH} (=23.7 ps). This type of behaviour can not be ruled out because $\tau_{(0)}$ is the root average of $\tau_{(1)}$ and $\tau_{(2)}$. Such variations have been reported in the earlier work [16] of the author using Higasi, Koga and Nakamura method and also in the observations of HIGASI et al. [23].

Table II

Relaxation time evaluated using Higasi method and corresponding activation parameters

Compound	T K	α	τ_{OH}	ΔF_e kJ mol^{-1}	ΔH_e kJ mol^{-1}	ΔS_e J mol^{-1} deg^{-1}
(A) 3-chloroaniline	297	.08	16.3	11.4		−16.5
	305	.01	14.1	11.4	6.5	−16.0
	313	—	12.8	11.5		−15.9
	321	.01	11.3	11.5		−15.6
(B) 4-chloro-3-nitroaniline	297	0.27	23.7	12.3		−12.1
	305	0.25	21.1	12.4	8.7	−12.1
	313	0.16	20.0	12.7		−12.7
	321	0.05	17.5	12.7		−12.5
(C) 4-chloro-2-nitroaniline	297	0.16	33.0	13.1		−8.4
	305	0.11	30.2	13.2	10.6	−8.5
	313	0.06	25.5	13.3		−8.6
	321	0.10	20.2	13.2		−8.1
(D) 2-chloro-4-nitroaniline	297	0.12	37.2	13.4		−11.8
	305	0.11	33.3	13.6	9.9	−12.1
	313	0.17	31.0	13.8		−12.5
	321	0.16	25.8	13.8		−12.5

The enthalpies associated with the various processes involved in the dielectric absorption have been found to be $\Delta H\tau_{OH}$ (=8.7 kJ mol^{-1}), $\Delta H\tau_{(2)}$ (=9.6 kJ mol^{-1}), $\Delta H\tau_{(0)}$ (=4.9 kJ mol^{-1}); ΔH_{η} (=10.5 kJ mol^{-1}). The enthalpy for the average process $\Delta H\tau_{(0)}$ is not very accurate due to irregular variation of $\tau_{(0)}$ because $\tau_{(0)}$ is the square root of the product of $\tau_{(1)}$ and $\tau_{(2)}$ and $\tau_{(1)}$ is irregularly varying with the temperature. The enthalpy associated with most probable relaxation τ_{OH} for the molecule **B** (=8.7 kJ mol^{-1}) has been found to be greater than **A**. This is in accordance with the bigger shape and size of the molecule **B** in comparison to molecule **A**.

The enthalpy, free energies and entropies are reported in Table II. The free energy ΔF_{ε} (=12.3—12.7 kJ mol^{-1}) and ΔS_{ε} (=12.1—12.5 J mol^{-1} deg^{-1}) have been found in the range of temperature 297—321 K. The entropy found to be negative is similar to the molecule **A** and a slightly high value of free energy is due to high value of relaxation time in this molecule. These observations are in agreement with the earlier results of many workers [4, 5, 16, 24].

(C) *4-Chloro-2-nitroaniline*

The distribution parameter α for this molecule has been found to be in the range of 0.06—0.16. The most probable relaxation time τ_{OH} for this molecule has been found to be 33.0 ps at 297 K. The relaxation time for this molecule has been found to be higher than that of **B** (=23.7 ps), this can be attributed to the greater hindrance offered by —NO_2 group to the rotation of —NH_2 group in the position 2 than in the position 3.

The dielectric absorption has been further resolved which gave rise to two relaxation times $\tau_{(1)}$ (=21.7 ps) and $\tau_{(2)}$ (=34.6 ps). The average relaxation time for this molecule has been found to be 26.2 ps at 297 K.

The enthalpies involved in the various processes have been found to be $\Delta H\tau_{(2)}$ (=14.7 kJ mol^{-1}), $\Delta H\tau_{(0)}$ (=9.8 kJ mol^{-1}), $\Delta H\tau_{OH}$ (=10.6 kJ mol^{-1}). The enthalpy associated with τ_{OH} for this molecule has been found to be greater than that of **A** and **B**. The enthalpy for the most probable relaxation process (=10.6 kJ mol^{-1}) can be compared with the enthalpy of the average relaxation process (=9.8 kJ mol^{-1}) within the experimental error, suggesting that the two processes are similar to one another.

The free energy ΔF_{ε} (13.1—13.3 kJ mol^{-1}) and a negative entropy ΔS_{ε} (=8.1—8.6 J mol^{-1} deg^{-1}) have been found in the temperature range 297—321 K. The free energy has been found to be greater than **A** and **B** and the negative value of entropy is in agreement with the results obtained by previous workers [4, 5, 16, 24].

(D) *2-Chloro-4-nitroaniline*

The distribution parameter α for this compound has been found to be in range of (0.11—0.17) in the range of temperature 297—321 K. The most probable relaxation time for this molecule has been found to be 37.2 ps which is sufficiently high in comparison to the other three molecules. Obviously this results from greater steric hindrance offered by —NH_2 group to the rotation of molecule by forming the intra-

molecular hydrogen bond between hydrogen atom of $—NH_2$ group and chlorine atom at position 2. The intramolecular hydrogen bonding is responsible for lowering the distribution parameter in comparison to the molecule **B** and **C** and increasing the overall relaxation time of the molecule. This is in agreement with the observations of SMYTH et al. [27] that the presence of $—NO_2$ group at the *para* position aids the delocalization of π-electrons between the nitrogen atom of $—NH_2$ group and the ring, which results in the intramolecular hydrogen bond, and consequently is responsible for long mean relaxation time and smaller distribution parameter for the *p*-nitro substituted aniline in benzene.

$\tau_{(2)}$ is very close to the most probable relaxation time τ_{OH}, showing that molecular process predominates in the system. Slight increase in α value with the temperature may be due to breaking of intramolecular hydrogen bond.

The enthalpies associated with different processes $\Delta H\tau_{(2)}$ and $\Delta H\tau_{OH}$ ($=9.9$ kJ mol^{-1}), $\Delta H\tau_{(0)}$ ($=9.0$ kJ mol^{-1}), ΔH_η ($=10.5$ kJ mol^{-1}) have been reported in Tables II., III. When compared to the enthalpies of molecule **A** and **B**. the

Table III

Relaxation times $\tau_{(1)}$, $\tau_{(2)}$ and $\tau_{(0)}$ and enthalpy of activation $\Delta H\tau_{(2)}$, $\Delta H\tau_{(0)}$, $\Delta H\eta$ Using Higasi, Koga and Nakamura method

Compound	T K	$\tau_{(1)}$ ps	$\tau_{(2)}$ ps	$\tau_{(0)}$ ps	$\Delta H\tau_{(2)}$ kJ mol^{-1}	$\Delta H\tau_{(0)}$ kJ mol^{-1}	$\Delta H\eta$ kJ mol^{-1}
(A) 3-chloroaniline	297	14.2	18.3	16.1			
	305	13.3	15.3	14.3	8.4	6.1	10.5
	313	12.9	12.5	12.7			
	321	11.2	11.7	11.4			
(B) 4-chloro-3-nitroaniline	297	12.7	31.1	19.9			
	305	12.7	28.8	18.8	9.6	4.9	10.5
	313	14.6	24.2	18.8			
	321	16.2	18.7	16.2			
(C) 4-chloro-2-nitroaniline	297	21.7	34.6	26.2			
	305	21.7	31.9	26.3	14.7	9.8	10.5
	313	21.4	26.6	23.8			
	321	16.5	22.5	20.4			
(D) 2-chloro-4-nitroaniline	297	23.7	37.5	29.8			
	305	23.2	34.1	28.1	9.9	9.0	10.5
	313	18.5	33.6	24.9			
	321	17.1	29.0	22.3			

enthalpy of molecule **D** ($=9.9$ kJ mol^{-1})>**B** ($=8.7$ kJ mol^{-1})>**A** ($=6.5$ kJ mol^{-1}). This may be due to the greater hindrance offered by $—NO_2$ group in para position. The more rigid nature of this molecule in comparison to **B** is perhaps responsible for the high value of enthalpy.

The free energy ΔF_ε ($=13.4$—13.8 kJ mol^{-1}) and ΔS_ε ($=11.8$—12.1 J mol^{-1}deg^{-1}) have been reported in Table II. The ΔS_ε has been found to be negative, showing that fewer configurations are possible in the activated state and the activated state is more ordered than the normal state. These results are in agreement with our previous studies [4, 5, 16] and the study of BRANIN and SMYTH [24].

Conclusion

All the four investigated aniline molecules have been found to be flexible. The flexibility is small in the case of 3-chloroaniline (**A**), the rest three molecules 2-chloro-4-nitroaniline (**D**), 4-chloro-2-nitroaniline (**C**) and, 4-chloro-3-nitroaniline (**B**) have been found to be more flexible in microwave region under investigation. Although molecules **B**, **C** and **D** are of the same size and shape, still their behaviour in the microwave field, the relaxation time, distribution parameter, and dipolar relaxation parameters are found to be different. The relaxation times of the molecules are increasing as the flexibility is decreasing. These observation are consistent with our previous observations [4, 5].

Relaxation time of 4-Chloro-3-nitroaniline (=23.7 ps) is sufficiently small as compared to the compounds (**C**) and (**D**). This probably appears due to the vacant position 2 in this molecule. FONG et al. [28] have interpreted their results of larger relaxation times of 2,6-dimethyl aniline as compared to 2,5-dimethyl aniline in terms of greater steric hindrance offered to the rotation of $—NH_2$ group in the former molecule.

In the case of 2-Chloro-4-nitroaniline the relaxation time has been found to be the longest. This is attributed to the formation of hydrogen bond between the chlorine atom at position 2 and the hydrogen of $—NH_2$ group. These results are in agreement with the observation of SMYTH et al. [27].

Acknowledgement

S. K. Saxena and C. L. Gupta are grateful to the University Grants Commission, New Delhi (India) for the award of Teacher Fellowship under Faculty Improvement Programme. We also thank to U.G.C. for supporting the work and granting financial assistance from time to time.

References

[1] *Fischer, E.:* Phys. Z. **40**, 645 (1939).
[2] *Srivastava, H. N.:* J. Sci. Ind. Res. B. **19**, 149 (1960).
[3] *Ahmad, S. I.:* Indian J. Pure and Appl. Phys. **2**, 70 (1964).
[4] *Mehrotra, N. K., T. C. Pant and M. C. Saxena:* Trans. Faraday Soc. **65**, 2079 (1969).
[5] *Mathur, A., A. Kumar and M. C. Saxena:* Il Nuovo Cimento **46**, B 57 (1978).
[6] *Eloranta, J. K., P. K. Kadaba:* Trans. Faraday Soc. **67**, 1355 (1971).
[7] *Tucker, S. W. and S. Walker:* J. Chem. Phys. **52**, 2545 (1970).
[8] *Grubb, E. L. and C. P. Smyth:* J. Amer. Chem. Soc. **83**, 4879 (1961).
[9] *Williams, G.:* Trans. Faraday Soc. **64**, 1219 (1968).
[10] *Stockhausen, M.:* Z. Naturforsch. **19a**, 1317 (1964).
[11] *Klages, G.:* Umschau Wiss. Techn. **66**, 330 (1966).
[12] *Chitoku, K. and K. Higasi:* Bull. Chem. Soc. Japan **39**, 2160 (1966).
[13] *Roberts, S., A. von Hippel:* J. Appl. Phys. **17**, 610 (1946).
[14] *Dakin, T. W. and C. N. Work:* J. Appl. Phys. **18**, 789 (1947).
[15] *Higasi, K.:* Bull. Chem. Soc. Japan **39**, 2157 (1966).
[16] *Saxena, S. K., C. K. Misra, J. P. Shukla and M. C. Saxena:* Acta Phys. et Chem. (Szeged), **25**, 47 (1979).
[17] *Higasi, K., Y. Koga and M. Nakanura:* Bull. Chem. Soc. Japan, **44**, 988 (1971).
[18] *Chitoku, K., K. Higasi:* Bull. Chem. Soc. Japan, **44**, 992 (1971).

[19] *Viz, J. K., K. K. Srivastava:* Bull. Chem. Soc. Japan, **46,** 1112 (1973).
[20] *Misra, C. K., J. P. Shukla, M. C. Saxena:* Adv. Mol. Relax. and Inter. Processes, **15,** 181 (1979).
[21] *Glasstone, S., K. J. Laidler and H. Eyring:* "The Theory of Rate Process". McGraw Hill Book Co., New York, p. 548 (1941).
[22] *Cole, K. S. and R. H. Cole:* J. Chem. Phys. **2,** 341 (1941).
[23] *Koga, Y., M. Takahashi and K. Higasi:* Bull. Chem. Soc. Japan, **47,** 697 (1974).
[24] *Branin, F. H. (Jr), C. P. Smyth:* J. Chem. Phys. **20,** 1121 (1952).
[25] *Holland, R. S., C. P. Smyth:* J. Phys. Chem. **59,** 1088 (1955).
[26] *Viz, J. K., I. Krishna and K. K. Srivastava:* Bull. Chem. Soc. Japan, **46,** 17 (1973).
[27] *Antoney, A. A., F. K. Fong, C. P. Smyth:* J. Phys. Chem. **68,** 2035 (1964).
[28] *Fong, F. K., J. P. McTague, S. K. Garg, C. P. Smyth:* J. Phys. Chem. **70,** 3567 (1966).

ИЗУЧЕНИЕ ДИЭЛЕКТРИЧЕСКОГО ПОГЛОЩЕНИЯ В ХЛОР- И НИТРОЗАМЕЩЕННЫХ АНИЛИНАХ В БЕНЗОЛЕ

С. К. Саксена, Ц. Л. Гупта, М. Н. Шарма и М. Ц. Саксена

Проведено изучение диэлектрического поглощения четырех замещенных анилинов вицинального 3-хлоранилина (**A**), 4-хлоро-3-нитроанилина (**B**), 4-хлоро-2-нитроанилина (**C**), 2-хлоро-4-нитроанилина (Д) в разбавленных растворах в микроволновой области длин волн 3,11 см. Рассчитывали диэлектрическое поглощение по методу Хигаши, Кога и Накамура, по которому получены два релаксационных времени. Значения τ_1 и τ_2' значительно различались для молекул **B** и **C**, указывая на гибкость структуры этих молекул в микроволновом поле. Полученные резильтаты находятся в хорошем соответствии с данными, имеющимися в литературе.

INVESTIGATION OF NUCLEOTIDE-METAL ION SYSTEMS, III. STUDY OF THE ATP—Ni(II) SYSTEM

By

J. CSÁSZÁR and L. KISS

(Department of General and Physical Chemistry, A. József University, Szeged)

(Received October 7. 1980)

The Ni(II) complex of ATP-5' [ATP] with composition $NiCl_2.ATPH_2.11\,H_2O$ has been prepared. The spectral and electrochemical behaviours of this compound have been studied and conclusions drawn on the site of coordination, supporting that in solution the Ni(II) ion is bound to the β- and γ-phosphate groups and a distorted octahedral NiO_6 microsymmetry is formed.

Introduction

In previous papers [1, 2] we surveyed the possible species which can be formed by means of interaction between the transition metal ions and nucleotides. The biological importance of these compounds is a proved fact, but the views relating to the structures of these compounds and to the coordination sites of the metal ions are very different [3—6].

In contrast to the earlier investigations our aim was to isolate the Ni(II)-ATP compound in a crystalline form and to contribute to a better knowledge of this system by physico-chemical study of the product.

Results and discussion

A 1:1 mixture of concentrated aqueous solutions of $NiCl_2.6\,H_2O$ and $ATP.Na_2$ was poured slowly under constant stirring into acetone cooled to about 278 K. The palegreen microcrystalline product was filtered, washed with ethanol and dried over P_2O_5 in vacuo. On the basis of the analytical data [$\%C_{calcd.}$: 14.42 (14.30); $\%H_{calcd.}$: 1.69 (1.63); $\%N_{calcd.}$: 8.41 (8.53); $\%Ni_{calcd.}$: 7.05 (7.08, titrimetric)], we regard the composition $NiCl_2.ATPH_2.11\,H_2O$ as probable. By alcoholic precipitation from a neutral mixture (buffered with NaOH to pH=7), BHATTACHARYYA ET AL. [7] isolated a product of formula $Na_2NiATP.4\,H_2O$.

Details of the physico-chemical experimental methods are given in a previous paper [1]. In the pH-metric titration curve of an aqueous mixture of the Ni(II) salt and $ATP.Na_2$, the second buffer region — characteristic of the ligand — disappears, indicating formation of the 1:1 complex. The stability constants of this compound, $\lg K_1[NiATPH]=2.72\pm0.02$ and $\lg K_2[NiATP]=5.02\pm0.02$, are known from the literature [8].

The solid sample is paramagnetic, with BM=3.12 (T=298 K), indicating the presence of two unpaired electrons and of a six-coordinated, strongly distorted octahedral structure.

The molar conductivity (Λ_M=185 Ω^{-1} cm^{-1}) differs slightly from the value measured for the Co(II)-ATP compound [2]. For a millimolar solution of $Na_2NiATP.4\,H_2O$ the value Λ_M=218 Ω^{-1} cm^{-1} is given by BHATTACHARYYA et al. [7]. The Λ *vs.* $\sqrt{c}$ relationship indicates a weak 1:2 type electrolyte, which is consistent with the composition suggested above.

The polarographic behaviour of the Ni(II)—ATP complex is different from that of the Co(II), Cu(II) and Zn(II) complexes. In 0.1 mol dm^{-3} KNO_3 supporting electrolyte, the half-wave potential of the Ni(II)→Ni(O) reduction step (−1.043 V *vs.* N.C.E.) is shifted in the positive direction in the presence of $ATP.Na_2$ (−0.950 V *vs.* N.C.E.). In both cases the electrode reactions are irreversible. Further investigations relating to this phenomenon are in progress.

The reflectance spectrum of the crystalline product, the absorption spectrum of a solution made from it, and that of the mixture containing the components in the ratio 1:1 are practically identical, and indicate unambiguosly the presence of a six-coordinated species.

The three characteristic bands can be assigned to the $^3A_{2g}(F)\rightarrow{}^3T_{2g}(F)$ [ν_1], $^3T_{1g}(F)$ [ν_2], $^3T_{1g}(P)$ [ν_3] $d-d$ transitions [9]. The spectrum does not change in the presence of an excess of $ATP.Na_2$, indicating that dissociated or hydrated species are not present in considerable amount. The measured and the calculated parameters are listed in Table I.

Table I

Measured and calculated parameters of the complex

	Refl. spectrum	Soln. spectrum
ν_1	8 750 cm^{-1}	8 850 cm^{-1}
ν_2	14 200 cm^{-1}	14 500 cm^{-1}
ν_3	23 400 cm^{-1}	25 600 cm^{-1}
Dq	875 cm^{-1}	885 cm^{-1}
B	757 cm^{-1}	903 cm^{-1}
β	0,70	0,83
LFSE	10 500 cm^{-1}	10 620 cm^{-1}

The calculated interelectronic repulsion parameter B and the nephelauxetic parameter β indicate predominantly ionic bonds [10]. In the crystalline state, presumably because of the stabilizing effect of the lattice energies, the bonds are more covalent. The β value calculated from the solution spectrum is the same as in the case of the $[Ni(H_2O)_6]^{2+}$ ion, proving that the ligand field strengths of ATP and of H_2O are approximately the same.

The solution spectrum is only slightly influenced by the pH. In the range pH=2—10 the positions of the bands remain almost unchanged. With increasing pH, there are almost no changes in the intensities of the ν_1 and ν_2 bands, whereas the ν_3 band changes to a greater extent (in $4\cdot10^{-2}$ mol dm^{-3} solution E=0.252-0.340).

By means of the magnetic moment and the 10 Dq value a spin — orbital coupling constant of $\lambda=-233$ cm^{-1} can be calculated for the crystalline substance [e.g. 11]. Considering the value $\lambda_{ion}=-315$ cm^{-1} and the relationship $\alpha^2=\lambda/\lambda_{ion}$, we obtain α=0.84, which is identical with the β value calculated only from the spectral data.

The spectrum and the calculated parameters suggest that the binding sites of the Ni(II) ion are in the phosphate chain. Even if there is a weak interaction with

the N_7 atoms of the purine ring in the crystalline state, it ceases to exist in solution. If Ni—N bonds were present, a more covalent bond character (*i.e.* a larger Dq and a smaller β value) and band splitting (low symmetry) would be expected.

The infrared spectrum of the Ni(II) complex differs slightly from that of free ATP.Na_2. The main frequencies are: 3380 s (νNH+νOH), 1711 s (?), 1664 m (νC=N), 1628 w, 1528 w, 1247 s (νP=O), ~1097 s, 1012 s (P—O+C—O), 924 m (P—O—P), 834 w, 640 w, ~535 m. Unfortunately the νOH and νNH bands totally overlap, so that the possible C_6-NH_2-Ni(II) interaction can not be observed.

On the above basis, we have taken the formation of a low-stability high-spin 1:1 complex into consideration. We assume that the binding sites of the Ni(II) ion are primarily on the β- and γ-phosphate groups. It is unlikely that the metal ion forms a direct bond with the N_7 atom of the adenine part or with the C_6-NH_2 group, though from a steric point of view this possibility can not be excluded. On the basis of ^{1}H-NMR investigations some authors [12] consider possible the formation of an outer sphere complex [Ni—HOH···N_7].

In this case, with the linkage of a further three H_2O molecules the Ni(II) ion becomes six-coordinated, having a NiO_6 microsymmetry. This is the conformation which is mostly in accordance with the experimental data. Therefore, as regards the possible structures I and II, we prefer the latter.

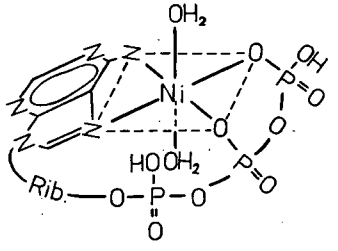

I.

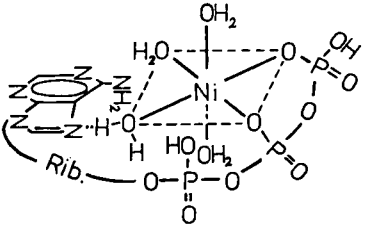

II.

Japanese authors [13] suggest that the binding of metal ion on the phosphate chain is the likeliest, based on LCAO calculations. This is supported by the facts that for a given metal ion the stability constants increase in the sequence AMP< <ADP<ATP, and for ATP, CTP and ITP these constants remain the same within experimental error, indicating the unimportant role of the ring. It is worth mentioning that the calculated stability constants values are of the same order as is characteristic of M-O systems, but are considerably lower than the values calculated for M-N, O systems [14, 15].

* * *

The authors are indebted to CHINOIN Pharmaceutical and Chemical Works for financial support.

References

[1] *Császár, J. and L. Kiss:* Acta Chim. Hung. (Budapest) in press.
[2] *Kiss, L. and J. Császár:* Acta Chim. Hung. (Budapest) in press.
[3] *Phillips, R. S. J.:* Chem. Rew. **66**, 501 (1966).
[4] *Izatt, R. M., J. J. Christensen and J. G. Rytting:* Chem. Rev. **71**, 439 (1971).
[5] *Weser, U., M. Doemnicke:* Z. Naturforschg. **25**, 592 (1970).
[6] *Swift, T. J. et al.:* Biochemistry **10**, 843 (1971).
[7] *Bhattacharyya, R. G. and J. Bhaduri:* J. Inorg. Nucl. Chem. **40**, 733 (1978).
[8] *Taqui-Khan, M. M., A. E. Martell:* J. Amer. Chem. Soc. **66**, 10 (1962).
[9] *Ballhausen, C. J.:* Introduction to Ligand Field Theory, McGraw-Hill, London, 1962.
[10] *Jørgensen, C. K.:* Absorption Spectra and Chemical Bonding in Complexes, Pergamon, New York, 1962.
[11] *Schläfer, H. L., G. Gliemann:* Einführung in die Ligandenfeldtheorie, Akad. Verlag, Frankfurt/Main, 1967.
[12] *Glassman, T. A., C. Cooper, L. W. Harrison and T. J. Swift:* Biochemistry **10**, 843 (1971).
[13] *Fukui, K., A. Imamura and C. Nagata:* Bull. Chem. Soc. Japan **36**, 1450 (1963).
[14] *Britzinger, H.:* Helv. Chim. Acta **44**, 935 (1961).
[15] *Tu, A. T. and M. J. Heller:* Metal ions in biological systems, Vol. 1., p. 1., Ed.: H. Siegel, Marcel Dekker Inc. New York, 1974.

ИССЛЕДОВАНИЕ СИСТЕМ НУКЛЕОТИДЫ-ИОНЫ МЕТАЛЛОВ, III ИЗУЧЕНИЕ СИСТЕМЫ АТП—Ni(II)

Й. Часар и Л. Киш

Синтетизирован комплекс АТП—5′ (АТР) с Ni(II) состава $NiCl_2.ATPH_211\,H_2O$. Изучены спектроскопические и электрохимические свойства соединений и сделаны заключения относительно строения координационной структуры, основываясь на том, что Ni(II) ионы в растворах связаны с β- и γ-фосфатными группами и образуются деформированные октаэдрические микросимметрии группы NiO_6.

BATHOCHROME BANDENVERSCHIEBUNG UND HOHE REVERSIBILITÄT BEI PHOTOCHEMISCHER TRANS-CIS-ISOMERISIERUNG VON β-ARYL-SUBSTITUIERTEN DIPHENYLPHOSPHINYL- UND DIPHENYLTHIOPHOSPHINYL-TRANS-ETHYLENEN*

Von

D. GLOYNA und K.-G. BERNDT

Humboldt Universität Berlin, Sektion Chemie
WB Organische Chemie, DDR-104 Berlin, DDR

(Eingegangen am 27, August 1980)

Die monochromatische Bestrahlung der Titelverbindungen in verdünnter Lösung führt in kinetisch einheitlicher Reaktion zu photostationären Zuständen (photochemische $A \rightleftharpoons B$-Gleichgewichte), die sich reversibel durch Änderung der Bestrahlungswellenlänge ineinander überführen lassen. Es wurden bis zu 1000 reversible Zustandsänderungen bestimmt. Die thermische Rückreaktion $A \leftarrow B$ ist bei Raumtemperatur nicht meßbar. Die bei der Bestrahlung der Titelverbindungen beobachtete bathochrome Verschiebung der längstwelligen Absorptionsbande wird auf sterische und elektronische Wechselwirkung der Phosphor-Gruppierung mit dem Styren-Gerüst zurückgeführt.

Die präparative Zugänglichkeit von β-aryl-substituierten trans-Ethylen-diphenylphosphinoxiden **1** [1, 2] und -diphenylphosphinsulfiden **2** [3] wurde in jüngster Zeit durch Aldehyd-Olefinierungen nach HORNER unter Verwendung unsymmetrisch P-substituierter Methylen-bis-P(X)-Verbindungen (X=O, S) so verbessert, daß nunmehr eine gezielte Untersuchung der Eigenschaften dieser Substanzklassen vom Standpunkt der systematischen Abwandlung der Struktur möglich wird. Zum photochemischen Reaktionsverhalten dieser Substanzklassen finden sich unseres Wissens bisher keine Angaben. Es wird bei **1** und **2** in verdünnter flüssiger und fester Lösung [4] entsprechend der Struktur der Verbindungen durch eine reversible *trans-cis*-Isomerisierung geprägt. In dieser Arbeit berichten wir über die photochemische *trans-cis*-Isomerisierung der ω-Diphenylphosphinyl-*trans*-styrene **1a**—**1e** sowie des β-(3-Indolyl)-*trans*-ethylen-diphenylphosphinoxids **1f** in verdünnter flüssiger Lösung.

	a	b	c	d	e	f
R	C_6H_5	4—$N(CH_3)_2$—C_6H_4	4—OCH_3—C_6H_4	4—Cl—C_6H_4	4—CN—C_6H_4	3—Indolyl

* 23. Mitteilung über Darstellung und Eigenschaften von aryl-substituierten Ethylenen.

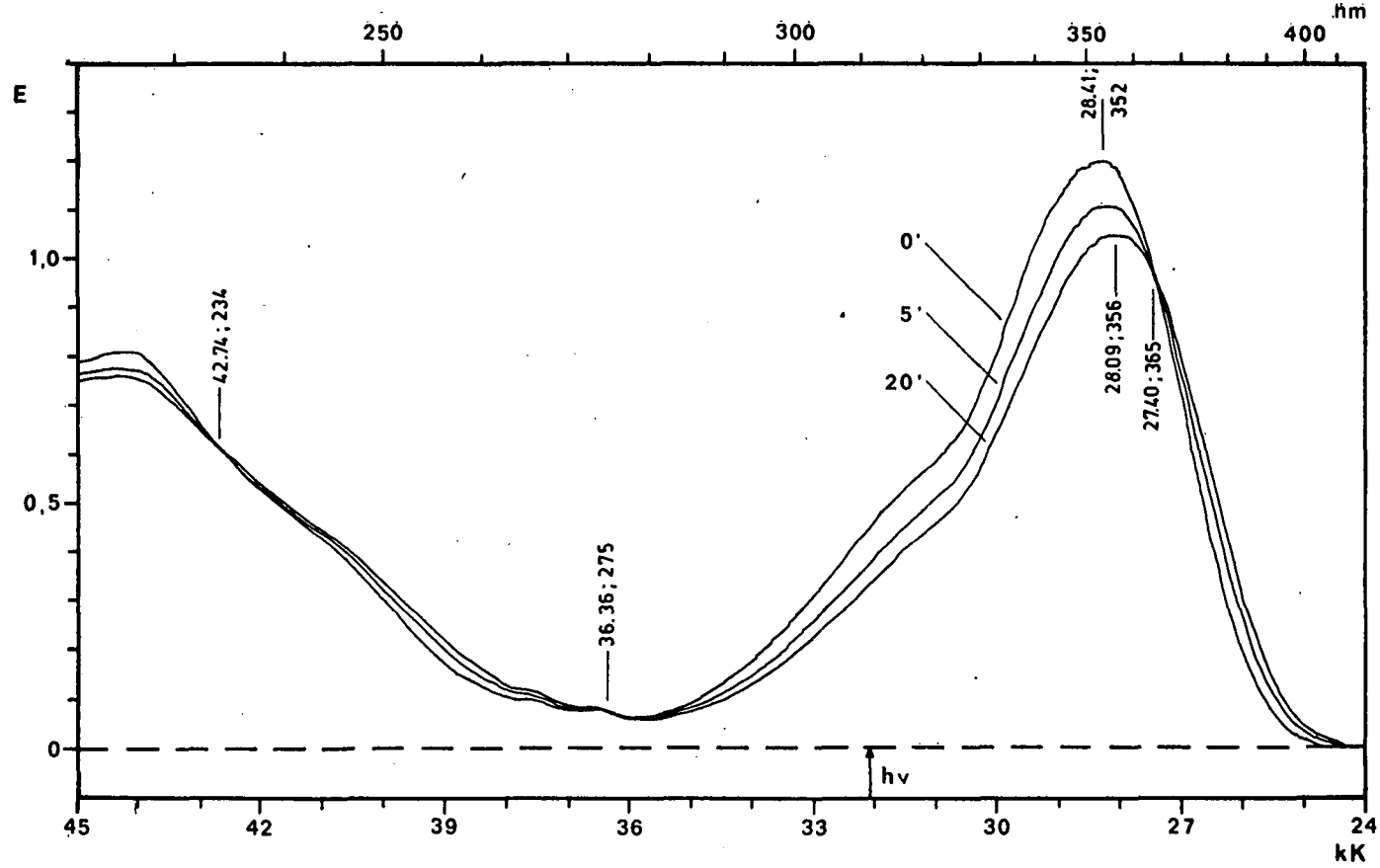

Abb. 1. Spektrale Änderungen für 4-Dimethylamino-ω-diphenylphosphinyl-*trans*-styren **1b** in 95-proz. Ethanol bei Bestrahlung mit 312 nm bis zum Erreichen des photostationären Zustandes (nach 20 Min.) bei 20 °C; $c_A = 3{,}7 \cdot 10^{-5}$ mol/l

Wie wir fanden, bedingt die stereo-elektronische Wechselwirkung der stark elektronenziehenden, raumerfüllenden P(O)-Gruppe mit dem Aryl-ethylen-Gerüst einige Besonderheiten im Vergleich zu ähnlich strukturierten Ethylenen oder zu Stilbenen. Monochromatische Bestrahlung von **1** im Bereich der längstwelligen Absorptionsbande führt nämlich überraschenderweise zu einer bathochromen Verschiebung dieser Bande, verbunden mit einer Extinktionsverminderung (siehe Abb. 1 und 2). Dabei scheint der Betrag dieser Verschiebung bei **1a**—**1e** von der Natur des 4-ständigen Substituenten im Styren-Gerüst abzuhängen sowie auch vom ω-ständigen Akzeptorsubstituenten, wie erste analoge Versuche mit **2** zeigten. Weitere Versuche dazu sind im Gange. Die beobachtete bathochrome Verschiebung ist am größten bei Donator-Akzeptor-Substitution, also bei **1b**. Bei *trans*-Stilbenen beobachtet man dagegen ausnahmslos eine hypsochrome Verschiebung der längstwelligen Absorptionsbande [5] von ca. 10—30 nm, da die *cis*-Stilbene als Photoreaktionsprodukte infolge sterischer Hinderung bei kürzeren Wellen absorbieren. Ausgeprägter ist diese hypsochrome Verschiebung bei Bestrahlung von Thioindigo oder thioindigoiden Verbindungen [6]. Die Erklärung dieser Hypsochromie durch Nichtplanarität [7] der *cis*-Isomeren infolge sterischer Hinderung wird hier auf Grund quantenchemischer Rechnungen neuerdings in Frage gestellt und stattdessen im wesentlichen auf unterschiedliche elektronische Wechselwirkungen der Heteroatome in den planaren *trans*- und *cis*-Isomeren zurückgeführt [8]. ω-Substituierte, mit **1** und **2** formal vergleichbare Styrene zeigen kaum eine Bandenverschiebung beim Übergang in die *cis*-Isomeren. So absorbieren sterisch nicht gehinderte ω-Nitro-*cis*-styrene nur wenig kürzerwellig als die *trans*-Isomeren [9]. Auch das Isomerenpaar des mit **1b** vergleichbaren 4-Dimethylamino-ω-cyano-styrens weist im Bereich der längstwelligen Absorptionsbande nur geringe Unterschiede auf [10]. Allerdings ist „der Schwerpunkt der ersten Absorptionsbande *der* cis-Form eher langwellig als kurzwellig gegenüber der *trans*-Verbindung verschoben", was mit annähernd gleicher Mesomerie infolge annähernd gleicher sterischer Situation in beiden Isomeren erklärt wird [10].

Die bathochrome Bandenverschiebung bei **1** und **2** kann durch starke elektronische Wechselwirkung der Substituenten im Styren-Gerüst und durch sterische Faktoren bedingt sein. Die sterische Hinderung zwischen den 2-ständigen Aromatenprotonen des Styren-Gerüstes und der großen tetraedrisch konfigurierten Diphenylphosphinyl-Gruppe im *cis*-Isomeren kann zur Verdrillung um die Ethylenbindung führen. Es ist bekannt, daß Verdrillung um eine C-C-Doppelbindung eine bathochrome Verschiebung der längstwelligen Absorptionsbande bewirkt [11—13]. Die elektronische Wechselwirkung der Substituenten in **1** und **2** ist besonders stark, wenn R insgesamt Donator-Eigenschaften aufweist (also bei **b**, **c** und **f**), wie unsere absorptions- und emissionsspektroskopischen Messungen zeigen [14]. ^{1}H—NMR-, ^{31}P—NMR- und IR-spektroskopische Untersuchungen ergeben, daß die Elektronendichte bei P(O)-substituierten Styrenen **1** (u. a. **1a**—**1e**) an den Ethylen-C-Atomen und am P-Atom vom 4-ständigen Substituenten im Styren-Gerüst abhängig ist, ebenso die P=O-Valenzschwingung [1, 15]. Dies deutet insgesamt bei Vorliegen eines Donator-Akzeptor-Systems in **1** auf eine alternierende Verteilung der π-Elektronendichte, wie sie für den Polymethin-Zustand im DÄHNEschen Sinne [16, 17] charakteristisch ist. Charakteristisch für den Polymethin-Zustand ist auch eine bathochrome Verschiebung der längstwelligen Absorptionsbande [18] bei monochromatischer Bestrahlung, wie dies bei **1** und **2** beobachtet wird. Aus diesen Befunden

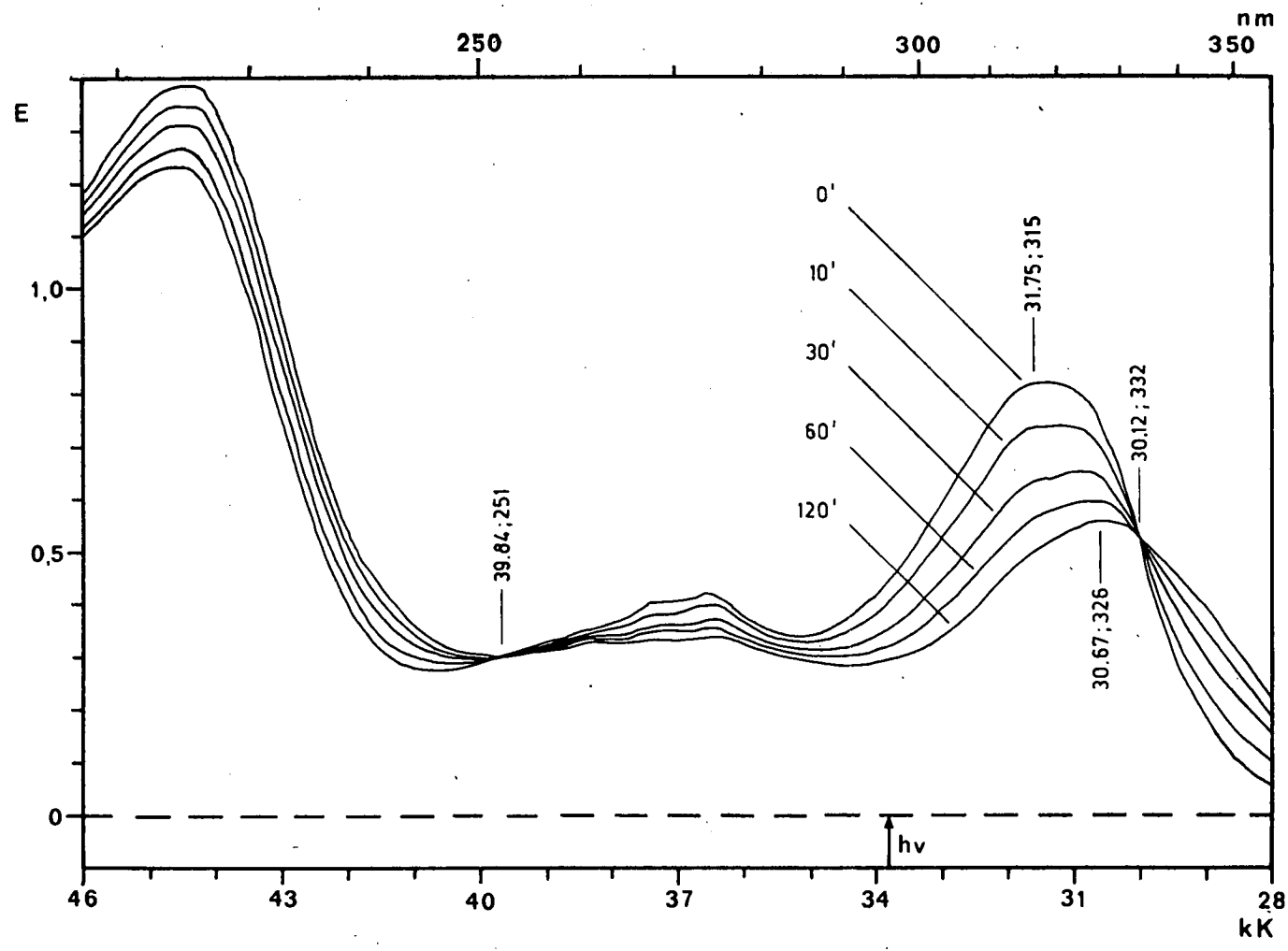

Abb. 2. Spektrale Änderungen für *β*-(3-Indolyl)-*trans*-ethylen-diphenylphosphinoxid **1f** in 95-proz. Ethanol bei Bestrahlung mit 296 nm bis zum Erreichen des photostationären Zustandes (nach 120 Min.) bei 20 °C; $c_A = 3{,}0 \cdot 10^{-5}$ mol/l

leiten wir ab, daß zumindest bei **1** eine polymethinähnliche π-Elektronenstruktur vorliegt. Die starke Wechselwirkung der Substituenten im Falle einer Donator-Akzeptor-Substitution bewirkt in **1** einen gleitenden Übergang der aromatisch-olefinischen Struktur in den besonderen Bindungszustand des Polymethins.

Die monochromatische Bestrahlung von **1** und **2** führt in jedem Fall zu einem photostationären Zustand. Mit Methoden der qualitativen kinetischen Analyse nach MAUSER kann gezeigt werden, daß ein Zwei-Komponenten-System (AB-System) vorliegt. So machen mehrere isosbestische Punkte [19] im Extinktions-Zeit-Diagramm (siehe Abb. 1 und 2) ein AB-System wahrscheinlich, die gefundene Linearität des Extinktionsdifferenzen-Diagramms [20] sowie des Extinktions-Diagramms [21, 22] beweist es im Rahmen der photometrischen Genauigkeit des verwendeten Spektrometers. Bestrahlungen bei verschiedenen Wellenlängen im Bereich der längstwelligen Absorptionsbande ergeben photostationäre Zustände verschiedener quantitativer Zusammensetzung (siehe auch Tab. 1), die sich ineinander über-

Tabelle 1

Maximum der längstwelligen Absorptionsbande λ^{max} von **1** *und* **2** *und der trans-cis-Gemische im photochemischen Gleichgewichtszustand $\lambda^{max}_{tr/cis}$ sowie isosbestische Punkte λ_i in Abhängigkeit von der Bestrahlungswellenlänge λ_{exc} und des Lösungsmittels (LM) bei 20 °C*[a]

	LM	λ_{exc} (nm)	λ^{max} [b] (nm)	$\lambda^{max}_{tr/cis}$ (nm)	λ_i (nm)
1a	Ethanol[c]		265		
		289		268	223, 242, 289
2a	Ethanol[c]		265		
		254		264	224, 243, 300
1b	Ethanol[c]		352		
		312		356	
		365		354	234, 275, 364
	Benzen		344		
		313		353	
		365		349	282, 354
	n-Heptan		335		
		313		340	
		365		335	286, 340
2b	n-Propanol		352		
		320		356	366
1c	Ethanol[c]		287		
		302		297	231, 252, 315
1d	Ethanol[c]		272		
		254		275	
		280		273	227, 246
	n-Heptan		269		
		254		275	
		280		273	225, 244, 284
1f	Ethanol[c]		315		
		296		326	
		312		323	251, 332
		334		321	
		365		317	

[a] Genauigkeit ±0,5 nm; [b] Mittelwerte aus 3—5 Einzelmessungen gleicher Genauigkeit; [c] 95-prozentig

führen lassen durch Variation der Bestrahlungswellenlänge. Das bedeutet, es liegt ein photoreversibles AB-System vor. Die quantitative Zusammensetzung solcher photochemischer Gleichgewichte wird durch die ZIMMERMAN-Gleichung [23] gegeben.

$$\left(\frac{c_A}{c_B}\right)_{\lambda_{exc}} = \left(\frac{\varphi_A}{\varphi_B}\right)_{\lambda_{exc}} \left(\frac{\varepsilon_B}{\varepsilon_A}\right)_{\lambda_{exc}}$$

mit c_A, c_B = Konzentration von A bzw. B im photostationären Zustand, der durch Bestrahlung bei der Wellenlänge λ_{exc} erreicht wird

φ_A = Quantenausbeute für $A \rightarrow B$
φ_B = Quantenausbeute für $B \rightarrow A$
ε_A, ε_B = Extinktionskoeffizient von A bzw. B bei λ_{exc}

Es reichert sich die Substanz eines AB-Systems im photochemischen Gleichgewicht an, die bei der verwendeten Bestrahlungswellenlänge am wenigsten absorbiert. Die quantitative Analyse der photochemischen Gleichgewichte bei **1** und **2** wird später gegeben. Der nur geringe Anteil von Nebenreaktionen bei der photoreversiblen $A \rightleftarrows B$-Umwandlung von **1** und **2** bedingt eine relativ hohe Zyklenzahl[1], z. B. bei **1b** von ca. 1000 und bei **1f** von ca. 300 Zyklen in Ethanol bei Anregung mit 312 nm und 365 nm. Bei den bestrahlten Lösungen wurden nach 5tägigem Stehen im Dunkeln keine spektralen Veränderungen gemessen. Das thermodynamische Gleichgewicht ist bei Raumtemperatur „eingefroren", d. h. die thermische Rückreaktion $B \rightarrow A$ bei Raumtemperatur sehr langsam.

Eine Bestrahlung von **1a** im präparativen Maßstab in Ethanol bei 280 nm, die bis zur Erreichung des photochemischen Gleichgewichtes durchgeführt wurde, lieferte schließlich den Beweis, daß es sich bei dem AB-System tatsächlich um *trans-cis*-Isomere handelt. Die ^{1}H—NMR-Analyse des isolierten Photoreaktionsgemisches ergab ein *trans-cis*-Gemisch [4], aus dem sich chromatographisch das reine *cis*-Isomere abtrennen ließ. Es ist mit authentischem Material identisch, wie die Tabelle 2 zeigt.

Tabelle II

Schmelzpunkt, Molpeak (70 eV) und UV-Spektrum von ω-Diphenylphosphinyl-trans-styren **1a** *und dessen Photoreaktionsprodukt*

	Schmp. (°C)	M$^+$ (*m/e*)	*UV* (95-proz. Ethanol) λ^{max} (nm)	ε^{max} (1 mol^{-1} cm^{-1})
1a, trans	165 165—167 [24]	304	265	25 900
cis- **1a**	103 103—104 [25]	304	269[a]	19 500[a]

[a] Mittelwert aus 3 Messungen gleicher Genaugkeit

[1] Hierunter verstehen wir die Anzahl der reversiblen Umwandlungen zweier photostationärer Zustände ineinander bis zur Verminderung der Extinktion auf die Hälfte des ursprünglichen Wertes.

Am isolierten Reaktionsgemisch konnten dünnschichtchromatographisch keine Hinweise auf Spaltung der P—C-Bindung als Nebenreaktion während der Bestrahlung erhalten werden, obwohl die eingestrahlte Energie bei 280 nm (427 kJ mol^{-1}) beträchtlich die Dissoziationsenergie der P—$C_{aromat.}$-Bindung (293 kJ mol^{-1} [26]) übertrifft.

Experimenteller Teil

Die präparative Darstellung der Verbindungen ist in [1] beschrieben. Die UV-Spektren wurden mit dem Gerät Specord UV/VIS (Fa. VEB Carl Zeiss Jena) aufgenommen, die Massenspektren mit dem Gerät MAT CH—6 (Fa. Varian). Die Bestrahlungen wurden in Küvetten (d=1,000 cm) an $2 \cdot 10^{-5}$ bis $4 \cdot 10^{-5}$ molaren luftgesättigten Proben bei Raumtemperatur in einer Eigenbau-Apparatur mit stabilisiertem Hg-Höchstdruckbrenner bzw. Xenon-Höchstdruckbrenner (Fa. VEB Narva Berlin) durchgeführt. Zur Aussonderung der angegebenen Wellenlängen diente ein Hochleistungsmonochromator (Fa. Bausch & Lomb Inc. Rochester). Die Halbbandbreite des Anregungslichtes betrug 6 nm. Bei der Bestrahlung von **1a** im präparativen Maßstab wurde ein Metallinterferenzfilter (Fa. VEB Carl Zeiss Jena) mit einer Halbbandbreite von 20 nm verwendet. Die Probenkonzentration betrug in diesem Fall $5 \cdot 10^{-3}$ mol l^{-1}.

Die Zyklenzahl wurde extrapoliert aus ca. 20 Messungen bei Annahme eines linearen Abfalls der Extinktion mit zunehmender Anzahl von AB-Umwandlungen.

Die Dünnschichtchromatographie des Photoreaktionsproduktes von **1a** wurde mit nichtaktivierten Kieselgel-Platten (Fa. Merck Darmstadt) nach der üblichen Methode durchgeführt. Schichtdicke: 0,25 mm; Laufmittel: Benzen/Aceton (8:2); Entwickler: zuerst J_2 in CCl_4, danach 0,1 m KJ in verdünnter H_2SO_4.

* * *

Wir danken Herrn Prof. Dr. Henning für Unterstützung bei der Durchführung dieser Arbeit, Herrn Dr. sc. Grupe für die Aufnahme zweier Massenspektren.

Literatur

[1] *Gloyna, D., K.-G. Berndt, H. Köppel und H.-G. Henning:* J. Prakt. Chem. **318,** 327 (1976).
[2] *Gloyna, D., K.-G. Berndt, H. Köppel und H.-G. Henning:* J. Prakt. Chem. **319,** 451 (1977).
[3] *Gloyna, D.:* in Vorbereitung.
[4] *Berndt, K.-G.:* Diplomarbeit, Humboldt-Universität Berlin, 1973.
[5] *Schulte-Frohlinde, D., H. Blume und H. Güsten:* J. Phys. Chem. **66,** 2486 (1962).
[6] *Wyman, G. M.:* Chem. Comm. **1971,** 1332.
[7] *Wyman, G. M., B. M. Zarnegar:* J. Phys. Chem. **77,** 831 (1973).
[8] *Sühnel, J., K. Gustav, R. Paetzold und J. Fabian:* Z. Physik. Chem. (Leipzig) **259,** 17 (1978).
[9] *Miller, D. B., P. W. Flanagan und H. Shechter:* J. Org. Chem. **41,** 2112 (1976).
[10] *Lippert, E., W. Lüder:* Z. Physik. Chem. (Frankfurt/M.) **33,** 60 (1962).
[11] *Jaffé, H. H., M. Orchin:* J. Chem. Soc. **1960,** 1078.
[12] *Lüttke, W., M. Klessinger:* Chem. Ber. **97,** 2342 (1964).
[13] *Momicchioli, F., I. Baraldi und M. C. Bruni:* Faraday Trans. II. **68,** 1556 (1972).
[14] *Berndt, K.-G., D. Gloyna:* in Vorbereitung.
[15] *Schleinitz, K. D., H. Köppel, M. Siegmund, D. Gloyna und L. Alder:* Poster on International Conference on Phosphorus Chemistry, Halle 1979; Abstracts of Papers II, Nr. 160, p. 290

[16] *Dähne, S.:* Z. Chem. **5**, 441 (1965).
[17] *Dähne, S., D. Leupold:* Angew. Chem. **78**, 1029 (1966).
[18] *Baumgärtner, F., E. Günther, G. Scheibe:* Ber. d. Bunsenges. **60**, 570 (1956).
[19] *Mauser, H.:* Z. Naturforsch. **23b**, 1021 (1968).
[20] *Mauser, H.:* Z. Naturforsch. **23b**, 1025 (1968).
[21] *Mauser, H., H.-J. Niemann, R. Kretschmer:* Z. Naturforsch. **27b**, 1349 (1972).
[22] *Mauser, H., V. Starrock, H.-J. Niemann:* Z. Naturforsch. **27b**, 1354 (1972).
[23] *Zimmerman, G., L. Chow, U. Paik:* J. Amer. Chem. Soc. **80**, 3528 (1958).
[24] *Kabačnik, M. I., T. J. Medved, E. I. Matrosov:* Doklady Akad. Nauk SSSR **162**, 339 (1965).
[25] *Aguiar, A. M., D. Daigle:* J. Org. Chem. **30**, 3527 (1965).
[26] *Hartley, S. B., W. S. Holmes, J. K. Jacques, M. F. Mole und J. C. Coubrey:* Quart. Rev. **17**, 204 (1963).

БАТОХРОМНЫЙ СДВИГ ПОЛОС И ВЫСОКАЯ ОБРАТИМОСТЬ РЕАКЦИИ ПРИ ФОТОХИМИЧЕСКОЙ ТРАНС-ЦИС ИЗОМЕРИЗАЦИИ β-АРИЛЗАМЕЩЕННЫХ ТРАНС ДИФЕНИЛФОСФИНИЛ И ДИФЕНИЛТИОФОСФИНИЛ ЭТИЛЕНОВ

Д. Глойна и К. Г. Берндт

Монохроматическое облучение изучаемых соединений в раздавленных растворах приводит к кинетически простой реакции (фотохимическое равнивесие $A \rightleftharpoons B$), которая является обратимой и управляемой изменением длины волны облучающего света. Определено до 1000 изменений состояния. Термическая обратная реакция $A \rightarrow B$ при комнатной температуре не может быть определена. Батохромный сдвиг более длинноволновых полос поглощения объясняется стерическим и электронным взаимодействием фосфоривых групп со стирольным скелетом.

CHEMISTRY OF 1,3-BIFUNCTIONAL COMPOUNDS, XXIII.* AMINOALKYL ESTERS OF XANTHENE-9-CARBOXYLIC ACID, II.** CHOLINOLYTIC AND BRONCHODILATOR ACTIVITY OF QUATERNARY SALTS OF NEW DIAMINOALKYL-XANTHENE-9-CARBOXYLATES

By

K. FELFÖLDI, M. LASZLAVIK, M. BARTÓK

Department of Organic Chemistry,
József Attila University, 6720 Szeged, Hungary
and

E. KÁRPÁTI

Pharmacological Laboratory
Chemical Works of Gedeon Richter Ltd.,
1475 Budapest P.O.B. 27, Hungary

(Received September 30, 1980)

Quaternary salts of diaminoalkyl esters of xanthene-9-carboxylic acid were synthetized, and their cholinolytic and bronchodilator activities were examined as referred to atropine. The compounds were prepared by quaternization of the esters obtained from the appropriate diaminoalcohol and xanthene-9-carboxylic acid chloride. The connection was studied between the activity and the number of carbon atoms in the substituents. An outstandingly good effect was observed for two compounds.

The quaternary salts of aminoalkyl esters of xanthene-9-carboxylic acid are known to possess ganglion-blocking activity [1]. Some of them (Banthin, Probanthin) also display a strong cholinolytic effect [2]. It has further been reported [3] that the quaternary salts of certain esters of diaminoalcohols exhibit ganglion-blocking and hypotensive activity. Accordingly, we considered that the quaternary salts of diaminoalkyl-xanthene-9-carboxylates too migh well possess cholinolytic activity.

The innervation of the respiratory tract is known to be in part parasympathetic, and in part sympathetic. The parasympathetic innervation is ensured by the vagal nerve. The innervation of the vagus ensures the tonicity of the respiratory tract [4], and transection of the nerve or chemical blocking of the postganglionic efferent pathways results the dilation of the airways. Since the state of the airways is a decisive factor as regards the extent of pulmonary resistance [5], the possibility of influencing the tonicity of the respiratory tract with pharmacons is of primary impor-

* Part XXII: *M. Bartók, K. Felföldi, G. Bozóki—Bartók:* Helv. Chim. Acta: **63**, 2172 (1980)
** Part I: *K. Felföldi, Á. Molnár, M. Bartók:* Acta Chim. (Budapest) **91**, 333 (1976).

tance in respiratory diseases. In asthma, histamine brings about constriction of respiratory tracts directly, but nevertheless the main direction of the effect is a reflex one, and this arises *via* the mediation of the vagal nerve. This is proved by the fact that the asthmatic attacks of dogs can be reduced by cooling of the vagus or by administration of atropine [6]. From the animal-experimental and clinical results it appears that acetylcholine or an enhanced parasympathetic activity plays a decisive role in the pathomechanism of chronic respiratory obstruction. In this case, cholinolytics are more effective than sympathomimetics, they have a longer duration of action, and they are free of side-effects [7]. In asthma, the sympathomimetics are the more effective, but combined administration of the two types of drug, with their different mechanisms of action, results in a greater and more lasting reaction than any one of them alone [8]. For this reason, after determining the cholinolytic activities of our new compounds, we also examined them with regard to bronchodilator activity.

A close correlation was found between the cholinolytic and bronchodilator activities of the new compounds: the two activities vary in parallel. Both effects depend to a large extent on the numbers of carbon atoms in the hydrocarbon chain and in the substituents on the nitrogen atoms (Table III), similarly as was observed for the quaternary salts of aminoalkyl-xanthene-9-carboxalates with simpler structures [9].

In both respects, the highest activity is displayed by **21**. The activity changes are correlated most strongly with the variation in m, the maximum occurring for $m=3$ (see **20**, **21**, **23**, **26**, **27** and **28**). The increase of n from two to three likewise raises the activities (see the pairs **18** and **20**, and **19** and **21**). With the increase of the number of carbon atoms in the substituents R_1 and R_2 ($n=m=3$), the activities vary according to a maximum curve (see **16**, **17**, **21** and **24**). If R_1 and R_2 form a ring with the nitrogen, the activities decrease strongly (see **21** and **25**).

Increase of the number of carbon atoms in the substituent R_3 or the quaternizing alkyl group reduces the activity values (see **21** and **22**, and **21** and **23**).

High activities are similarly to be observed for **29**, which has a slightly different structure.

The esters were prepared by the reaction of the appropriate diaminoalcohol and xanthene-9-carboxylic acid chloride in anhydrous acetone or benzene. After boiling for a short time, the base was obtained in the customary way from the precipitating hydrochloride salt, and was quaternized in a mixture of acetone and methanol. Two methods were used to prepare the diaminoalcohols: reaction of the appropriate diamine with haloalcohol (Method A), or reaction of dialkylamino-alkyl chloride with alkylamino-alcohol (Method B). Different methods were employed to prepare two of the diaminoalcohols **9** and **14** (see Experimental section). The dialkylamino-alkyl chlorides were prepared by known methods [10, 11]. A new methods was used to prepare 3-methyl- and ethylamino-propanol-1.

Experimental

Pharmacology. The pupilla diameter in mice (CFLP) was determined by the method of PULEWKA et al [12]. Various doses of the substances were administered subcutaneously to groups of 10 animals. The peak pupilla dilations were averaged and plotted against log dose. The relative potencies were calculated from dose-response curves.

The antispasmodic effects were examined on isolated guinea-pig ileum by the method of MAGNUS [13]. Acetylcholine (ACh) was employed as agonist. The examination materials were tested on 10 preparations per dose, and the relative potencies were calculated from the ED_{50} values [14].

Isolated, intact guines-pig trachea was prepared according to the method of FARMER and COLEMAN [15]. The trachea was stimulated by square-wave pulse of supramaximal voltage and 1 msec duration, repeated for 5 sec with a frequency of 20 Hz in each minute. Cumulative dose-response curves were plotted from the inhibition of the rise in intraluminal pressure. For each substance 10 preparations were used. The relative potencies were calculated from the pA_2 values [16].

The bronchial resistance of guinea-pigs was measured on the basis of the method of KONZETT and RÖSSLER [17, 18]. The inhibition of the bronchostriction induced with intravenous ACh injections was plotted against log dose. The relative potencies

Table I

Physical constants of

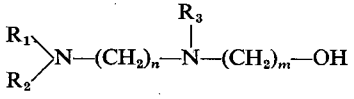

Compd.	R_1	R_2	R_3	n	m	Formula	B. p. °C (Hgmm)	n_D^{20}	Yield	Method
1[a]	CH_3	CH_3	CH_3	2	2	$C_7H_{18}N_2O$	85—88 (30)	1.4555	44	A
2	CH_3	CH_3	CH_3	3	3	$C_9H_{22}N_2O$	88—97 (7)	1.4612	43	A
3	C_2H_5	CH_3	CH_3	3	3	$C_{10}H_{24}N_2O$	118—120 (25)	1.4585	38	A
4[b]	C_2H_5	C_2H_5	CH_3	2	2	$C_9H_{22}N_2O$	136—138 (30)	1.4585	84	A
5	C_2H_5	C_2H_5	CH_3	2	3	$C_{10}H_{24}N_2O$	142—144 (30)	—	72	A
6	C_2H_5	C_2H_5	CH_3	3	2	$C_{10}H_{24}N_2O$	124—126 (8)	—	77	B
7	C_2H_5	C_2H_5	CH_3	3	3	$C_{11}H_{26}N_2O$	145—146 (15)	1.4608	74	B
8	C_2H_5	C_2H_5	C_2H_5	3	3	$C_{12}H_{28}N_2O$	118—120 (6)	1.4636	48	A
9	C_2H_5	C_2H_5	CH_3	3	4	$C_{12}H_{28}N_2O$	123—125 (4)	1.4614	42	—
10	C_2H_5	C_2H_5	CH_3	3	5	$C_{13}H_{30}N_2O$	125—127 (3)	1.4645	68	B
11	C_3H_7	C_3H_7	CH_3	3	3	$C_{13}H_{30}N_2O$	111—112 (3)	1.4696	75	A
12	$-(CH_2)_4-$		CH_3	3	2	$C_{10}H_{22}N_2O$	147—150 (30)	—	62	A
13	$-(CH_2)_4-$		CH_3	3	3	$C_{11}H_{24}N_2O$	157—160 (30)	—	42	A
14	X[c]	CH_3	CH_3	3	3	$C_{11}H_{26}N_2O_2$	150—154 (2)	1.4793	51	—

[a] Lit. [20] b.p. 52 °C (1 Hgmm), n_D^{20}: 1.4550
[b] Lit. [20] b.p. 96 °C (7 Hgmm), n_D^{20}: 1.4580
[c] X: 3-hydroxypropyl-1

Table II

Physical constants of dimethoiodide quaternary salt of

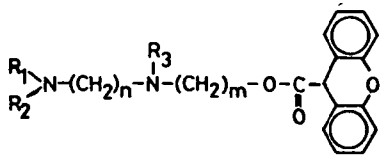

Compd.	R_1	R_2	R_3	*n*	*m*	Formula	Melting point, °C
15	CH_3	CH_3	CH_3	2	2	$C_{23}H_{32}I_2N_2O_3$	217—218
16	CH_3	CH_3	CH_3	3	3	$C_{25}H_{36}I_2N_2O_3$	193—195
17	CH_3	C_2H_5	CH_3	3	3	$C_{26}H_{38}I_2N_2O_3$	176—178
18	C_2H_5	C_2H_5	CH_3	2	2	$C_{25}H_{36}I_2N_2O_3$	199—200
19	C_2H_5	C_2H_5	CH_3	2	3	$C_{26}H_{38}I_2N_2O_3$	186—188
20	C_2H_5	C_2H_5	CH_3	3	2	$C_{26}H_{38}I_2N_2O_3$	189—190
21	C_2H_5	C_2H_5	CH_3	3	3	$C_{27}H_{40}I_2N_2O_3$	156—157
22	C_2H_5	C_2H_5	C_2H_5	3	3	$C_{28}H_{42}I_2N_2O_3$	154—156
23[a]	C_2H_5	C_2H_5	CH_3	3	3	$C_{29}H_{44}I_2N_2O_3$	142—143
24	C_3H_7	C_3H_7	CH_3	3	3	$C_{29}H_{44}I_2N_2O_3$	175—176
25	$-(CH_2)_4-$		CH_3	3	3	$C_{27}H_{38}I_2N_2O_3$	180—181
26	$-(CH_2)_4-$		CH_3	3	2	$C_{26}H_{36}I_2N_2O_3$	218—219
27	C_2H_5	C_2H_5	CH_3	3	4	$C_{28}H_{42}I_2N_2O_3$	149—151
28	C_2H_5	C_2H_5	CH_3	3	5	$C_{29}H_{44}I_2N_2O_3$	143—145
29	X[b]	CH_3	CH_3	3	3	$C_{41}H_{48}I_2N_2O_6$	194—195

[a] Diethoiodide [b] X: 3-(xanthene-9-carbonyloxy)-propyl-1

werecalculated from dose-response curves. For each substance and each dose, 6—9 experiments were performed. The substances were administered intravenously.

Guinea-pigs were placed individually in plexi-glass boxes exposed to an aerosol of a 1% aqueous ACh solution. The time elapsed between the beginning of the aerosol exposure and severe dyspnea in individual animals was recorded as the prostration time, a prolongation of which was considered indicative of bronchodilator activity. The substances were administered subcutaneously, and the maximum enhancement of the prostration time was evaluated as percentage inhibition compared to the control group. The relative potency was calculated from the dose-response curves. A total of 12 animals were used per dose.

Table III

Pharmacological properties of quaternary salts

Compd.	Cholinolytic activity[a]		Bronchodilator activity[a]		
	Pupil size	ACh-induced contraction of ileum	Isolated trachea	Bronchial resistance	ACh-induced prostration
15	0.52	0.04	0.05	0.02	0.09
16	42	3.1	11	35	42
17	95	7.2	17	57	61
18	0.31	0.05	0.01	0.03	0.08
19	2.9	0.31	0.12	0.21	6.2
20	3.7	0.29	0.21	0.17	7.1
21	311	25	60	270	214
22	45	2.9	9.6	17	44
23	101	6.2	12.3	65	63
24	15	1.5	5.7	19	11
25	89	5.6	15	34	57
26	4.2	0.36	0.17	0.09	7.3
27	27	1.8	0.97	22	15
28	0.62	0.07	0.05	0.05	0.08
29	305	107	50	157	131

[a] Atropine = 100

Chemistry. Constants relating to the diaminoalcohols and quaternary salts prepared are listed in Tables I and II. The melting and boiling point values are not corrected. The tlc examinations were made on Kieselgel HF (Merck) plates, with ethanol-diethylamine (96:4, v/v) as solvent mixture, and the Draggendorf reagent as developer. The quaternary salts were recrystallized from aqueous ethanol, the yield being in general 40—60%. The C, H and N analyses were within 0.4% of the theoretical for all compounds.

3-Methylamino-propanol-1

A solution of 3-chloro-propanol-1 (71 g, 0.75 mole) and methylamine (62 g, 2 mole) in EtOH (400 ml) was shaken for 15 hr at 130 °C in an autoclave. After cooling, the EtOH was distilled off and the residue was dissolved in concentrated aqueous KOH solution. The organic phase was separated, dried and distilled. Yield

37 g (55%), b.p. 95—100 °C (30 Hgmm), n_D^{20}: 1.4450; lit. [19] b.p. 175—177 °C (750 Hgmm), n_D^{20}: 1.4479.
3-Ethylamino-propanol-1 was prepared in an analogous manner. Yield 48%, b.p. 96—98 °C (30 Hgmm), n_D^{20}: 1.4452; lit. [19] b.p. 184—187 °C (750 Hgmm), n_D^{22}: 1.4475.

Method A. 3-[N-Methyl-N-(3-dipropylamino-propyl)]-amino-propanol-1 (**11**)

3-Methylamino-propanol-1 (17 g, 0.19 mole), 3-dipropylamino-propyl-chloride (34.4 g, 0.2 mole) and anhydrous K_2CO_3 (35 g) were stirred in EtOH (150 ml) during boiling for 15 hr. After filtration of the cooled reaction mixture, the filtrate was evaporated and the residue was distilled. Yield 35 g (75%).

Method B. 3-[N-Methyl-N-(3-diethylamino-propyl)]-amino-propanol-1 (**7**)

N,N-Diethyl-*N'*-methyl-propane-1,3-diamine (Fluka) (16.6 g, 0.115 mole), 3-chloropropanol-1 (11 g, 0.116 mole) and anhydrous K_2CO_3 (15 g) were stirred in EtOH (75 ml) during boiling for 15 hr. The mixture was worked up as in Method A. Yield 17.2 g (74%).

N,N'-Dimethyl-N,N'-bis(3-hydroxypropyl)-propane-1,3-diamine (**14**)

A solution of 3-methylaminopropanol-1 (8.9 g, 0.1 mole) in EtOH (40 ml) was added dropwise with stirring to a mixture of 1,3-dibromopropane (10.1 g, 0.05 mole) and anhydrous K_2CO_3 (15 g) in EtOH (75 ml), and the reaction mixture was then boiled for 15 hr. After filtration, the filtrate was evaporated and the residue was distilled. Yield 5.5 g (51%), m.p. of dihydrochloride 144—146 °C.

4-[N-Methyl-N-(3-diethylamino-propyl)]-aminobutanol-1 (**9**)

A mixture of *N,N*-diethyl-*N'*-methylpropane-*1,3*-diamine (20.2 g, 0.14 mole) and butyrolactone (12 g) was heated at 100° for 24 hr. The reaction product was dissolved in abs. Et_2O (100 ml), the solution was added with stirring and cooling to a solution of $Li[AlH_4]$ (4.7 g, 0.12 mole) in Et_2O (100 ml), and the reaction mixture was then boiled for 6 hr. With cooling and stirring, 9 ml water and then 9 ml 65% NaOH solution were added dropwise to the reaction mixture. The Et_2O solution was evaporated and the residue was distilled. Yield 12.6 g (42%).

3-[N-Methyl-N-(3-diethylamino-propyl)]-amino-propyl-xanthene-9-carboxylate dihydrochloride and dimethoiodide (**21**)

A solution of diaminoalcohol **7** (5.2 g, 0.025 mole) in Me_2CO (20 ml) was added dropwise with stirring and cooling to a solution of xanthene-9-carboxylic acid chloride (6.4 g, 0.026 mole) in Me_2CO (40 ml), and the reaction mixture was

then boiled for 20 min. An EtOH—HCl solution was added to the still hot mixture, and after cooling the precipitated dihydrochloride salt was filtered off and recrystallized from EtOH. Yield 9.6 g (80%), m.p. of dihydrochloride salt 195—196 °C.

The dihydrochloride salt (4.8 g, 0.01 mole) was dissolved in cold NaOH solution. After Et_2O extraction, the Et_2O solution was dried and evaporated. The residue was dissolved in Me_2CO (40 ml), MeI (3 g) was added, and the mixture was boiled for 20 min and then cooled. The dimethoiodide (**21**) which separated out was filtered off and recrystallized from EtOH. Yield 5 g (72%).

References

[1] *Cusic, J. W., R. A. Robinson:* J. Org. Chem. **16**, 1921 (1951).
[2] *Johnson, E. A., D. R. Wood:* Brit. J. Pharmacol. **9**, 218 (1954).
[3] *Adamson, D. W., J. W. Billinghurit:* Nature **177**, 523 (1956).
[4] *Nadel, J. A., J. G. Widdicombe:* Ann. N.Y. Acad. Sci. **109**, 712 (1963).
[5] *Macklem, P. T., J. Mead:* J. Appl. Physiol. **22**, 395 (1967).
[6] *Gold, W. M., P.Y.C.Yu.:* J. Appl. Physiol. **33**, 719 (1972).
[7] *Poppius, H., Y. Salorinne:* Brit. med. J. **4**, 134 (1973).
[8] *Petrie, G. R., K. N. V. Palmer:* Brit. med. J. **1**, 430 (1969).
[9] *Nádor, K.:* Progress in Drug Research (Birkhäuser Verlag), **2**, 323 (1960).
[10] *Gilman, H., D. A. Shirley:* J. Am. Chem. Soc. **66**, 1889 (1944).
[11] *Leonard, F., L. Simet:* J. Am. Chem. Soc. **77**, 2857 (1955).
[12] *Pulewka, P.:* Arch. exp. Path. Pharmak. **168**, 307 (1932).
[13] *Magnus, R.:* Pflüer's Arch. **102**, 123 (1904).
[14] *Litchfield, J. T., F. Wilcoxon:* J. Pharmacol. exp. Therap. **96**, 99 (1949).
[15] *Farmer, J. B., R. A. Coleman:* J. Phar. Pharmac. **22**, 461 (1970).
[16] *Arunlakshama, O., H. O. Schild:* Brit. J. Pharmac. Chemother. **14**, 48 (1959).
[17] *Konzett, H., R. Rössler:* Arch. exp. Path. Pharmak., **195**, 71 (1940).
[18] *Gardner, D. G.:* Brit. J. Pharmac. Chemother. **41**, 128 (1971).
[19] *Schlögl, K., R. Schlögl:* Monatsh. **95**, 922 (1964).
[20] *Korsunov, M. A., P. H. Bodnaryuk:* Zh. Org. Khim. **5**, 1947 (1969).

ХИМИЯ 1,3-БИФУНКЦИОНАЛЬНЫХ СОЕДИНЕНИЙ, XXIII. АМИНОАЛКИЛЬНЫЕ ЭФИРЫ КСАНТЕНО-9-КАРБОКСИЛЬНЫХ КИСЛОТ, II. ХОЛИНОЛИТИЧЕСКАЯ И БРОНХОДИЛАТОРНАЯ АКТИВНОСЬ ЧЕТВЕРТИЧНЫХ СОЛЕЙ НОВЫХ ДИАМИНОАЛКИЛ-КСАНТЕНО-9-КАРБОКСИЛАТОВ

К. Фелфелди, М. Лаславик, М. Барток и Э. Карпати

Синтезированы четвертичные соли диаминоалкильных эфиров ксантено-9-карбоксильных кислот и изучены их холинолитическая и бронходилаторная активность в сравнении с атропином. Соединения были синтезированы при кватернизации эфиров, полученных из соответствующих диаминоспиртов и хлорангидридов ксантено-9-карбоксильных кислот. Изучена связь между активностью действия и числом углеродных атомов в заместителях. Исключительно хороший эффект найден для двух соединений.

CHEMISTRY OF 1,3-BIFUNCTIONAL COMPOUNDS, XXIV* PREPARATION AND PHARMACOLOGY OF CYCLOALKYLAMINOPROPYL TRIMETHOXYBENZOATES

By

K. FELFÖLDI, M. LASZLAVIK, M. BARTÓK

Department of Organic Chemistry,
Attila József University, 6720 Szeged, Hungary
and

E. KÁRPÁTI

Pharmacological Laboratory,
Chemical Works of Gedeon Richter Ltd.,
1475 Budapest P.O.B. 27, Hungary

(Received September 30, 1980)

3,4,5-Trimethoxybenzoate esters of 3-(*N*—R—*N*-cycloalkyl)-aminopropanols were synthetized. The quaternary salts of the esters display considerable pharmacological activity, and in particular a coronary vasodilator effect.

The aminoalcohols and their esters are widely used in therapy. Such compounds are prepared in large numbers from plant extracts and also synthetically. Depending on their structures, they can have many effects, the most important being those on the nervous system, the musculature and the vascular system.

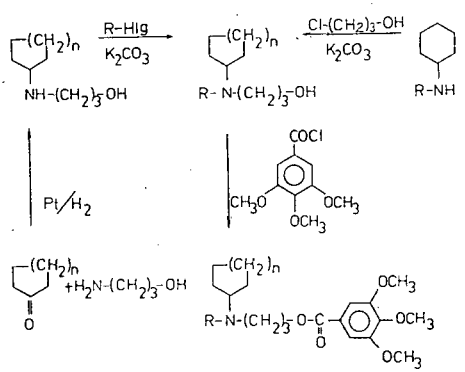

Scheme of the preparation of the esters

* Part XXIII: see reference [3].

We reported earlier [1—3] on the synthesis of piperidino-, morpholino-, heptamethylenimino- and diaminoalkylpropyl esters. The new compounds possess valuable local anaesthetic, coronary vasodilator, cholinolytic and bronchodilator properties. In the present paper an account is given of the synthesis (see the reaction scheme) and pharmacological activities of some 3-(*N*—R—*N*-cycloalkyl)-aminopropyl trimethoxybenzoates. It is known [5] that diphenylpropylaminoalkyl esters with similar structures have coronary vasodilator, spasmolytic and hypotensive effects. The new compounds were subjected to pharmacological examination in the Pharmacological Laboratory of the Chemical Works of Gedeon Richter Ltd. The coronary vasodilator effects were investigated on isolated rat heart [4], and the pharmacological characteristics were compared with those of Persantin (Dipyridamole), previously employed effectively in therapy. The compound exhibiting the most striking properties was 3-[*N*-(3-phenylallyl)-*N*-cyclohexyl]-aminopropyl trimethoxybenzoate HCl (**13a**) (Table I). The flow enhancement indicates the extent of the vasodilation.

Table I
Pharmacological data of the compounds **13a**

Compound	Doses g	Flow enhancement %
Persantin	5	11.8
	50	32.4
13a	5	35.9
	50	64.9

Experimental

The temperatures given in Table II are uncorrected. The purities of substances were checked by thin-layer chromatography too (Kieselgel (Merck) plate, developing solvent: 4% diethylamine—petroleum ether; detecting agent: Draggendorf reagent). Most of the chemicals used were commercial products of Fluka, but some were prepared by known methods. Apart from a few exceptions (see below), the tertiary aminoalcohols were obtained by the reaction of the appropriate 3-cyclo-alkylaminopropanol-1 and alkyl halide. The esters were produced with a yield of 40—70% by the reaction of the aminoalcohol and 3,4,5-trimethoxybenzoyl chloride; the hydrochloride was purified by repeated recrystallization from ethanol. Quaternary salts were prepared by a known method.

3-Cycloheptylaminopropanol-1

0.15 g PtO_2 was prehydrogenated for 1 h at room temperature in 30 ml ethanol, at a hydrogen pressure of 1.5 atm. Next, 30 ml of an ethanolic solution of 33.6 g (0.3 mole) cycloheptanone and 22.5 g (0.3 mole) 3-aminopropanol-1 was added to the catalyst, and hydrogenation was continued for a further 5 h. The catalyst was filtered off, the reaction mixture was evaporated, and the residue was distilled. The product weighed 37.5 g (73% yield), with b.p. 140—142 °C (6 Hgmm), and n_D^{25}: 1.4906.

Similar means were used to prepare 3-cyclopentylaminopropanol-1 (80%), b.p. 192—196 °C (5 Hgmm), n_D^{27}: 1.4883; 3-cyclohexylaminopropanol-1 (65%), m.p. 66—69 °C; and 3-cyclooctylaminopropanol-1 (78%), b.p. 146—148 °C (4 Hgmm), n_D^{22}: 1.4965.

Table II

3-(N-R-substituted-N-cycloalkyl)-aminopropyl-alcohols and their 3,4,5-trimethoxybenzoate esters

No.	c-alkyl	R	B.p. (°C) Hgmm	n_D^{20}	Yield (%)	Salts of trimethoxybenzoat esters			
						Formula	M.p. (°C)	Analysis Calc. C	Analysis Found H
1	c-hexyl	CH_3>CH– CH_3	104—106 4	—	32	$C_{22}H_{36}ClNO_5$	HCl 162—163	61.45 61.41	8.25 4.17
2	c-hexyl	CH_2=CH-CH_2–	114—117 4	—	30	$C_{22}H_{34}ClNO_5$	HCl 118—119	61.74 61.35	8.01 8.03
3a	c-hexyl	CH_3-CH =CH-CH_2–	121—125 5	—	40	$C_{23}H_{36}ClNO_5$	HCl 105—106	62.50 62.18	8.20 7.82
3b	c-hexyl	—"—	121—125 5	—	—	$C_{24}H_{38}INO_5$	CH_3I 129—130	52.65 52.57	6.99 6.63
4	c-hexyl	CH_3-C(Cl)=CH-CH_2–	145—146 5	—	56	$C_{24}H_{37}ClJNO_5$	CH_3I 125—126	49.53 49.42	6.41 6.30
5	c-hexyl	CH≡C-CH_2–	118—120 6	1.4962	40	$C_{22}H_{32}ClNO_5$	HCl 138—139	61.90 61.67	7.57 7.37
6	c-hexyl	CH_3O-CH_2-CH_2–	123—125 6	1.4763	25	$C_{22}H_{36}ClNO_6$	HCl 121—122	59.20 58.90	8.10 7.90
7	c-hexyl	NC-CH_2-CH_2–	168—172 8	1.4887	37	$C_{22}H_{33}ClN_2O_5$	HCl 163—164	59.80 59.78	7.55 7.30
8	c-hexyl	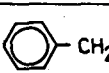 CH_2–	188—192 6	1.5272	67	$C_{26}H_{36}ClNO_5$	HCl 147—148	65.45 65.25	7.40 7.20

9	*c*-hexyl	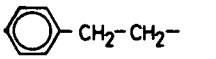	182—185 6	1.5242	50	$C_{28}H_{40}INO_5$	CH_3I 112—114	56.25 55.95	6.75 6.71
10	*c*-hexyl	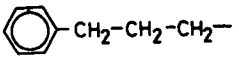	158—160 4	1.5217	52	$C_{29}H_{42}INO_5$	CH_3I 100—101	57.10 56.95	6.92 7.10
11	*c*-hexyl	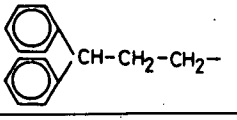	80—81[a]	—	40	$C_{34}H_{44}ClNO_5$	HCl 128—130	70.15 69.95	7.62 8.62
12	*c*-hexyl	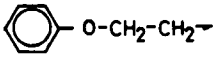	205—210 5	1.5228	41	$C_{27}H_{38}ClNO_6$	HCl 115—116	63.80 64.07	7.54 7.22
13a	*c*-hexyl	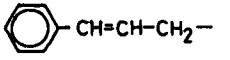	195—196 3	—	70	$C_{28}H_{38}ClNO_5$	HCl 158—159	66.72 66.47	7.60 7.33
13b	*c*-hexyl	—"—	—	—	—	$C_{29}H_{40}INO_5$	CH_3I 148—150	57.14 56.95	6.61 6.81
14	*c*-pentyl	—"—	188—190 5	1.5325	70	$C_{27}H_{36}ClNO_5$	HCl 130—131	66.04 65.85	7.24 7.42
15	*c*-heptyl	—"—	192—196 4	1.5388	65	$C_{29}H_{40}ClNO_5$	HCl 165—166	67.23 66.90	7.78 7.97
16	*c*-octyl	—"—	204—208 3	—	42	$C_{30}H_{42}ClNO_5$	HCl 145—146	67.71 67.44	7.95 8.03
17[b]	*c*-hexyl-methyl	—"—	—	—	—	$C_{30}H_{42}INO_5$	CH_3I 135—136	55.78 55.50	6.79 6.89

[a] Melting point
[b] Aminoalcohol was not isolated

Tertiary aminoalcohol preparation (Standard method)

A mixture of 0.2 mole secondary aminoalcohol, 0.22 mole alkyl halide and 25 g anhydrous potassium carbonate was boiled under stirring for 15 h. After cooling of the reaction mixture, the inorganic salt was filtered off, the filtrate was evaporated, and the residue was distilled.

In the cases of aminoalcohols **1** and **2**, the appropriate secondary amine (Fluka), *i.e.* isopropyl cyclohexyl amine or allyl cyclohexyl amine, was reacted with 3-chloropropanol-1 by the above method.

3-[N-cyclohexyl-N-(2-methoxyethyl)]-aminopropanol-1 (**6**)

29.4 g (0.3 mole) cyclohexanone and 22.5 g (0.3 mole) 2-methoxyethylamine were reacted together under reductive conditions (Pt, H_2), and the 2-methoxyethyl cyclohexyl amine obtained as product was reacted without purification with 3-chloropropanol-1 in the presence of potassium carbonate as above.

3-[N-cyclohexyl-N-(2-cyanoethyl)]-aminopropanol-1 (**7**)

A mixture of 31.2 g (0.2 mole) 3-cyclohexylaminopropanol-1 and 11.7 g (0.22 mole) acrylonitrile was boiled for 2 h, and the resulting product was purified by distillation.

3-Hexahydrobenzylaminopropanol-1

20 ml anhydrous benzene solution of 20 g (0.2 mole) ethyl acrylate was added dropwise at 0 °C under stirring to 25 g (0.22 mole) aminomethylcyclohexane (Fluka), the reaction mixture was then stirred for 2 h at room temperature and subsequently filtered, the filtrate was evaporated, and the residue was distilled. The resulting ethyl β-hexahydrobenzylaminopropionate weighed 30 g (61% yield), with b.p. 164—168 °C (30 Hgmm) and n_D^{25}: 1.4780.

100 ml anhydrous ether solution of 30 g (0.14 mole) ethyl β-hexahydrobenzylaminopropionate was added dropwise under cooling and stirring to 50 ml anhydrous ether solution of 3.2 g (0.085 mole) $Li[AlH_4]$. The reaction mixture was then boiled for 2 h. Next, 6.5 ml water and 6.5 ml 70% sodium hydroxide solution were added under cooling. The ether phase was dried and evaporated, and the residue was distilled. The product weighed 13 g (54%), with b.p. 118—122 °C (2 Hgmm) and m.p. 39—41.5 °C.

The infrared spectra of some esters were recorded. Characteristic bands: $\nu C{=}O$: 1720 cm^{-1}; ester and ether bonding $\nu_{as}C{-}O{-}C$ and $\nu_s C{-}O{-}C$: 1260, 1230, 1130 and 1010 cm^{-1}; $\nu C{=}C$: **2**: 1650 cm^{-1}, **3a, b**: 1680 cm^{-1}, **4**: 1670 cm^{-1}, **13a, b, 15, 16**: 1660 cm^{-1}; $\nu{\equiv}N^+{-}H$: 2500 cm^{-1}; **7**: $\nu C{\equiv}N$: 2290 cm^{-1}; **5**: $\nu{\equiv}C{-}H$: 3300 cm^{-1}, $\nu C{\equiv}C$: 2145 cm^{-1}.

Acknowledgements

The authors wish to express their thanks to Gizella Bartók-Bozóki for performance of the analyses and recording of the infrared spectra, and to Gizella Koródi for assistance in the synthesis work.

References

[1] *Felföldi, K., Á. Molnár, M. Bartók:* Acta Chim. (Budapest) **90**, 75 (1976).
[2] *Felföldi, K., Á. Molnár, M. Bartók:* Acta Chim. (Budapest) **91**, 333 (1976).
[3] *Felföldi, K., M. Laszlavik, M. Bartók, E. Kárpáti:* Acta Phys. et Chem. Szeged, preceding paper.
[4] *Vanremoortere, E.:* Arch. int. Pharmacodyn. **95**, 466 (1953).
[5] *Nakumara, K., K. Hidehiko, A. Jiro:* Ger. Offen. 1 802 656 (1969); C.A. **71**, 123912x (1969).

ХИМИЯ 1,3-БИФУНКЦИОНАЛЬНЫХ СОЕДИНЕНИЙ, XXIV СИНТЕЗ И ФАРМАКОЛОГИЧЕСКОЕ ДЕЙСТВИЕ ЦИКЛОАМИНОПРОПИЛ-ТРИМЕТОКСИБЕНЗОАТОВ

К. Фелфелди, М. Лаславик, М. Барток и Э. Карпати

Синтезированы 3,4,5-триметоксибензоатные эфиры 3-(*N*—R—*N*-циклоалкил)-аминопропанолов. Четвертичные соли эфиров обладают значительной фармакологической активностью, в частности, венечным вазодилятаторным эффектом.

CHEMISTRY OF 1,3-BIFUNCTIONAL COMPOUNDS, XXV* SYNTHESIS OF SOME ESTERS CONTAINING SUBSTITUTED PIPERIDINE AND TETRAHYDROPYRIDINE SKELETONS

By

K. FELFÖLDI, Á. MOLNÁR, M. BARTÓK and R. A. KARAKHANOV

Department of Organic Chemistry,
Attila József University, 6720 Szeged, Hungary

(Received September 30, 1980)

The synthesis and pharmacologic characteristics of 3-piperidinyl esters were reported earlier [1]. The present paper describes the synthesis of 43 esters containing substituted piperidine and tetrahydropyridine skeletons. Most of the new esters display a coronary vasodilator effect.

In this work esters of *N*-substituted-4-piperidinol and various 4-substituted-piperidinyl and tetrahydropyridinylpropyl esters were synthetized. Some *N*-alkyl-4-piperidinyl esters are known to exhibit valuable pharmacological properties, *e.g.* local anaesthetic, reserpine-like, parasympatholytic, hypotensive, ganglion blocker, and central nervous system tranquillizing effects [2—8]. It is similarly known [9] that the 1-(3-aroylpropyl)-4-aryl-1,2,3,6-tetrahydropyridines display analgetic, spasmolytic and central nervous system tranquillizing effects. The new compounds we have prepared were subjected to pharmacological investigation in the Pharmacological Laboratory of the Gedeon Richter Pharmaceutical Works. Mainly the coronary vasodilator effect was found to be significant, particularly in the case of **18**, *N*-(3-methylbutyl)-4-piperidinylxanthene-9-carboxylate.

Experimental

The temperature values given in the Tables have not been corrected. The courses of the reactions and the purities of the end-products were examined by, among others, thin-layer chromatography. Of the compounds used, 4-piperidinol, 4-(pyrrolidinyl-1)-piperidine, 4-(piperidinyl-1)-piperidine and 1,4-dioxa-8-azaspiro [4,5]-decane were Fluka products, while 4-phenyltetrahydropyridine, 4-*p*-chlorophenyltetrahydropyridine and 4-hydroxy-4-*p*-chlorophenylpiperidine were made available by the Gedeon Richter Pharmaceutical Works. The aminoalcohols were prepared by reacting the appropriate secondary amine with alkyl halide or with 3-chloropropyl alcohol [1, 10, 11], and purified by distillation or recrystallization. The *N*-cyanoethyl-4-pipe-

* Part XXIV: see reference [11].

Table I
N-substituted-4-piperidinols

No.	R	B.p. (°C) Hgmm	n_D^{20}	Yield %
1[a]	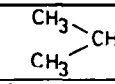	110—114 20	1.4750	58
2	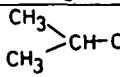	84—86 5	1.4674	62
3	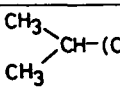	124—126 2	1.4710	75
4	$CH_2=CH-CH_2-$	98—100 8	1.4907	79
5	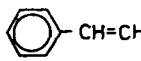	111—113[b]	—	35
6	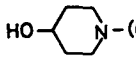	202—204[b]	—	40

[a] Lit. [12]: b.p. 113—114 °C (23 Hgmm)
[b] Melting point

ridinol necessary for the preparation of esters **25** and **26** was obtained by the reaction of acrylonitrile and 4-piperidinol [11]; the reaction product was acylated without further purification. The esters were obtained from the reaction of the appropriate aminoalcohol and acid halide, and purified by recrystallization from ethanol.

References

[1] *Felföldi, K., Á. Molnár, M. Bartók:* Acta Chim. (Budapest) **90**, 75 (1976).
[2] Brit. pat. 899 605 (1962); C. A. **59**, 7497f (1963).
[3] *Renz, J., J. P. Bourquin:* Swiss. pat. 383 777 (1960); C. A. **62**, 7734f (1965).
[4] *Ganellin, C. R., R. G. W. Spickett:* J. Med. Chem. **8**, 619 (1968).
[5] *Biel, J. H.:* U. S. pat. 2 856 407 (1958); C. A. **53**, 5292a (1959).
[6] *Coon, S. B., D. Papa:* J. Org. Chem. **20**, 774 (1955).
[7] *Moffet, R. B.:* J. Med. Chem. **7**, 319 (1964).
[8] *Cusic, J. W.:* U. S. pat. 2 650 230 (1953); C. A. **48**, 11500c (1954).
[9] *Janssen, P. A. J.:* J. Med. Pharm. Chem. **1**, 281 (1959). U. S. pat. 2 973 363 (1961); C. A. **35**, 15514e (1961).
[10] *Felföldi, K., Á. Molnár, M. Bartók:* Acta Chim. Budapest **91**, 333 (1976).
[11] *Felföldi, K., M. Laszlavik, M. Bartók, E. Kárpáti:* Acta Phys. et Chem. Szeged, preceding paper.
[12] *McElvain, S. M., K. Rorig:* J. Am. Chem. Soc. **70**, 1820 (1948).

ХИМИЯ 1,3-БИФУНКЦИОНАЛЬНЫХ СОЕДИНЕНИЙ, XXV СИНТЕЗ НЕКОТОРЫХ ЭФИРОВ, ИМЕЮЩИХ ЗАМЕЩЕННЫЕ ПИПЕРИДИНОВЫЕ И ТЕТРАГИДРОПИРИДИНОВЫЕ СКЕЛЕТЫ

К. Фелфелди, А. Молнар, М. Барток и Р. А. Караханов

В работе описан синтез 43 эфиров, имеющих замещенные пиперидиновые и тетрагидропиридиновые скелеты. Болшинство синтезированных эфиров обладает венечным вазодилятаторным действием.

Table II

Z—CH_2—CH_2—CH_2—OH

No.	Z	B.p. (°C) Hgmm	M.p. (°C)	Yield %	Formula	Analysis Calc./Found		
						C	H	N
7	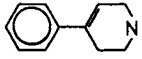	168—172/1	—	75	$C_{14}H_{16}NO$	78.50 78.25	7.52 7.72	6.53 6.82
8	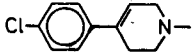	178—184/1	189—190*	65	Methoiodide $C_{13}H_{21}ClINO$	45.76 45.40	5.37 5.39	3.65 3.65
9	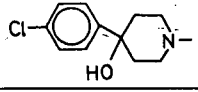	—	106—107 236—238*	74	$C_{14}H_{20}ClNO_2$	62.33 62.12	7.47 7.45	5.19 5.27
10	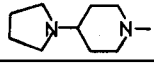	158—160/1.5	57—58	70	$C_{12}H_{24}N_2O$	68.10 67.71	11.30 11.43	13.20 13.60
11	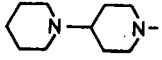	152—154/1	38—40	70	$C_{13}H_{26}N_2O$	69.00 68.87	11.60 11.53	12.37 12.52
12	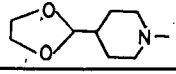	—	84—85	45	$C_{10}H_{19}NO_3$	59.70 59.65	9.53 9.45	6.96 6.72

* Melting point of methioiodide

Table III

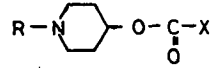

No.	R	X	Formula	M.p. (°C)	Analysis Calcd./Found C	Analysis Calcd./Found H
13	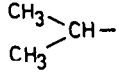	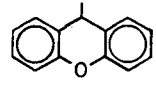	$C_{22}H_{26}ClNO_3$	HCl 147—148	68.12 67.99	6.72 6.32
14	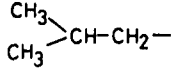	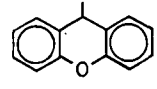	$C_{23}H_{28}ClNO_3$	HCl 194—195	68.73 68.36	7.02 7.04
15	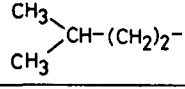	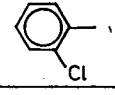	$C_{17}H_{25}Cl_2NO_2$	HCl 176—178	58.96 58.68	7.28 7.48
16	—"—	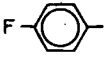	$C_{17}H_{25}ClFNO_2$	HCl 208—210	61.90 61.78	7.64 7.64
17	—"—	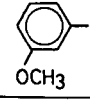	$C_{18}H_{28}ClNO_3$	HCl 177—178	63.24 63.14	8.25 8.43
18	—"—	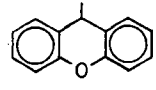	$C_{24}H_{30}ClNO_3$	HCl 206—208	69.30 69.05	7.27 7.41
19	$CH_2=CH-CH_2-$	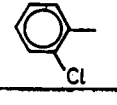	$C_{15}H_{19}Cl_2NO_2$	HCl 160—163	56.97 56.76	6.06 6.06

20	—"—	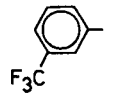	$C_{16}H_{19}ClF_3NO_2$	HCl 140—142	54.94 54.61	5.47 5.57
21	—"—		$C_{16}H_{22}ClNO_3$	HCl 173—175	61.33 61.12	7.11 7.09
22	—"—	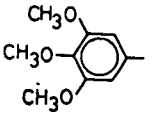	$C_{18}H_{26}ClNO_5$	HCl 199—201	58.17 58.13	7.03 7.29
23	—"—	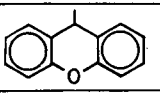	$C_{22}H_{24}ClNO_3$	HCl 132—134	68.47 68.13	6.27 6.48
24	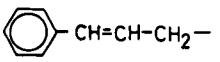		$C_{22}H_{26}ClNO_3$	HCl 177—179	68.12 67.94	6.75 6.59
25	$NC-(CH_2)_2-$	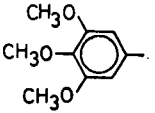	$C_{18}H_{26}ClN_2O_5$	HCl 159—160	56.20 56.40	6.35 6.46
26	—"—	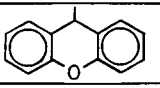	$C_{22}H_{23}ClN_2O_3$	HCl 154—155	66.24 65.93	5.61 5.85
27	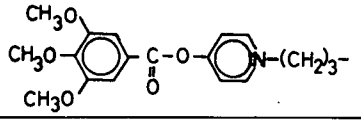	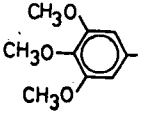	$C_{35}H_{48}Cl_2N_2O_{10}$	2 HCl 208—209	56.33 56.70	6.88 7.17
28	—"—	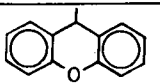	$C_{41}H_{44}Cl_2N_2O_6$	2 HCl 148—149	67.30 67.18	6.06 6.36

Table IV

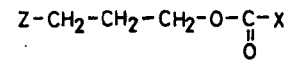

No.	Z	X	Formula	M.p. (°C)	Analysis Calc./Found		
					C	H	N
29	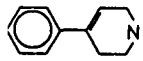	$-CH_3$	$C_{16}H_{22}ClNO_2$	HCl 159—161	66.48 65.84	7.32 7.42	4.85 5.00
30	—"—	$-C(CH_3)_3$	$C_{19}H_{28}ClNO_2$	HCl 173—174	67.54 67.81	8.53 8.47	4.15 4.25
31	—"—		$C_{21}H_{24}ClNO_2$	HCl 175—176	70.48 70.41	6.76 6.94	3.91 3.70
32	—"—	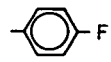	$C_{21}H_{23}ClFNO_2$	HCl 187—188	67.10 66.88	6.44 6.14	3.73 3.95
33	—"—	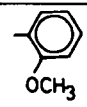	$C_{22}H_{26}ClNO_3$	HCl 163—164	68.12 68.18	6.76 6.90	3.61 3.70
34	—"—	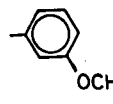	$C_{22}H_{26}ClNO_3$	HCl 181—182	68.12 67.93	6.76 6.98	3.61 3.55
35	—"—	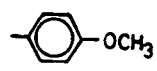	$C_{22}H_{26}ClNO_3$	HCl 174—175	68.12 67.85	6.76 6.68	3.61 3.47
36	—"—	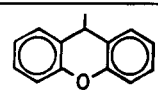	$C_{28}H_{28}ClNO_3$	HCl 171—172	72.33 72.38	5.85 6.14	3.30 3.15

37	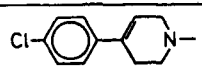	$-CH_3$	$C_{16}H_{21}Cl_2NO_2$	HCl 172—173	58.19 58.00	6.41 6.20	4.24 4.40
38	—"—		$C_{21}H_{23}Cl_2NO_2$	HCl 174—175	64.29 64.24	5.91 5.73	3.57 4.03
39	—"—		$C_{21}H_{22}Cl_2FNO_2$	HCl 179—182	61.47 61.23	5.40 5.26	3.41 3.65
40	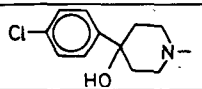		$C_{21}H_{25}Cl_2NO_3$	HCl 161—162	61.47 61.05	6.14 5.85	3.41 4.03
41	—"—		$C_{21}H_{24}Cl_2FNO_3$	HCl 177—178	58.88 58.64	5.65 5.69	3.27 3.68
42	—"—		$C_{21}H_{24}Cl_2FNO_3$	HCl 179—180	58.88 58.69	5.65 5.62	3.27 4.06
43	—"—	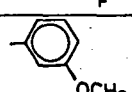	$C_{22}H_{27}Cl_2NO_4$	HCl 160—161	60.00 59.92	6.18 6.41	3.18 3.42
44	—"—	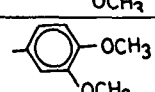	$C_{23}H_{29}Cl_2NO_5$	HCl 181—182	58.72 58.66	6.21 6.43	2.98 3.05
45	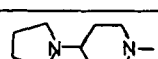		$C_{19}H_{30}Cl_2N_2O_2$	2 HCl 263—265	58.61 58.60	7.77 7.80	7.19 7.18
46	—"—	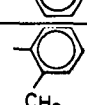	$C_{20}H_{32}Cl_2N_2O_2$	2 HCl 258—260	59.55 59.25	8.00 8.23	6.95 6.80
47	—"—	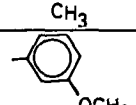	$C_{20}H_{32}Cl_2N_2O_3$	2 HCl 250—254	57.28 57.08	7.69 7.81	6.68 6.88

Table IV (cnntinned)

No.	Z	X	Formula	M.p. (°C)	Analysis Calc./Found C	H	N
48	—"—	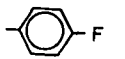	$C_{19}H_{20}Cl_2FN_2O_2$	2 HCl 262—265	56.05 55.85	7.09 7.25	6.88 7.12
49	—"—	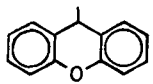	$C_{26}H_{34}Cl_2N_2O_3$	2 HCl 242—245	63.28 62.95	6.95 7.27	5.67 5.31
50	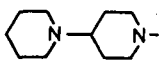		$C_{20}H_{32}Cl_2N_2O_2$	2 HCl 260—262	59.65 59.45	8.05 8.14	6.94 6.81
51	—"—	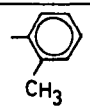	$C_{21}H_{34}Cl_2N_2O_2$	2 HCl 258—262	60.43 60.18	8.21 8.31	6.70 6.74
52	—"—	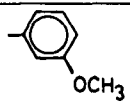	$C_{21}H_{34}Cl_2N_2O_3$	2 HCl 261—264	58.40 58.20	7.15 7.35	6.47 6.45
53	—"—	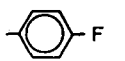	$C_{20}H_{31}Cl_2FN_2O_2$	2 HCl 273—276	57.01 56.85	7.40 7.31	6.65 6.78
54	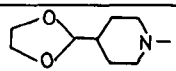	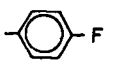	$C_{17}H_{23}ClFNO_4$	HCl 209—211	55.46 55.26	6.44 6.25	— —
55	—"—	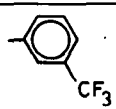	$C_{18}H_{23}ClF_3NO_4$	HCl 177—178	52.76 52.95	5.66 5.86	— —

PREPARATION AND PHARMACOLOGY OF ESTERS OF HYDROXYMETHYLPYRIDINES

By

F. NOTHEISZ, K. FELFÖLDI, M. BARTÓK

Department of Organic Chemistry,
Attila József University, 6720 Szeged, Hungary
and

E. KÁRPÁTI

Pharmacological Laboratory,
Chemical Works of Gedeon Richter Ltd.,
1475 Budapest P.O.B. 27, Hungary

(Received September 30, 1980)

Various esters of hydroxymethylpyridine were synthetized and their pharmacological properties were investigated. Some of the compounds (**1, 8** and **9**) displayed better anti-arrhythmic effects than that of the quinidine used as reference substance.

We earlier described the synthesis and pharmacological properties of numerous (mainly 1,3-) aminoalkyl esters [1—5]. In some cases considerable local anaesthetic [1], coronary vasodilator [4, 5] and bronchial spasmolytic [3] effects were found. In the present work the synthesis of various esters of hydroxymethylpyridines is reported, together with pharmacological data. A number of benzoate esters of hydroxymethylpyridine are known in the literature [6—9]; a few of these possess important pharmacological (particularly cholinergic and hypotensive) effects [10—13]. The new derivatives we prepared have been examined with regard to their action in inhibiting cardiac arrhythmia in anaesthetized cats [14]. This inhibitory effect is expressed in an elevation of the electric fibrillation threshold of the heart. The extent of the effect was calculated as the percentage increase in the fibrillation threshold compared to the level in the untreated control animals, and in Table I the results are compared with those for quinidine,

Table I

Pharmacologycal data of some esters

Compound	Elevation of the fibrillation threshold (%)	
	2 mg/kg	1 mg/kg
1	—	27.6
2	—	13.5
7	14.1	—
8	—	32.1
9	—	34.8
15	14.2	—
Quinidine	34.5	20.6

Table II

Physical constants of pyridinemethanols

Compound	B.p. (°C) Hgmm	M.p. (°C) of hidrochlorid	Analysis Calc./Found C	H	Cl⁻	B.p. Lit. [11]
2-pyridinemethanol	95—100 5	105—106	49.50 49.30	5.54 5.77	24.35 24.52	124—127 23
3-pyridinemethanol	136—138 10	116—118	49.50 49.34	5.54 5.82	24.35 24.70	142—144 14
4-pyridinemethanol	115—120 5	178—180	49.50 49.25	5.54 5.62	24.35 24.60	147—148 15

employed successfully as an anti-arrhythmic in therapy. In some cases (**1**, **8** and **9**) an improved effect is observed. The esters were prepared from the corresponding hydroxymethylpyridine on the basis of previous descriptions [11]. 2-Hydroxymethylpyridine was prepared from 2-picoline [11, 15], and 3- and 4-hydroxymethylpyridines from the ethyl esters of nicotinic and isonicotinic acids by a further modification of a known method [16].

Experimental

The temperature values given in Tables II—V have not been corrected. The purities of the compounds were checked by, among others, thin-layer chromatography. Of the compounds used, nicotinic acid, isonicotinic acid and 2-picoline were Fluka products. The customary method was followed to prepare the ethyl esters.

4-Hydroxymethylpyridine

A solution of 60 g (0.4 mole) of the ethyl ester of isonicotinic acid in 400 ml abs. ether was added dropwise during 1.5 h to a solution of 10 g (0.38 mole) $Li[AlH_4]$ in 600 ml abs. ether; 64 ml water was next added. The reaction mixture was filtered, and the white precipitate was extracted with 2×200 ml ethanol. The organic phases were combined, and after a 12-h standing period the solution was again filtered. The filtrate was evaporated to dryness, and the residue was distilled. Yield 25.6 g (59%).

3-Hydroxymethylpyridine

This was prepared in a similar way as the 4-substituted compound, from the ethyl ester of nicotinic acid. Yield 63%.

Table III

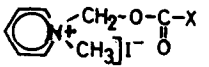

No.	X	M.p. (°C)	Formula	Analysis Calc./Found C	H	N
1		154—155	$C_{14}H_{13}ClINO_2$	43.16 43.14	3.36 3.43	3.60 3.50
2	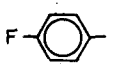	178—180	$C_{14}H_{13}FINO_2$	45.05 44.93	3.52 3.62	3.75 3.85
3	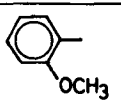	152—153	$C_{15}H_{16}INO_3$	46.77 46.94	4.19 4.22	3.64 3.55
4	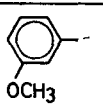	162—163	$C_{15}H_{16}INO_3$	46.77 46.80	4.19 4.21	3.64 3.60
5	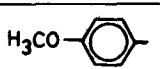	180—181	$C_{15}H_{16}INO_3$	46.77 46.93	4.19 4.10	3.64 3.58
6	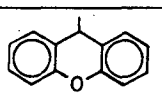	157—159	$C_{21}H_{18}INO_3$	55.04 54.88	3.74 4.10	3.06 3.00

Table IV

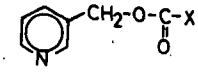

No.	X	M.p. (°C)	Formula	Analysis Calc./Found		
				C	H	N
7	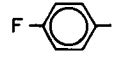	HCl 141—143	$C_{13}H_{11}ClFNO_2$	58.33 57.96	4.12 4.48	5.23 5.10
8	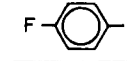	Methoiodide 132—133	$C_{14}H_{13}FINO_2$	45.05 44.75	3.52 3.67	3.75 3.55
9	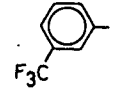	Methoiodide 138—139	$C_{15}H_{13}F_3INO_2$	42.58 42.15	3.10 2.92	3.31 3.45
10	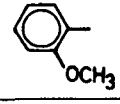	HCl 151—152	$C_{14}H_{14}ClNO_3$	60.20 60.14	5.04 5.09	5.00 5.15
11	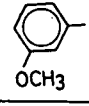	HCl 136—137,5	$C_{14}H_{14}ClNO_3$	60.20 60.39	5.04 5.19	5.00 4.92
12	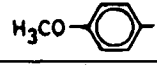	Methoiodide 172—173	$C_{15}H_{16}INO_3$	46.77 46.87	4.19 4.20	3.64 3.75
13	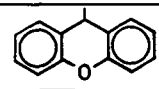	Methoiodide 150—151	$C_{21}H_{18}INO_3$	55.04 54.85	3.74 4.08	3.06 3.00
14	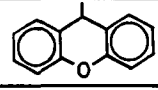	Ethoiodide 141—142	$C_{22}H_{20}INO_3$	55.95 55.63	4.24 4.46	2.98 3.05

Table V

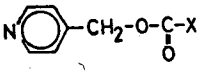

No.	X	M.p. (°C)	Formula	Analysis Calc./Found		
				C	H	N
15	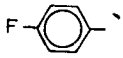	HCl 198—200	$C_{13}H_{11}ClFNO_2$	58.33 58.15	4.12 4.30	5.25 5.05
16	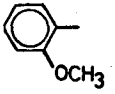	HCl 188—190	$C_{14}H_{14}ClNO_3$	60.20 60.35	5.04 5.08	5.00 4.87
17		HCl 182—183	$C_{14}H_{14}ClNO_3$	60.20 60.42	5.04 4.99	5.00 4.82
18	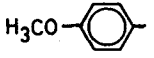	HCl 186—188	$C_{14}H_{14}ClNO_3$	60.20 60.08	5.04 4.85	5.05 5.15
19	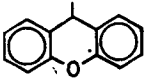	HCl 170—172	$C_{20}H_{16}ClNO_3$	68.09 67.75	4.29 5.05	3.97 4.12
20	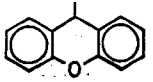	Methoiodide 187.5—189	$C_{21}H_{18}INO_3$	55.04 55.12	3.74 3.44	3.06 3.20

2-Picoline-N-oxide

46.6 g (0.5 mole) 2-picoline was dissolved in 300 ml glacial acetic acid, 50 ml 30% H_2O_2 was added, and the solution was kept for 3 h at 70—80 °C. After the addition of a further 35 ml H_2O_2, the reaction mixture was heated for an additional 9 h. The volume was then evaporated to 100 ml, 100 ml water was added, and the solution was evaporated to dryness. The residue was dissolved in 250 ml chloroform and the solution washed with sodium carbonate solution. After drying, the chloroform was evaporated off, and the residue was distilled. Yield 40 g (74%), with b.p. 130—135 °C at 20 mm Hg (lit. [15]: b.p. 123—125 °C at 15 mm Hg), and n_D^{20}: 1.5895.

Acetate ester of 2-hydroxymethylpyridine

40 g (0.37 mole) 2-picoline-N-oxide was added dropwise to 75 ml gently boiling acetic anhydride, and the reaction mixture was boiled for 20 min and then distilled. Yield 42.7 g (77%), with b.p. 128—130 °C at 30 mm Hg (lit. [15]: b.p. 115—118 °C at 22 mm Hg), and n_D^{20}: 1.4966.

2-Hydroxymethylpyridine

A mixture of 42.7 g (0.28 mole) of the acetate ester of 2-hydroxymethylpyridine and 100 ml 27% sodium hydroxide solution was stirred for 12 h at room temperature, and then extracted with chloroform (pH=7—8). The chloroform solution was dried and evaporated to dryness, and the residue was distilled. Yield 15.2 g (54%).

Acknowledgements

The authors wish to express their thanks to Gizella Bozóki—Bartók for performance of the microanalysis, and to Gizella Koródi for assistance with the syntheses.

References

[1] *Felföldi, K., Á. Molnár, M. Bartók:* Acta Chim. (Budapest) **90**, 75 (1976).
[2] *Felföldi, K., Á. Molnár, M. Bartók:* Acta Chim. (Budapest) **91**, 333 (1976).
[3] *Felföldi, K., M. Laszlavik, M. Bartók, E. Kárpáti:* Acta Phys. et Chem. Szeged **26**, 163 (1980).
[4] *Felföldi, K., M. Laszlavik, M. Bartók, E. Kárpáti:* Acta Phys. et Chem. Szeged **26**, 171 (1980).
[5] *Felföldi, K., Á. Molnár, M. Bartók, R. A. Karakhanov:* Acta Phys. et Chem. Szeged **26**, 177 (1980).
[6] *Zymálkowski, F.:* Arch. Pharm. **287**, 505 (1954).
[7] *Fromherz, K., H. Spielberg:* Helv. Physiol. et Pharmacol. Acta **6**, 42 (1948).
[8] *Ponci, R., A. Baruffini, F. Gialdi:* Farmaco Ed. Sci. **18**, 288 (1963).
[9] *Eistert, B., W. Kurze, G. W. Müller:* Annalen **732**, 1 (1970).
[10] *Jezo, J., F. Selecky, P. Sefcovic:* Pharmazie **13**, 195 (1958).
[11] *Vejdelek, Z. J., V. Trcka:* Chem. listy **52**, 1622 (1958).
[12] *Cousse, H., G. Mouzin:* Chim. Ther. **8**, 297 (1973).

[13] *Rorig, K. J.:* U. S. pat. 3 100 775 (1963); C. A. **60**, 2903g (1964).
[14] *Szekeres, L., J. Papp:* British J. Pharmacol. **17**, 167 (1964).
[15] *Boekelheide, V., W. J. Linn:* J. Am. Chem. Soc. **76**, 1286 (1954).
[16] *Protiva, M.:* Chem. listy **45**, 20 (1951).

СИНТЕЗ И ФАРМАКОЛОГИЧЕСКОЕ ДЕЙСТВИЕ ЭФИРОВ ГИДРОКСИМЕТИЛПИРИДИНОВ

Ф. Нотейс, К. Фелфелди, М. Барток и Э. Карпати

Синтезирован ряд гидроксиметилпиридинов и изучено их фармакологическое действие. Некоторые из изученных соединений (**1, 8, 9**) обладают лучшим антиаритмическим действием, чем хинидин, применявшийся в качестве эталона.

ИЗУЧЕНИЕ КОМПЛЕКСООБРАЗОВАНИЯ 1,3-ОКСАЗАЦИКЛОАЛКАНОВ С МЕТАНОЛОМ МЕТОДОМ ИК-СПЕКТРОСКОПИИ

А. А. ЛАПШОВА, Л. Е. САЛОВА, В. В. ЗОРИН, Т. Ф. АХУНОВ, Р. А. КАРАХАНОВ, С. С. ЗЛОТСКИЙ и Д. Л. РАХМАНКУЛОВ

Уфимский нефтяной институт, Уфа

(Поступило в редакцию 30. сентября 1980 г.)

Определены энтальпии водородных связей и константы равновесия Н-комплексов метанола с 1,3-оксазациклоалканами и изучена связь строения с их основностью.

Кислотно-катализируемые превращения 1,3-дигетероциклоалканов, во многом зависят от их основности [1—3].

Для выяснения механизма этих превращений, а также характера распределения электронной плотности в молекуле 1,3-оксазациклоалкана может оказаться полезным изучение их комплексов с метанолом.

В настоящей работе определены энтальпии водородных связей и константы равновесия Н-комплексов метанола с 1,3-оксазациклоалканами и изучена связь строения с их основностью.

Для определения констант основности и энтальпии образования водородных связей 1,3-оксазациклоалканов (I—XI) в комплексах с метанолом использовался метод ИК-спектроскопии [4—6].

В ИК-спектрах разбавленных растворов метанола в CCl_4 $[CH_3OH]=$ $=0{,}02$ моль/л наблюдается одиночная узкая полоса поглощения с максимумом при 3542 $см^{-1}$, соответствующая валентным колебаниям ОН-групп мономерных молекул метанола (ν_M).

При введении в систему 1,3-оксазациклоалкана в ИК-спектре появляются две новые полосы поглощения, смещенные в сторону низких частот, обусловленных колебаниями ОН-группы молекул метанола в комплесках с 1,3-оксазациклоалканами с водородной связью:

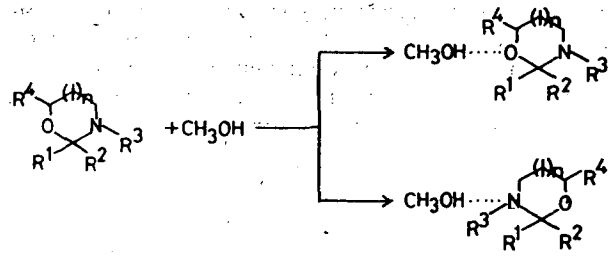

Для вычисления энтальпий водородных связей и констант равновесия K_B мы использовали зависимость между относительным сдвигом частоты $(\nu_M - \nu_K/\nu_M)$ и энтальпий образования водородной связи $-\Delta H = 18{,}5$ $(\nu_M - \nu_K/\nu_M)$ [5], а также связь сдвига полосы $(\nu_M - \nu_K)$ с величиной $\lg K_B$ [7], где ν_K-частота максимума полосы поглощения ОН-группы метанола, входящего в состав комплекса с Н-связью.

Полученные результаты (табл. 1) свидетельствуют о том, что 1,3-оксазациклоалканы образуют Н-комплексы, причем водородная связь в них осуществляется как с неподеленными парами электронов атома азота так и атома кислорода. Сопоставление величин ΔH_O и ΔH_N показывает, что энтальпия водородной связи в комплексе с атомом азота выше, чем с атомом кислорода.

Однако, константа равновесия K_B в случае Н-комплексов кислорода выше, чем у азота, что может быть связано с заметным проявлением энтропийного фактора. Последнее, очевидно, связано с тем, что атом азота более экранирован, чем атом кислорода и вследствие возникающих стерических препятствий концентрация Н-комплексов с атомом азота ниже.

Замена алкильного (I, II, IX) заместителя при атоме азота на фенильный (X) несколько понижает энтальпию водородной связи и константы основности K_O и K_N в Н-комплексах кислорода и азота, что, очевидно, вызвано понижением электронной плотности на атомах кислорода и азота в результате ее смещения к фенильному заместителю.

Введение алкильного заместителя во второе положение незначительно изменяет энтальпию водородной связи и константы основности K_O и K_N Н-комплексов с атомами азота и кислорода.

Введение фенильного заместителя во второе положение гетероцикла (VI) заметно уменьшает константу K_O.

В случае 3-изобутил-2,2-циклопентаметилен-1,3-оксазациклопентана значение H_O и H_N несколько выше, чем в случае производных альдегидов, что, очевидно, связано с повышением основности атома кислорода и азота.

Следует отметить, что в случае *N*-пропилпиперидина (XIV) энтальпия водородной связи несколько выше, чем в случае *N*-пропилморфолина (XII) и *N*-трет. бутил-1,3-оксазациклогексана (XI). По-видимому, при введении атома кислорода в цикл и по мере его приближения к атому азота, основность последнего уменьшается.

В случае соединения XIII, когда два атома азота находятся в положении 1 и 3 энтальпия водородной связи остается примерно на том же уровне, что и в 1,3-оксазациклогексане (XI).

Следует отметить, что энтальпия водородной связи метанола с атомом кислорода в 1,3-диоксациклопентане заметно меньше, чем в 1,3-оксазациклопентанах. Последнее, очевидно, связано с уменьшением электронной плотности на кислороде при замене группы *N*—R на атом кислорода. В 1,4-диоксациклогексане атомы кислорода обладают большей основностью, чем в 1,3-диоксациклопентане и это может быть связано с взаимным уменьшением электронной плотности на атомах кислорода при передвижении их из положений 1 и 4 в положения 1 и 3.

Таблица I

Термодинамические параметры H-комплексов метанола с 1,3-оксазациклоалканами

№	Соединение	$\Delta\nu_0$, $см^{-1}$	$-\Delta H_0$, ккал/моль	$\Delta\nu_N$, $см^{-1}$	$-\Delta H_N$, ккал/моль	K_0, л/моль	K_N, л/моль
I.	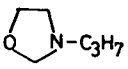	143,5	3,7	321	5,5	1,65	0,66
II.	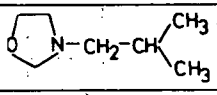	136	3,6	266,5	5,0	1,9	0,61
III.	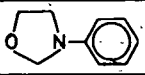	96	3,0	256	4,905	0,96	0,31
IV.	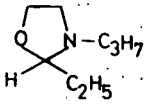	136	3,576	343,5	5,68	1,37	0,335
V.	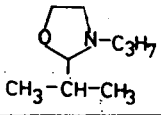	136	3,575	295	5,265	1,48	1,00
VI.	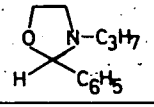	121	3,37	250	5,13	0,97	0,49
VII.	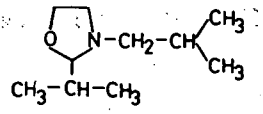	125	3,427	292	5,24	1,65	0,59
VIII.	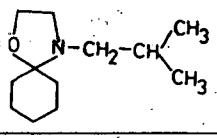	139	3,61	358	5,80	2,015	0,814
IX.	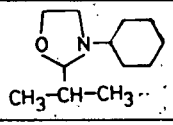	143	3,67	316	5,45	1,70	0,99
X.	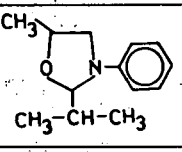	113	3,26	236	4,71	1,53	0,62
XI.	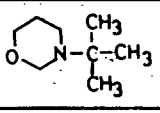	146	3,704	346	5,702	0,17	2,56

Таблица 1 (продолжение)

№	Соединение	$\Delta\nu_0$, $см^{-1}$	$-\Delta H_0$, ккал/моль	$\Delta\nu_N$, $см^{-1}$	$-\Delta H_N$, ккал/моль	K_0, л/моль	K_N, л/моль
XII.	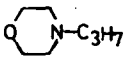	136	3,575	372	5,914	0,42	2,28
XIII.	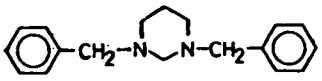	—	—	343,5	5,68	—	4,14
XIV.	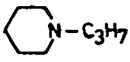	—	—	400	6,13	—	5,28
XV.		122	3,386	—	—	1,58	—
XVI.		90	2,91	—	—	0,72	—

Экспериментальная часть

Исходные 1,3-оксазациклопентаны были получены ацетализацией аминоалканов [8—10] с карбонилсодержащими соединениями по известной методике [11]. Чистоту реагентов контролировали хроматографически и ИК-спектрометрически. Концентрация метанола в CCl_4 была постоянной и составляла 0,02 моль/л, при этом самоассоциация молекул метанола отсутствовала.

Концентрация оснований—0,2 моль/л. Спектры записывались на приборе ИКС—14 с призмой LiF в области 2800—3800 $см^{-1}$ при постоянной толщине слоя 5 мм и температуре 25 °С.

Литература

[1] *Кантор, Е. А.:* Канд. диссерт. БГУ, Уфа, 1974.
[2] *Максимова, Н. Е.:* Канд. диссерт. МИНХ и ГП, Москва, 1974.
[3] *Закощанский, В. М., Г. С. Идлис, С. К. Огородников, В. С. Федоров:* Ж. орг. хим. **9**, 931 (1975).
[4] *Перелыгин, И. С., Т. Ф. Ахунов:* Опт. и спектр. **30**, 679 (1974).
[5] *Перелыгин, И. С., Т. Ф. Ахунов:* Ж. прикл. спектр. **18**, 696 (1973).
[6] *Латыпова, Ф. Н., Т. Ф. Ахунов, С. С. Злотский, Л. Е. Салова, Д. Л. Рахманкулов:* Ж. прикл. хим. **50**, 223 (1977).
[7] *Gordy, W., S. C. Stanford*: J. Chem. Phys. **9**, 215 (1940).
[8] *Notheisz, F., M. Bartók, V. Remport*: Acta Phys. et Chem. Szeged, **18**, 89, 197 (1972).
[9] *Felföldi, K., Á. Molnár, M. Bartók:* Acta Chim. Hung. **90**, 75 (1976).
[10] *Felföldi, K., Á. Molnár, M. Bartók:* Acta Chim. Hung. **91**, 333 (1976).
[11] *Апьок, Й., М. Бартос, Р. А. Караханов, Н. И. Шуйкин:* Изв. АН СССР, сер. хим. **1968**, 2352.

IR SPECTROSCOPIC INVESTIGATION OF COMPLEX FORMATION BETWEEN 1,3-OXAZACYCLOALKANES AND METHANOL

J. A. Lapshova, L. E. Salova, V. V. Zorin, T. F. Akhunov, R. A. Karakhanov, S. S. Zlotskii and D. L. Rakhmankulov

The enthalpy of the hydrogen-bond and the equilibrium constants of the complex-forming reactions between methanol and oxazacycloalkanes have been determined. A correlation has been found between the basicity and the structure.

THE INFLUENCE OF SURFACE MODIFICATION ON THE SEDIMENTATION AND RHEOLOGICAL CHARACTERISTICS OF FERRIC OXIDE SUSPENSIONS IN NON-AQUEOUS MEDIA

By

A. A. ABD-EL-HAKIM, J. BALÁZS and F. SZÁNTÓ

Department of Colloid Chemistry, Attila József University
Szeged, Hungary

(Received October 20, 1980)

Ferric oxide of the highest analytical purity was used to prepare products organophilized to various extents with an aqueous solution of ammonium stearate or a benzene solution of stearic acid. The selection of the degree of sorptive surface modification (organophilization) was made on the basis of the results of preliminary sedimentation and sorption studies. The surface properties of the products were investigated by immersion microcalorimetry. From this, conclusions were drawn as to the nature of the sorption, the specific surface area of the pigment, and the extent of coverage of the surface. The sediment volumes of the organophilized products were determined in organic media of different polarities. Detailed studies were made of the rheological properties of concentrated (coherent) suspensions in a paraffin oil medium of the products organophilized to various degrees. The parameters calculated from the correlation between the Bingham flow limit and the concentration of the suspension proved characteristic of the structures of the suspensions. Correlations were established between the results of adsorption, sedimentation and rheological examinations.

Introduction

Suspensions in organic media are finding ever wider application in modern technology. A knowledge of their properties is not only of interest from a theoretical aspect; it is also of fundamental importance during the preparation and use of, among others, varnish paints, oil-based boring muds, lubricating greases and metal-casting nucleus coating materials (black washes). The need often arises for the preparation of organosuspensions possessing suitable sedimentation constants and rheological properties (viscosity, flow limit, plasticity, tixotropy). For this task to be fully achieved, it is absolutely necessary to know the basic laws that govern the sedimentation and structure-forming properties of suspensions.

In suspensions in non-aqueous media the aggregation is generally more extensive than in suspensions in aqueous media. The explanation of this is that in the large majority of cases particles with polar surfaces are suspended in a less polar, or even an apolar medium, and consequently it is not possible for a lyosphere of appropriate thickness and structure to develop, this lyosphere leading to a substantial decrease in the interactions (adhesion forces) between the particles [1, 2].

The condition for the formation of incoherent suspensions, that there is practically no interaction at all between the particles of the disperse part, is only rarely

valid in the case of organosuspensions. Even at a relatively low suspension density, the flow gives rise to a considerable hydrodynamic interaction (which is not constant in space and time) between the particles. Generally accepted laws are available in connection with the stability and rheological properties of such incoherent or semicoherent systems [3—5]. The same can by no means be said in connection with the structure-forming, sedimentation and rheological properties of coherent (structured) suspensions. At the same time, the majority of real suspensions belong in this group, for the forces between the particles (termed adhesion forces below, in accordance with BUZÁGH [1]) cause aggregation leading to the development of a looser or more compact structure at the suspension densities employed in practice.

Fundamental investigations on the structure-forming characteristics of organosuspensions have been reported by VOET [5], MCDOWELL and USHER [6], ROSCOE [7], PARFITT [8] and REHBINDER [9, 10].

The stability of the structure developing in a structured system is governed by the number and strength of the binding points between the particles. The number of binding points is determined by the spatial filling of the disperse part, and by the dimensions and shape of the particles. The strengths of the linkages and the rate of their reformation after their shearing are determined primarily by the particle — particle and the particle — medium interactions, *i.e.* by the adhesion and the lyophility. If the lyophility of the particles of the disperse part towards the dispersion medium is increased, a decrease results in the magnitude of the adhesion forces between them, and hence in the structure-forming tendency of the system.

The lyophility and accordingly the properties of the structure developing in suspension can be regulated in the case of a given disperse part by the use of homogeneous organic media ensuring different degrees of wetting, and in the case of a given disperse part and a given dispersion medium by the modification of the interfacial layer between the medium and the particles with additives, generally tensides [2, 11, 12].

The influencing of the sedimentation and rheological properties of suspensions with tensides may be achieved in various ways:

(a) the lyosphere developing on the surface of the particles may be altered with tensides dissolved in the dispersion medium; or

(b) the particles of a hydrophilic disperse part, for example, may be organophilized by the adsorption or chemisorption of tensides prior to the formation of the suspension.

The literature [2, 8, 11—18] contains a reasonable number of research results involving studies on the effects of the tensides dissolved in the dispersion medium or the tensides used for organophilization on the stability and rheological properties of suspensions. However, it is much rarer [18, 19] to find publications in which investigations are made of the correlations between the interaction between the disperse part and the tenside (sorption), and the sedimentation and rheological properties of the suspensions.

We have therefore studied what changes occur in the sedimentation and rheological properties of ferric oxide suspensions in a paraffin oil medium (otherwise prepared in a fixed manner and with a fixed concentration) if:

(a) the stearic acid used to modify the interface is dissolved in the dispersion medium;

(b) the stearic acid is sorbed onto the surface of the ferric oxide from a benzene medium prior to preparation of the suspension;

(c) the ferric oxide in a water-*i*-propanol mixture is preliminarily reacted with the modifying stearate ion in the form of ammonium stearate.

A choice may be made from among these possibilities in, among others, the varnish paint industry, if the tensides are employed as dispersing, wetting or stabilizing agents.

Experimental

Materials. The ferric oxide used was Reanal Fe_2O_3 of the highest analytical purity, with a content of other oxides of less than 0.3%. The specific surface area of the ferric oxide was determined with the BET method in a nitrogen atmosphere and was found to be 7.0 m^2/g; this value did not change essentially as a result of the organophilization (surface modification). The dispersion medium was paraffin oil of pharmacopoeial quality. Fluka stearic acid of the highest analytical purity, and ammonium stearate prepared from stearic acid and ammonia gas, were used as wetting agents and for organophilization.

Methods. The surface of the ferric oxide was modified to various extents in a 10% suspension in benzene, by treatment with a 0.1% solution of stearic acid in benzene. In order to avoid the disturbing effect of water bound on the surface [20], before the suspension was prepared the ferric oxide was dried to constant weight at 105 °C in a vacuum drying-oven. The benzene was made anhydrous with metallic sodium. In the organophilization with ammonium stearate, a 10% aqueous suspension was prepared from the ferric oxide; an equivalent amount of ammonium stearate, in the form of a 0.1% aqueous solution also containing 33% *i*-propanol, was added to the suspension at 60 °C during vigorous stirring. After the adsorption equilibrium had been established (a period of 48 h proved sufficient for this in both cases), the ferric oxide was separated by centrifugation from the equilibrium solution, and then washed several times with the solvent. The washings were combined with the equilibrium solution. The organophilized samples were dried to constant weight at 60 °C in a vacuum drying-oven, powdered, and passed through a DIN—30 sieve.

The rheological investigations were carried out with a Haake rotary viscosimeter, with the use of a two-slit, thermostatable measuring vessel. The shear gradient was varied in the interval 1.62—262 sec^{-1}, in 10 stages. For the rheological measurements the suspensions were prepared in an Erweka rotatable homogenizer fitted with a closed agate vessel, in which the mild shear and homogenization are ensured by a fairly large agate ball. The suspension concentration was in all cases 35.9 g/100 g.

Results and discussion

The effects of the quantity of stearic acid or ammonium stearate on the sedimentation properties of ferric oxide suspensions in a benzene medium are shown in Fig. 1.

In pure benzene the ferric oxide gives a loose sediment with a large volume; the sedimentation occurs in an aggregated manner, with a sharp interface. As a

consequence of the adhesion decrease resulting both from the stearic acid and from the ammonium stearate, the sediment volume grows progressively smaller and the sedimentation becomes diffuse in character. It is also striking that the effect of the stearic acid is practically independent of the mode of its application. From the aspect of the sediment volume-diminishing effect, it is irrelevant whether the stearic acid is sorbed onto the surface of the ferric oxide particles and the suspension is then made in benzene, or whether the same quantity of stearic acid is dissolved in the dispersion medium (benzene) and hydrophilic ferric oxide is suspended in it. However, if the stearate ion reacts in the dissociated form in aqueous medium with the surface of the ferric oxide particles, and after drying the organophilized ferric oxide is suspended in an organic medium, then it is able to exert a larger adhesion-decreasing effect, and accordingly the sediment volume too naturally decreases to a greater extent.

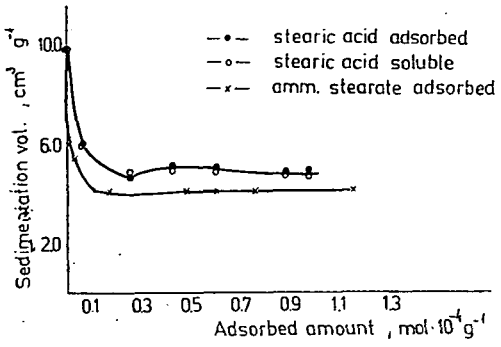

Fig. 1. The effects of the quantity of stearic acid or ammonium stearate on the sedimentation properties of ferric oxide suspensions in a benzene

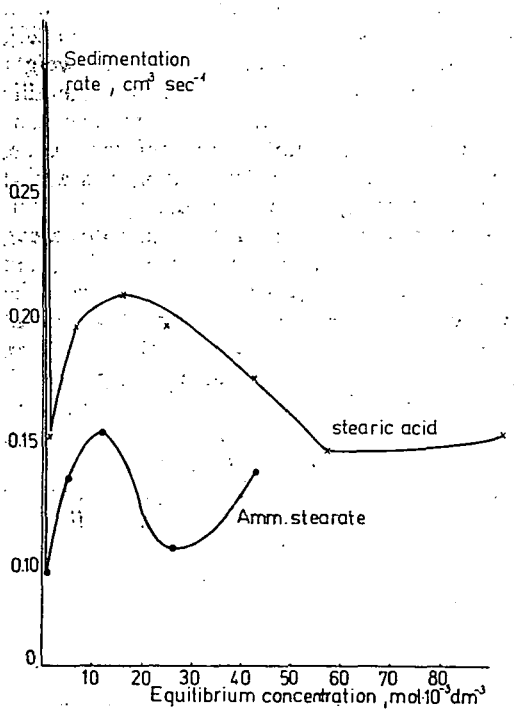

Fig. 2. The sedimentation rates of benzene suspensions of ferric oxide as functions of equilibrium concentration of stearic acid or ammonium stearate

These findings are supported by the results of sedimentation rate studies, which are illustrated in Fig. 2.

Fig. 2 shows the sedimentation rates of benzene suspensions of ferric oxide samples previously organophilized with stearic acid or ammonium stearate, as functions of the equilibrium concentration of stearic acid or ammonium stearate. In agreement with the data of earlier authors [2, 22—24], the sedimentation rate varies according to a complex (minimum-maximum) function with the quantity of the tenside. This complex correlation can be explained in that the sedimentation rate is influenced not only by the adhesion decrease resulting from the action of the adsorbed stearic acid or stearate ion, but at the same time by the disaggregation which takes place in parallel to this and by the increase in the

number of particles per unit volume too. Even so, however, it is quite clear that the ferric oxide samples organophilized with ammonium stearate in aqueous medium give suspensions that are more stable and sediment out at a substantially lower rate than the samples surface-treated with stearic acid.

The essential difference between the stearate adsorptions from the organic and the aqueous media is shown by the adsorption-desorption isotherms presented in Fig. 3.

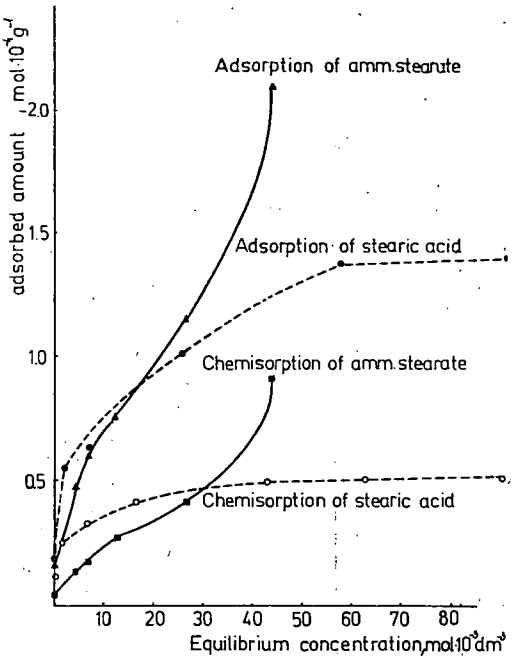

Fig. 3. The adsorption-desorption isotherm of stearic acid and ammonium stearate

On the basis of Fig. 3, it may be stated that in the first short section of the isotherms the equilibrium concentration is zero, and accordingly irreversible sorption may be assumed. During the further sorption of stearic acid the active sites on the surface of the ferric oxide particles rapidly become saturated and the adsorbed quantity increases. In this stage a considerable proportion of the amount of stearic acid adsorbed may be removed from the surface by extraction with the solvent. Subsequently, the concentration of the equilibrium solution gradually rises while the adsorbed quantity remains practically unchanged. The surface coverage calculated from the BET surface area of the adsorbent, the maximum amount chemisorbed and the surface area requirement of the stearic acid molecule (0.205 nm^2), does not attain 100%.

In the course of the sorption of ammonium stearate the situation is different. In this case, a measurable equilibrium concentration is already observed at comparatively low adsorbed amounts. On proceeding towards higher equilibrium concentrations, however, here too there are gradual increases in the quantities of both the reversibly and the irreversibly bound stearate ion. At the same time, our calculations indicate that the maximum quantity of chemisorbed stearate ensures total monomolecular coverage of the surface.

We also used immersion microcalorimetry to investigate the surface characteristics of the organophilized ferric oxide samples. These results will be reported in our following publication.

The effect of organophilization is manifested most markedly in the rheological properties of the concentrated suspensions. The degree of organophilization of the ferric oxide used for the rheological examinations was determined from the characteristic points of the adsorption-desorption isotherms.

Figure 4 depicts the branches of the equilibrium flow curves of paraffin oil

suspensions of ferric oxide organophilized to various extents with stearic acid, these results being obtained at increasing shear gradient values.

Fig. 4 shows that the Bingham flow limit found by extrapolation of the final linear section of the flow curve increases slightly on the action of a small amount of stearic acid, which is in good agreement with the variation of the sedimentation rate values in Fig. 2. As the quantity of stearic acid chemisorbed increases, the flow limit progressively decreases to a limiting value. The plastic viscosity values arising from the slopes of the linear sections do not vary substantially with the amount of stearic acid chemisorbed. Paraffin oil suspensions of the hydrophilic ferric oxide and of the ferric oxide organophilized to various extents are otherwise plastic systems, and display practically no thixotropy.

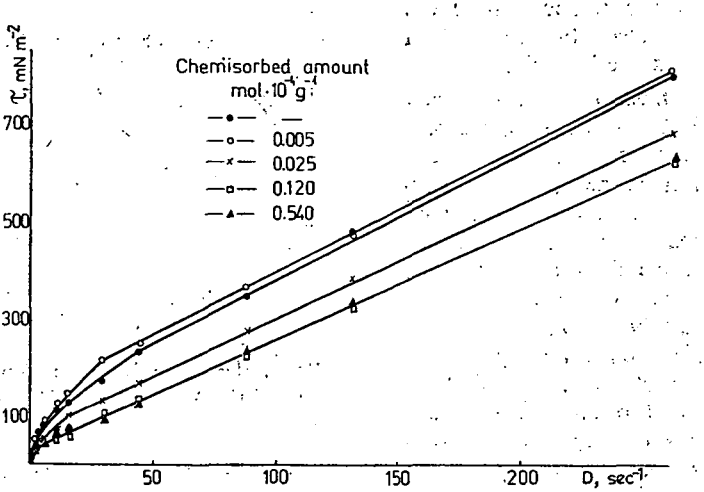

Fig. 4. Rheological curves of Fe_2O_3 organophilized with different quantities of stearic acid in paraffin oil

Essentially totally identical flow curves were obtained when the stearic acid was dissolved in paraffin oil and hydrophilic ferric oxide was always used in the suspension preparation.

If the preliminary organophilization of the ferric oxide was carried out with ammonium stearate in aqueous medium, under the same conditions the flow curves span a substantially larger shear stress interval (Fig. 5).

The suspension prepared with the hydrophilic ferric oxide is a form-retaining system possessing a relatively high Bingham flow limit (200 mNm^{-2}). In the case of a given suspension concentration, an increase in the amount of ammonium stearate causes the suspension to become progressively dilutely fluid, and its flow limit falls practically to zero. The adhesion decrease resulting from the organophilization, and the disaggregation occurring in parallel, are well observable in the colour of the suspensions too; this gradually changes from a dull light-red to a shiny dark-red.

If the ammonium stearate is dissolved in increasing amount in paraffin oil and the hydrophilic ferric oxide is suspended in it, the effect of the ammonium stearate is by no means so considerable. This is to be seen in Fig. 6, where it may readily be

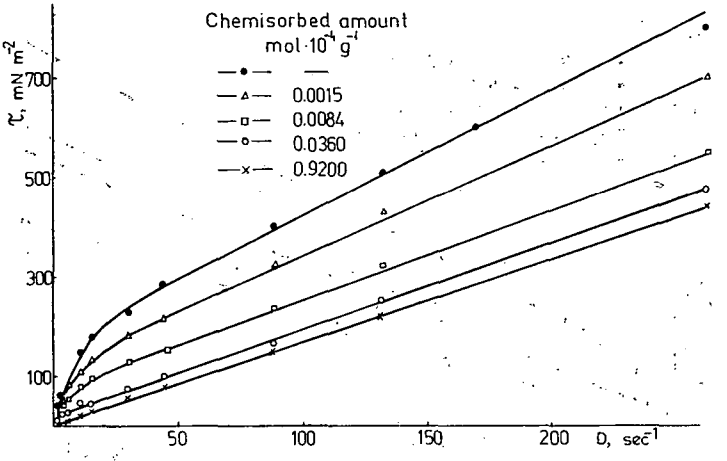

Fig. 5. Rheological curves of Fe_2O_3 organophilized with different quantities of ammonium stearate in paraffin oil

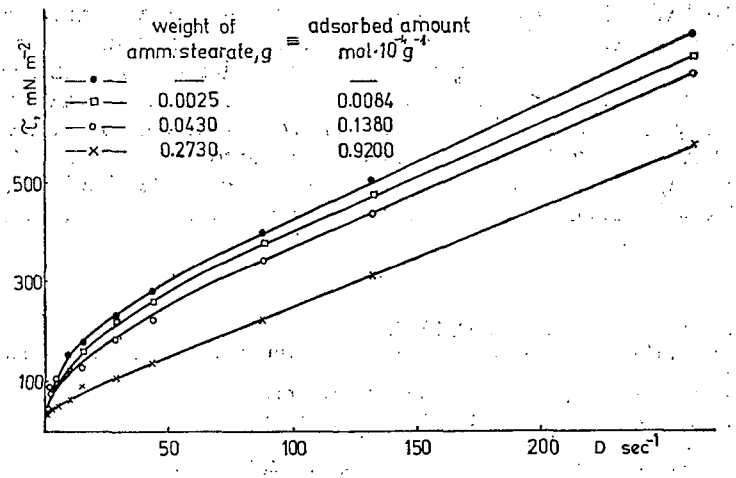

Fig. 6. Rheological curves of Fe_2O_3 in paraffin oil in presence of different amounts of ammonium stearate

observed that the flow limit has a value of only about 55 mNm^{-2}, even for the highest quantity of ammonium stearate.

Fig. 7 shows together the equilibrium flow curves of paraffin oil suspensions of the starting hydrophilic ferric oxide, and ferric oxides modified with the same quantity of dissolved or preliminarily adsorbed stearic acid or ammonium stearate.

From Fig. 7 too it may be stated quite clearly that the most extensive flow limit and plastic viscosity-decreasing effects can be obtained with the chemisorbed ammonium stearate.

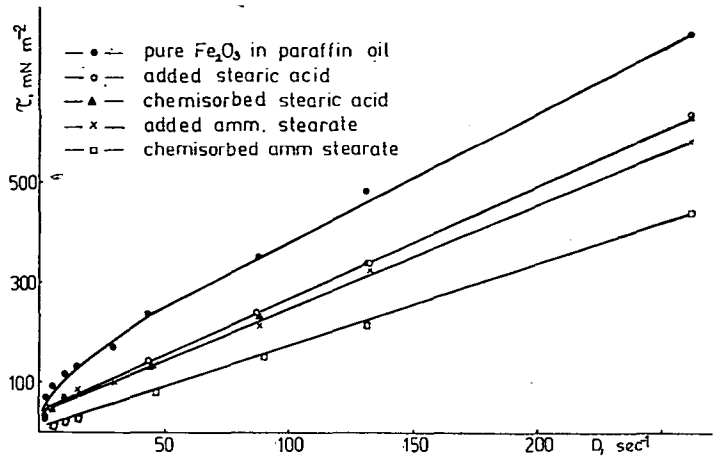

Fig. 7. Rheological curves showing the adsorbed and the added amounts of stearic acid and ammonium stearate

On the basis of the experimental results reported here, it may be said that concrete conclusions concerning the optimum conditions of organophilization of a pigment to be ground into a given dispersion medium may be drawn from the results of adsorption, sedimentation and rheological examinations that are relatively simple to carry out. Our experimental results may serve as additional data in support of the fact that not only the correct choice of the nature and quantity of the pigment and the tenside, but also the conditions of the pigment — tenside interaction exert a substantial influence on the practically important characteristics of varnish paints.

References

[1] *Buzágh, A.:* Kolloidchem. Beih. **32**, 114 (1930).
[2] *Szántó, F., B. Várkonyi, J. Balázs:* Nemvizes közegű szuszpenziók. A kémia újabb eredményei 5. Akadémiai Kiadó, Budapest, 1971.
[3] *Einstein, A.:* Ann. Physik. **19**, 289 (1906); **34**, 591 (1911).
[4] *Vand, V.:* J. Phys. Coll. Chem. **52**, 277, 300, 314 (1948).
[5] *Voet, A.:* J. Phys. Coll. Chem. **51**, 1037 (1947).
[6] *McDowell, C. M., F. L. Usher:* Proc. Roy. Soc. A. **131**, 564 (1931).
[7] *Roscoe, R.:* Flow properties of disperse systems. Chap. 1 Ed. Hermans, I. I., North Holland Publ. Company. Amsterdam (1953).
[8] *Parfitt, G. D.:* Dispersion of Powders in Liquids. Elsevier, Amsterdam (1969).
[9] *Rehbinder, P. A.:* Disc. Faraday Soc. **18**, 151 (1954).
[10] *Rehbinder, P. A.:* Rheol. Acta **1**, 361 (1961).
[11] *Szántó F., J. Balázs, M. Sümegi:* Magyar Kémikusok Lapja **9**, 458 (1970).
[12] *Szántó, F., J. Balázs, M. Sümegi:* Magyar Kémiai Folyóirat **76**, 531 (1970); **76**, 655 (1970); **76**, 659 (1970); **78**, 118 (1972).
[13] *Grinberg, M.:* Farbe und Lack **71**, 205 (1965).
[14] *Horkay, F., F. Szántó:* Plaste und Kautschuk **11**, 691 (1964).
[15] *Konsztantyinova, V. V., G. V. Belugina, Sz. H. Zakijeva, P. A. Rehbinder:* Kolloidn. Zh. **25**, 555 (1963).
[16] *Belugina, G. V., V. V. Konsztantyinova, Sz. H. Zakieva, P. A. Rehbinder:* Kolloidn. Zh. **32**, 177 (1970).

[17] *Erman, V. U., Sz. W. Tolsztaja, A. B. Taubman:* Lakokrasz. Mat. **2**, 25 (1969).
[18] *Balázs, J., F. Szántó, M. Sümegi, I. V. Tóth:* Kolorisztikai Értesítő **117**, 1973/3—4.
[19] *Ermilov, P. I.:* Diszpergirovannija pigmentov. "Himija" Moszkva, 1971.
[20] *Husbands, D. I., W. Tallis, I. C. Waldsax, C. R. Woodings, M. I. Jaycock:* Powder Technology **5**, 31, 1971/72.
[21] Colorimetric Methods of Analysis V II A, 702.
[22] *Wolf, K. L.:* Physik und Chemie der Grenzflächen. Bd. II. Ed. Berlin—Göttingen—Heidelberg. 1959.
[23] *Szántó F., S. Veres:* Acta Phys. et Chem. (Szeged) **8**, 151 (1962); **9**, 157 (1963).
[24] *Horkay, F., F. Szántó:* Plaste u. Kautschuk **11**, 691 (1964).

ВЛИЯНИЕ ПОВЕРХНОСТНОЙ МОДИФИКАЦИИ ОКСИДА ЖЕЛЕЗА НА СЕДИМЕНТАЦИОННЫЕ И РЕОЛОГИЕСКИЕ ХАРАКТЕРИСТИКИ ЕГО СУСПЕНЗИЙ В НЕВОДНЫХ СРЕДАХ

А. А. Абу-Эл-Хаким, Я. Балаж и Ф. Санто

Оксид железа высокой степени чистоты использовался для получения органофилизованных до разной степени продуктов. Органофилизацию проводили стеаратом аммония из водной и стеариновой кислотой из бензольной среды. Поверхнохтные свойства продуктов были изучены с помощью иммерсионной микрокалориметрии. Проведено подробное исследование реологических свойств концентрированных суспензий, органофилизованных до разных степеней образцов, в среде парафинового масла. Найдено хорошее соответствие между результатами адсорбционных, седиментационных и реологических испытаний.

О ПРОДУКТАХ ВЗАИМОДЕЙСТВИЯ ХЛОРИДА ЛАНТАНА И КАПРИНАТА КАЛИЯ

Л. Д. СКРЫЛЕВ, В. Ф. САЗОНОВА, И. И. СЕЙФУЛИНА

Кафедра физической химии университета им. И. И. Мечникова, Одесса

И. А. АНДОР

Кафедра общей и физической химии университета им. Аттилы Йожефа, Сегед

(Поступило в редакцию 10 июня 1980 г.)

Получены способом двойного обмена лантановые соли каприновой кислоты при разных pH среды и выделены методом флотации. Установлен состав полученных продуктов методами криоскопии, термогравиметрии, инфракрасной спектроскопии и рентгенографии.

Свойства труднорастворимых производных редкоземельных элементов (РЗЭ), образующихся при введении в раствор солей РЗЭ мыл щелочных металлов, изучены мало. Вместе с тем, знание этих свойств необходимо в целом ряде случаев седиментационного [1], экстракционного [2] и флотационного [3] выделения РЗЭ.

Ниже изложены результаты физико-химического иследования продуктов взаимодействия $0{,}4\times10^{-4}$ mol·dm^{-3} водных растворов хлорида лантана ($LaCl_3$) и 0,07 mol·dm^{-3} водных растворов каприната калия ($KO_2C(CH_2)_8CH_3$).

Объекты и методы исследования

Для приготовления водного расствора хлорида лантана использовали соль $CaCl_3\cdot6\,H_2O$ марки «х.ч.». Водный раствор каприната калия получали путем нейтрализации (при нагревании) дважды перекристализованной из спиртового раствора каприновой кислоты, водным раствором гидроксида калия [4]. Концентрация каприната калия в растворе была ниже его критической концентрации мицеллообразования [5]. После получения раствор, для предотвращения гидролиза, подщелачивали до pH 11,6.

Капринат калия к растворам хлорида лантана добавляли в количестве, стехиометрически необходимом для образования средней соли состава $La[O_2C(CH_2)_8CH_3]_3$. Взаимодействие хлорида лантана с капронатом калия протекало быстро и сопровождалось образованием высокодисперсного осадка, который отделяли от раствора флотацией [3] в стеклянной колонке диаметром 40 и высотой 200 mm. Дном колонки служил фильтр Шотта № 4, через который подавали воздух со скоростью $1{,}3\times10^{-6}$ m$^3\cdot$s^{-1}. Продукт после флотации сушили на воздухе при 293 K до постоянной массы.

Требуемые значения pH растворов устанавливали после прибавления к ним раствора каприната калия с помощью 0,1 $mol \cdot dm^{-3}$ растворов HCl и KOH. Контроль за значением pH растворов осуществляли посредством pH-метра типа pH—340 со стеклянным электродом.

Молекулярную массу вещества, образующего осадок, определяли криоскопически [6], используя в качестве растворителя бензол.

Рентгенограммы осадков снимали на дифрактометре ДРОН—05. Съемку производили в медном излучении с никелевым фильтром в пределах брегговских углов от 1 до 20°. Рентгенограммы идентифицировали по рентгеновской картотеке ASTM.

ИК спектры таблетированных с KBr осадков получали на приборах Perkin Elmer и Unicam SP—1000. Интерпритацию спектров проводили в соответствии с известными корреляциями [7—9] и на основании сравнения ИК спектров осадков, каприната лантана (полученного по методике [10] и условно названного «эталоном») и каприновой кислоты. Последнее было обусловлено тем, что в растворе, содержащем капринат лантана (соль слабой кислоты и слабого основания) может иметь место гидролиз, приводящий, в зависимости от pH раствора, к загрязнению осадка свободной каприновой кислотой или гидроксидом лантана.

Термический анализ осадков проводили на дериватографе *MOM* G—425 в платиновом тигле в интервале температур 293—1073 *K*. Скорость нагрева при этом составляла 0,17 $K \cdot s^{-1}$. Навески образцов были в пределах 45—65 mg.

Эксперементальные результаты и их обсуждение

Проведенные криоскопические измерения показали, что из растворов с значением pH 4 флотируются осадки, которым с достаточным приближением соответствует средняя соль состава $La[O_2C(CH_2)_8CH_3]_3$ а из растворов с pH 8 и 10 — осадки, отвечающие составу основной соли $La(OH)[O_2C(CH_2)_8CH_3]_2$.

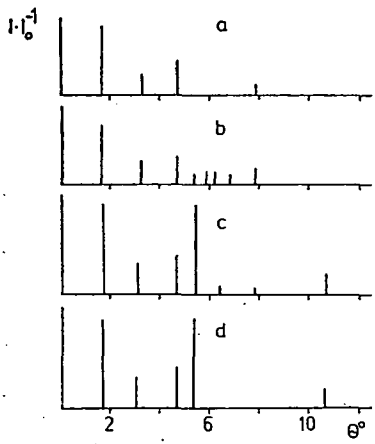

Рис. 1. Штрихрентгенограммы «эталона» — *a* и лантановых мыл, выделенных флотацией из растворов с значением pH 4 — *b*, 8 — *c* и 10 — *d*

Все выделенные флотацией осадки имеют кристаллическое строение и характеризуются наличием индивидуального набора межплоскостных расстояний *(рис. 1.)*. К сожалению, отсутствие в справочной литературе рентгенографических характеристик среднего и основного капринатов лантана не позволяло нам однозначно идентифицировать строение осадков. Вместе с тем, очевидно, что отсутствие на рентгенограммах осадков, выделенных из растворов с значением pH 4, линий, характерных для каприновой кислоты (масимумы в области 2,96; 3,66; 2,07; 5,07°), а на рентгенограммах осадков, выделенных из растворов с значением pH 8 и 10, линий, характерных для гидроксида

лантана (максимумы в области 1,94; 9,91; 10,5°) косвенно подтверждает сделанный выше на основании криоскопических измерений вывод о том, что в первом случае состав осадков отвечает формуле $La[O_2C(CH_2)_8CH_3]_3$, а во втором — $La(OH)[O_2C(CH_2)_8CH_3]_2$.

На основании ИК спектров можно придти к выводу, что состав осадка, выделенного из раствора с pH 4, идентичен составу «эталона», о чем свидетельствует полное сходство их ИК спектров *(рис. 2.* и *3*, кривая *3*, *4*.). Возможное

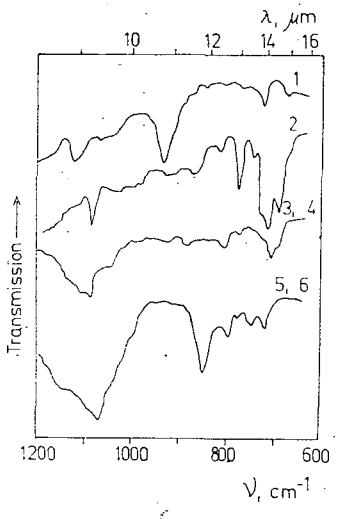

Рис. 2. ИК спектры каприновой кислоты — *1*, каприната калия — *2*, «эталона» — *3* и лантановых мыл, выделенных флотацией из растворов с значением pH 4 — *4*, 8 — *5* и 10 — *6* в интервале длин волн 1200—600 cm^{-1}

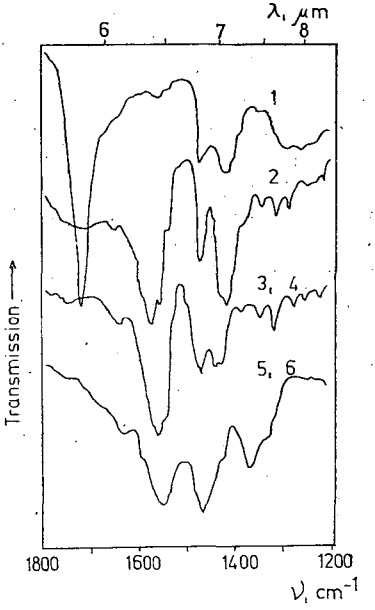

Рис. 3. ИК спектры каприновой кислоты — *1*, каприната калия — *2*, «эталона» — *3* и лантановых мыл, выделенных флотацией из растворов с значением pH 4 — *4*, 8 — *5* и 10 — *6* в интервале длин волн 1800—1200 cm^{-1}

включение каприновой кислоты в кристаллическую структуру осадка и эталона в более значительном количестве исключается, т. к. в их ИК спектрах отсутствует полоса, характерная для валентных колебаний карбонильной группы ($\nu C{=}O$ 1710 cm^{-1}, *рис. 3*, кривая *1*). Наличие же примеси свободной каприновой кислоты в осадках и «эталоне» исключается как по отсутствию выше описанной полосы, так и широкой характерной полосы при *940* cm^{-1}, соответствующей внеплоскостным деформационным колебаниям OH-группы (γOH) в димерном кольце карбоксилов кислот [7] (соотв. *рис. 2*, кривые *3—6* и кривая *1*).

Образование связи металл-кислород в солях карбоновых кислот приводит к образованию карбоксилатной группы COO^- с симметрией C_{2v} и появлению полос поглощения, соответствующих симметричным ($\nu_s CO_2^-$) и асимметрич-

ным ($\nu_{as}CO_2^-$) валентным колебаниям группы [8]. В осадках, полученных нами, максимум полосы соответствующей $\nu_{as}CO_2^-$ находится при приблизительно 1550 cm^{-1} *(рис. 3, кривые 3—6)*. К сожалению, интерпретация ИК спектров в области симметричных валентных колебаний группы CO_2^- затрудняется из-за наложения полос; характерных для деформационных колебаний метильных и метиленовых групп (1470, 1450, и 1445 cm^{-1}). Тем не менее полоса (или плечо), находящаяся при 1415 cm^{-1} *(рис. 3, кривые 3—6)* с наибольшей вероятностью [11] может быть отнесена к симметричным валентным колебаниям группы CO_2^-. Сравнения ИК спектров осадков со спектром исходного каприната калия *(рис. 2 и 3, кривая 2)* показывают, что в области появления полос $\nu_{as}CO_2^-$ в спектрах осадков наблюдается смещение максимума на -20 cm^{-1}. В области «прогрессии полос» [12] более четкое проявление эквидистантных гибридных полос, соответствующих деформационным и скелетным колебаниям алифатических цепей связанных с полярными группами, в капринате калия и в осадке, полученном при pH 4 (соотв. *рис. 3, кривые 2 и 3*), чем в осадках, полученных при pH 8 и 10 *(рис. 3, кривые 5 и 6)*, может указывать на большую поляризованность концевой карбоксилатной группы у первых.

ИК спектры осадков, «эталона» и каприната калия в области 1200—600 cm^{-1} в основном аналогичны. Однако, в спектрах осадков, выделенных из растворов с pH 8 и 10, появляется новая полоса при 850 cm^{-1}, которая может быть отнесена к колебаниям Me—OH [8, 9]. Наряду с этим, отсутствие узкой интенсивной полосы в области приблизительно 3600 cm^{-1} исключает наличие примеси гидроксида лантана в образцах.

Все осадки представляют кристаллогидраты, о чем свидетельствует наличие в их ИК спектрах широких полос поглощения в области 3430 cm^{-1} и 1630 cm^{-1} (соответсвенно, валентные и деформационные колебания OH-группы).

Таким образом, в соответствии с проведенным отнесением характеристических полос основных функциональных группировок осадков, можно утверждать, что взаимодействие хлоида лантана с капринатом калия, в принятых нами условиях, в растворе с pH 4 приводит к образованию средних мыл, не седержащих каприновой кислоты, а в растворах с pH 8 и 10 — основных мыл, без примеси гидроксида лантана.

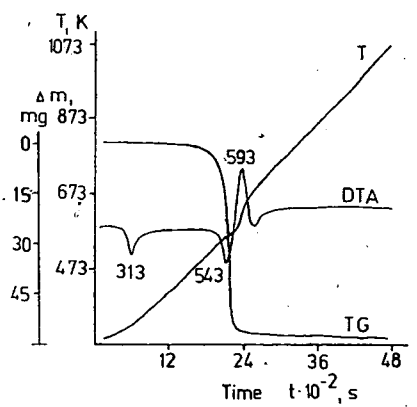

Рис. 4. Термогравиграмма каприновой кислоты

Исследование термической устойчивости осадков в присутствии воздуха подтвердило вывод об идентичности образцов мыл, выделенных из растворов с pH 8 и 10 (термогравиграммы осадков в основном одинаковы), и отличие их от образцов мыл, выделенных из растворов с pH 4.

Отсутствие примеси кислоты в осадке, выделенном из растворов с pH 4, подтверждается при сравнении термогравиграммы каприновой кислоты *(рис. 4)* и каприната лантана *(рис. 5)*: на кривой *DTA* лантанового мыла не наблюдается эффекта плавления кислоты *(рис. 4*, эндотерми-

ческий максимум при 313 K). Наличие кристализационной воды во всех рассматриваемых образцах подтверждается присутсвием на кривых *DTA* пиков дегидратации с экстремальными точками при 363 K (осадок из раствора с pH 4, *рис. 5*) и 393 K (осадки из раствора с pH 8 и 10, *рис. 6*). Количество кристализационной воды в осадках было определено на основании кривых TG, которое соответствовало в мольных соотношениях 1,5 H_2O в осадке выделенном при pH 4, 2 и 4 H_2O в осадках выделенных соответственно при pH 8 и 10.

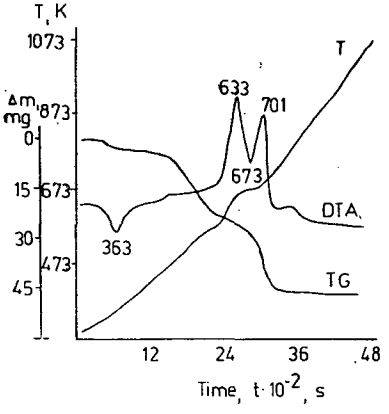

Рис. 5. Термогравиграмма лантанового мыла, выделенного из раствора с значением pH 4

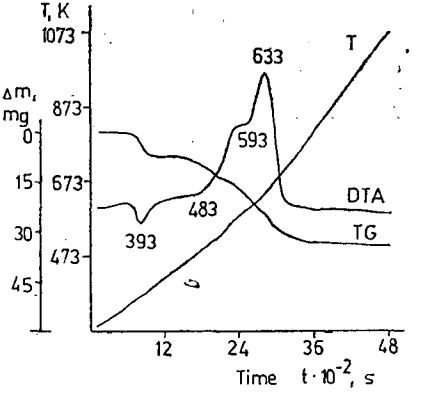

Рис. 6. Термогравиграмма лантанового мыла, выделенного из раствора с значением pH 10

Разложение осадков при повышенных температурах приводило к образованию одного и того же конечного продукта — оксида лантана.

Суммируя все выше изложенное, можно придти к заключению, что результаты криоскопических измерений, рентгенографического, ИК спектроскопического и термического исследований осадков, выделенных из растворов с различными значениями pH, согласуются между собой и находятся в хорошем соответствии с данными кондуктрометрического изучения взаимодействия хлорида лантана с капринатом калия, полученными нами ранее [13].

Литература

[1] *Серебренников, В. В.:* Химия редкоземельных элементов, т. 1 Изд. Томского унив., 1956.
[2] *Корпусов, Г. В., Р. Д. Корпусова, Г. Л. Вакс, Е. Н. Патрушева:* Ж. неорг. хим. **14**, 1912 (1969).
[3] *Скрылев, Л. Д., В. Ф. Сазонова, В. В. Менчук:* Изв. вузов. Горный ж. № **4**, 138 (1978).
[4] *Маркина, З. Н., Н. Н. Цикурина, Н. Э. Костова, П. А. Ребиндер:* Коллоиди. ж. **26**, 76 (1964).
[5] *Шинода, К., Т. Накагава, Б. Тамамуси, Т. Исемура:* Коллоидные поверхностно-активные вещества, «Мир», Москва: 1966, стр. 95.
[6] *Воробьев, Н. К.* (ред.): Практикум по физической химии, «Химия» Москва, 1975.
[7] *Беллами, Л.:* Инфракрасные спектры молекул, Изд. ИЛ, Москва, 1957.
[8] *Nakamoto, K.:* Infrared Spectra of Inorganic and Coordination Compounds, J. Wiley and Sons, New York. 1963. p. 197.

[9] *Nyquist, R. A., R. O. Kagel:* Infrared Spectra of Inorganic Compounds, Acad. Press, New York, London 1971.
[10] *Misra, S. N., T. N. Misra, K. P. Mehrotra:* Inorg. Nucl. Chem. **25**, 195 (1963).
[11] *Салимов, М. А., В. А. Пчелин, А. В. Керимбеков:* Ж. физ. хим. **37**, 2285 (1963).
[12] *Jones, R. N., A. F. McKay, R. G. Sinclair:* J. Amer. Chem. Soc. **74**, 2575 (1952).
[13] *Скрылев, Л. Д., В. Ф. Сазонова, М. Э. Корнелли, Н. А. Шумилина:* Изв. вузов. Химия и хим. технология, **21**, 491 (1978).

INVESTIGATION OF THE PRODUCTS OF THE REACTION BETWEEN La(III)CHLORIDE AND POTASSIUM CAPRATE

L. D. Skrylev, V. F. Sazonova, I. I. Seifulina and I. A. Andor

Lanthanum salts of capric acid were produced in solution at different pH values with the acid of a double exchange reaction and the products were separated by a flotation method. The compositions of the products were determined by cryoscopy, thermogravimetry, *IR* spectroscopy and *X*-ray diffraction methods.

LABORATORY NOTES
LIGHT THERMOSTAT FOR THE CULTIVATION OF HALOBACTERIUM HALOBIUM

By

M. ZÖLLEI, J. HEVESI and T. SZITÓ

Department of Biophysics, Attila József University, Szeged

(Received October 3, 1980)

A simple light thermostat was built for the cultivation of Halobacterium halobium. The advantage of this apparatus as compared to the climate chambers and phytotrons, which are generally applied for cultivation, is that it is easy to handle and the production cost is very low.

The apparatus

The frame of the thermostat is made of angle-bar and fixed on a wooden base (Fig. 1). The back and side walls are covered with textile-bakelite plates. The light-tubes are fitted to the internal walls, and the choke-coils to the external walls; thus, the choke-coils do not heat the interior compartment. The light thermostat is situated in a laboratory with a volume of approximately 50 m^3. A sketch of the apparatus is shown Fig. 2.

20 W, 220 V 35 light tubes are used for illumination and heating of the cultivation-space. The illumination can be employed in six grades of intensity. Two switches are connected in parallel to two groups of light tubes on the right hand wall, two switches to two groups of six light tubes on the left-hand wall, and one switch each to groups of six and seven light tubes on the rear wall. Accordingly the intensity of illumination, in the middle of the space where the cultivation tube is located, can be varied between 500 and 3500 lux. The front of the thermostat can be closed to different degrees by means of bakelite sheets, depending on the required temperature of the inner space. The top of the thermostat is open in order to let the superfluous heat out of the cultivation space and it can readily be conducted away from the laboratory. The laboratory is thermostated with a Lehel AK 2F climatizer.

The top of the compartment is bridged; from the center of the bridge an iron rod projects downwards and supports the cylindrical culture tube.

Results of cultivation

The culture medium was prepared in a standard manner [1]. A period of 1.5 h is necessary to warm the culture compartment to 38 °C. The climatizer thermostating the laboratory at 23—24 °C is switched on only after the culture compartment

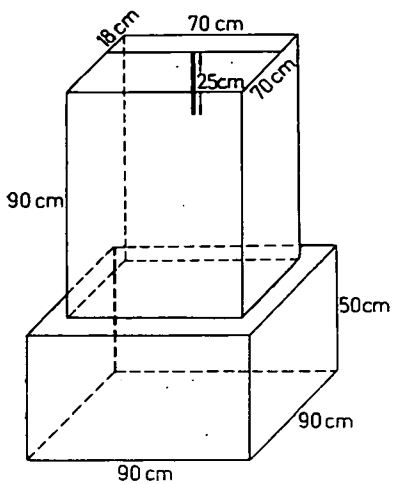

Fig. 1. Scale drawing of thermostat

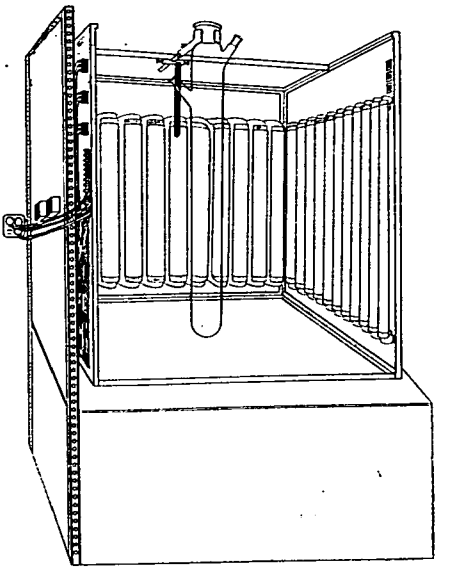

Fig. 2. Sketch of thermostat

and the laboratory can be maintaned at almost constant value. The culture is supplied with oxigen by two Cyklon air-pumps connected parallelly. The velocity and quantity of air passing through are regulated by a toroid-transformer operating the air pump. Our experimental results show that a flow rate of 25 $cm^3\ l^{-1}\ min^{-1}$ is optimum during the first 2.5—3 days of cultivation. After this period the flow rate is halved. 24 h after the beginning on the cultivation the cells are counted and the scattering spectrum of the culture is recorded. These operations are repeated at 14—16 h

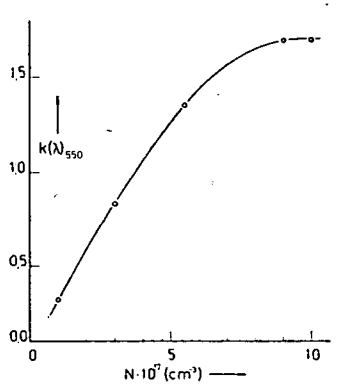

Fig. 3. Variations of intensities of light scattered by cell suspension and of absorbed light with the increase of the number of cells

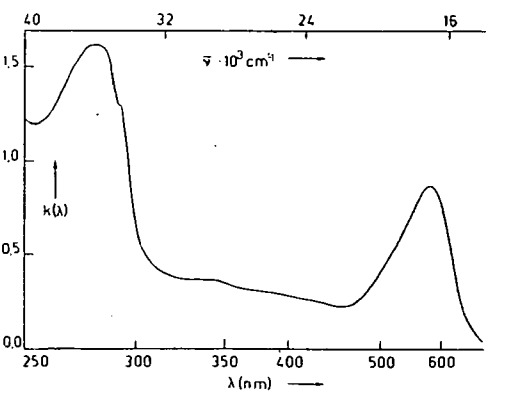

Fig. 4. Absorption spectrum of purple membrane

intervals. A calibration curve was prepared from the cell-counting data and the scattering spectra (Fig. 3). This can be used together with spectroscopic measurements to follow the development of the culture continously. At 38 °C with an air flow rate of 25 $cm^3\ l^{-1}\ min^{-1}$ and an illumination of 3500 lux, the cultivation lasts for about 60—70 h. Our results to date show that on average the quantity of cells obtained from each culture is 8 $gr\ l^{-1}$. The customary methods were used to obtain the purple membrane and to prepare the bacteriorhodopsin [1]. The absorption spectrum of the purple membrane was taken with a Specord UV-VIS Spectrophotometer (Fig. 4), and aggrees well with the spectra reported in the literature [2].

Acknowledgement

The authors wish to express their thanks to Dr. I. Horváth (Department of Zoology) for help in cell counting.

Literature

[1] *Oesterhelt, D., W. Stoeckenius:* Methods in Enzymology **31**, 667 (1974).
[2] *Becker, B. M., J. Y. Cassim:* Preparative Biochemistry, **5**, 161 (1975).

СВЕТОВОЙ ТЕРМОСТАТ ДЛЯ КУЛЬТИВИРОВАНИЯ БАКТЕРИЙ ТИПА HALOBAKTERIUM HALOBIUM

М. Зёллеи, Я. Хевеши и Т. Ф. Сито

Для культивирования бактерий типа Halobakterium halobium был создан простой световой термостат. По сравнению с обычно применяемой климатической камерой, т. е. фитотроном, преимущества установки состоят в простом управлении и малой стоимости.

BOOK REVIEWS

Liquid and Amorphous Metals

Editors: E. Lüscher and H. Coufal, NATO Advanced Study Institutes Series; Series E: Applied Sciences, Volume 36, Sijthoff & Noordhoff, Alphen aan den Rijn, The Netherlands and Germantown, Maryland, USA, 1980.

The Advanced Study Institute on Liquid and Amorphous Metals was held in Zwiesel, W. Germany, September 11—22, 1979. It was an Institute focusing attention to up-to-date theoretical and experimental results on the properties of disordered metallic systems.

The Introduction begins with a review by G. Fritsch and E. Lüscher. They clearly show how theory and experiment can be related at the various stages between microscopic point of view and macroscopic properties of liquid metals and alloys. In the next lecture a thorough survey of the atomic theory of liquid dynamics is given by A. Sjölander, who concludes that in order to have a consistent theory for liquids one would demand that both the statics and the dynamics should come out from the theory and only the interaction potential being the input.

Part 2 contains lectures on the theory of the disordered state, namely on the resistivity, structure and dynamics and collective excitations of liquid metals and alloys, as well as structural models, stability, dynamical properties, electronic structure and superconductivity of amorphous and glassy systems. As a succesful model for metallic and dielectric glasses a two level systems is discussed by H. Beck.

In Part 3 experimental results are presented. Neutron scattering experiments are reported on the way to reach sufficent accuracy to allow more than qualitative conclusions on interesting details of liquid dynamics. Nevertheless, most of the lectures in this part of the volume were devoted to the field of metallic glasses. Preparation, unique properties, applications and experimental results on the physical properties such as electron transport, mechanical, magnetic, optical and low temperature properties are reviewed. Ionic structure, glass formation, electron and Mössbauer spectroscopy and positron annihilation measurements are discussed, as well.

Completing the volume Part 4 contains contributed papers.

The book is of great value and highly recommended both to experts in material sciences and those who intend to get a comprehensive information on or to enter this important field.

I. Gyémánt

(Department of Theoretical Physics,
Attila József University, Szeged)

Topics in Current Chemistry Vol. 87: Micelles Springer-Verlag, Berlin—Heidelberg—New York, 1980

There is already a huge literature on association (micelle) colloids, primarily due to the extremely wide field of application, but also because of the numerous interesting theoretical questions connected with this. A series of excellent and very detailed handbooks deal with this topic, but in spite of this there has previously been a need for a book concisely reviewing the recent theoretical and experimental results relating to micelle formation. This volume fills this deficiency.

It is a particular merit of the book that systems involving organic (or more exactly apolar) media are not forgotten. Accordingly, the volume consists basically of two parts: "Micelles. Amphiphile Aggregation in Aqueous Solution" by B. Lindman and H. Wennerström (Divisions of Physical Chemistry 1 and 2, Chemical Center, University of Lund), and "Surfactants in Nonpolar Solvents. Aggregation and Micellization" by H.-F. Eicke (Institute for Physical Chemistry, University of Basel).

The first part of the book is divided into 7 chapters, covering 85 pages and with 317 literature references. Following the short introduction (Chapter 1), in Chapter 2 the authors discuss the experimental results relating to aqueous solutions of amphiphilic molecules, especially in the light of the

experimental facts concerning the CMC. In the opinion of the reviewer, this is an excellent, up-to-date survey of the effects of factors influencing the CMC and of the physico-chemical properties of the association systems, and will also be of outstanding value from an educational aspect. This chapter contains the phase diagrams of concentrated solutions of surface-active substances and of three-component systems, recent results relating to solubilization, and much new knowledge connected with nonionic tensides and short-chain compounds. Special mention should be made of the possibilities and results of application of the NMR technique.

In Chapter 3 the authors discuss the theories relating to micelle formation. The reviewer found the application of the theory of hydrophobic interactions to micelle formation, and considerations on the effects of temperature, to be of particular interest.

In Chapter 4 we find the most recent results concerning the size-distribution, structure and form of micelles, with special regard to the roles of the counterions; here too the material is based primarily on the results obtained by NMR.

Chapter 5 is devoted to dynamic questions, and chiefly the kinetics of micelle formation and solubilization, micellar catalysis, and the translational thermal motion of micelles.

Finally, in accordance with the importance of the question, Chapter 6 presents a detailed treatment of the topics of the electric interactions and ion distribution of ionic micellar systems in the light of the latest results, the salt effect, the dependence of the size and form of the micelles on the electrostatic effects, and a brief account of the interactions between micelles.

Chapter 7 contains the above-mentioned, fresh and well-selected literature references.

The second part of the book provides an excellent study of a field on which a review of this nature had not previously been published. This part too is divided into 7 chapters. In the introduction in the first chapter the author states that, of the association systems involving nonaqueous media, only those in expressedly apolar (nonpolar), *i.e.* hydrocarbon media will be dealt with, for only in this case do micelles develop (invert micelles, with orientations opposite to those of aqueous media systems). A good survey is given of the problems of interpretation and definition of the CMC in this case, which differs so much from the "classical" one.

After the CMC questions, here too the possibilities of theoretical treatment are to be found in Chapter 2, together with a deep and interesting analysis of the molecular interactions that may be involved. Special emphasis is laid on the role of the extremely small amount of water in the association; this was mainly demonstrated by the investigations of the author and his coworkers, in particular by means of NMR studies.

In Chapter 3 we find a very detailed analysis, based on the most recent experimental facts, of the effects of the molecular structure, the solvent and the temperature on the size and form of the micelles. Chapter 4 again gives results on the kinetics of the micellization process, while Chapter 5 presents a concise survey of the examination methods that may be employed in nonpolar media, including the most modern methods (not only NMR, but also the positron annihilation method, for instance). The brief Chapter 6 deals with solubilization and the formation of microemulsions, while Chapter 7 comprises an excellent literature collection, with 228 references.

This book will be of great interest and value not only to the specialists dealing with this topic and its applications, but to research workers and teachers in the entire field of surface chemistry and colloid chemistry.

F. Szántó

(Department of Colloid Chemistry
Attila József University, Szeged)

Radioactivity and Its Measurement Second Edition (SI Units) W. B. Mann, R. L. Ayres and S. B. Garfinkel Pergamon Press 1980, 282 pages

The book is a really refreshing lecture on radioactivity and its measurement because the concepts are introduced chronologically in a ready readable fashion even for those who have not received a special training in these disciplines. The first five chapters deal with the early history of radioactivity, the decay laws, the interactions of α, β and γ rays with matter which became the basis of detection, assay and identification of these radiations. These last points gain increasingly on importance because of the easy availability of different isotopic nuclides which led to a tremendous increase in the application of these isotopes in the different industries, sciences and medicine. Even though for clinical diagnosis the stable isotopic nuclides (like ^{13}C, ^{18}O, ^{34}S etc.) are nowadays preferred, the active varieties find extensive use as radiopharmaceuticals. Especially from this last point of

view is it of notable importance that the authors were associated with the preparation of NCRP Report №. 58, dealing with radioactivity measurement procedures, and as a consequence a good deal of reference has been given to it. As far as the closing three chapters are concerned they give the fundamentals of radiation detection and the principles of electronic equipment developed for processing and assaying radioactivity. These chapters contain more details about instrumentation, solid state detectors and the statistic rules of counting than NCRP Report 58 itself.

The book does not make use of complex mathematics, therefore, can be read easily even by beginners. Consequently, it is a good "first book" on radioactivity for those who want to apply radioactivity for one of the purposes mentioned and for students to find data and details not heard of in the lectures.

P. Fejes

(Department of Applied Chemistry,
Attila József University, Szeged)

Fundamenta Scientiae edited by B. Jurdant and M. Paty

The first issue of Fundamenta Scientiae was recently published by Pergamon Press. This brand new journal is intended to answer some of the most intriguing questions of our age.

The principal aim of this publication is stated by its editors to be "... not to lay down the rules of a hybrid discipline consisting of bits of philosophy of science, history of science, sociology, logic, etc., but rather to question established ways of thinking, to reexamine fundamental issues, to offset conventional imagery, to challenge the expert...".

The journal sets itself the ambitious task of determining the relationship between the sciences, placing them in their overall context. Another goal to be achieved is a constant redefinition of the ever-changing relationship between science and philosophy.

In the first issue of this bilingual journal, questions of common concern are discussed: Science as a Western phenomenon, by R. Rashed; Prédication et Grammaire Universelle, by R. Thom; Quality, form and globality: an assessment of catastrophe theory, by G. Marmo and B. Vitale; Science and development in Latin America — opposing forces, by J. Leite Lopes; Structure et fonction vues par un physiologiste, by C. H. Marx; The three little dinosaurs or a sociologist's nightmare, by B. Latour; An analysis of three historical theories in the natural sciences, by L. Reijnders; Probability and causality: a critique of "a probabilistic theory of causality" by Patrick Suppes, by D. J. Amit; and Histoire d'une redécouverte et de ses prolongements, by J. Riess.

It is hoped that Fundamenta Scientiae will be of great interest to the readership of Acta Physica et Chemica.

L. Seres

(Institute of General and Physical Chemistry,
Attila József University, Szeged)

A kiadásért felelős: Dr. Tandori Károly
1980
A kézirat nyomdába érkezett 1980. december 5. Megjelenés: 1981. június
Példányszám: 550. Ábrák száma: 51. Terjedelem: 10 (A/5) ív
Készült monószedéssel, íves magasnyomással, az MNOSZ 5601—50/A szabványok szerint
80-5248 — Szegedi Nyomda — F. v.: Dobó József igazgató

Information for Contributors

1. Manuscripts should be submitted to Prof. Pál Fejes, Institute of Applied Chemistry, József Attila University, Szeged, Rerrich tér 1, Hungary, H-6720.
2. The manuscripts must not exceed in any case 32 pages (Figures, legends, Tables and Summary included). Manuscripts should be submitted in duplicate.
3. The format of the text: A/4, double spaced, 25 lines per page and 50 characters per line. Title: all capital characters; underlined twice. Subtitle(s) should be written in new line(s) in normal writing, underlined also twice, first characters: capital. (See the following example).

STEREOCHEMICAL STUDIES

Studies on Cyclic-2-Hydroxycarboxylic Acids

By

PÁL KISS

Research Institute for Industrial Chemistry, Budapest
(Received.....)

4. After these comes the summary, which is followed by the text proper. If the parts of the paper are separated by secondary titles like: Introduction, Experimental etc., the following rule holds: secondary titles of equal rank are to be written in new lines, the first word with capital letter, otherwise running text underlined once.
   Example:
   Introduction
   Experimental part
5. The names of the authors in the running text are written in capital letters. Exceptions are the names in connection with scientific instruments, etc. where only the first letter should be capital.
6. Citations in the text with reference to the selected literature at the end of the paper are to be made with squared brackets, like: [5], [4, 9], [4—9].
7. To make printing easier, mathematical formulas are to be simplified as much as possible. Reference to mathematical equations is made by numbers in parenthesis, like: (16).
8. Tables should be typed on separate pages. Please supply numbers and titles for all tables (Numbering occurs with Roman numerals: Table I).
   Throughout the whole text the IUPAC nomenclature should be used.
   Insert of Tables in the text will be indicated at the appropriate place of the margin, like this: Table I.
9. Figures must be drawn clearly with Chinese ink on oily drawing paper, the thickness of lines as well as size of letters and symbols should be selected with care, the minimum size is nearly 0.3 cm. The maximum width of Figures is 24 cm, however, Figures of width equal or less than 12 cm are preferred.
   Please, use upwright writing on the Figures.
   In the case of real numbers points are used instead of commas.
   The place of Figures in the text is indicated on the margin like this: Figure 13.
   Please supply legends for all figures and compile these on separate sheets. Indicate only the number of the Figures in the original drawing, for this purpose use blue pencil.
10. Literature will be given under the heading References, like this: (on a separate sheet at the end of the manuscript)
    [1] Allinger, N. L., M. T. Tribble: J. Phys. Chem. 33, 1565 (1976).
    [2] Abraham, J. K., H. S. Hoover: Principles of Competitive Oxidation. McGraw-Hill, New York 1977, p. 133.

INDEX

I. Vass, N. Marek and J. Hevesi: A Polarization Spectrofluorimeter with On-Line Data Processing 111
B. Rácz, Zs. Bor, G. Szabó and S. Szatmári: Generation of Subnanosecond Pulses in Nitrogen Laser-Pumped Tunable Dye Lasers 117
B. Rácz and G. Szabó: Improved Model of Nitrogen Laser Pumped Dye Lasers 127
J. Hebling, Zs. Bor, B. Rácz, B. Német and I. Sánta: Generation of Nearly Transform-Limited Subnanosecond Light Pulses by Long Cavity Dye Laser 137
S. K. Saxena, C. L. Gupta, M. N. Sharma and M. C. Saxena: Dielectric Absorption Studies in Chloro and Nitro Substituted Anilines in Benzene 141
J. Császár and L. Kiss: Investigation of Nucleotide-Metal Ion Systems, III. Study of the ATP—Ni(II) Systems 151
D. Gloyna and K.-G. Berndt: Bathochromic Bandshift and High Reversibility in the cis-trans Isomerization of β-aryl-substituted Diphenylphosphinyl and Diphenylthiophosphinyl-trans-Ethylenes. (In German) 155
K. Felföldi, M. Laszlavik, M. Bartók and E. Kárpáti: Chemistry of 1,3-Bifunctional Compounds, XXIII. Aminoalkyl Esters of Xanthene-9-Carboxylic Acid, II. Cholinolytic and Bronchodilator Activity of Quaternary Salts of New Diaminoalkyl-Xanthene-9 Carboxylates 163
K. Felföldi, M. Laszlavik, M. Bartók and E. Kárpáti: Chemistry of 1,3-Bifunctional Compounds, XXIV. Preparation and Pharmacology of Cycloalkylaminopropyl Trimethoxybenzoates 171
K. Felföldi, Á. Molnár, M. Bartók and R. A. Karakhanov: Chemistry of 1,3-Bifunctional Compounds, XXV. Synthesis of Some Esters Containing Substituted Piperidine and Tetrahydropyridine Skeletons 177
F. Notheisz, K. Felföldi, M. Bartók and E. Kárpáti: Preparation and Pharmacology of Esters of Hydroxymethylpyridines 185
J. A. Lapshova, L. E. Salova, V. V. Zorin, T. F. Akhunov, R. A. Karakhanov, S. S. Zlotskii and D. L. Rakhmankulov: IR Spectroscopic Investigation of Complex Formation between 1,3-Oxazacycloalkanes and Methanol (In Russian) 193
A. A. Abd-El-Hakim, J. Balázs and F. Szántó: The Influence of Surface Modification on the Sedimentation and Rheological Characteristics of Ferric Oxide Suspensions in Non-Aqueous Media 197
L. D. Skrylev, V. F. Sazonova, I. I. Seifulina and I. A. Andor: Investigation of the Products of the Reaction between La(III) Chloride and Potassium Caprate. (In Russian) 207
M. Zöllei, J. Hevesi and T. Szitó: Light Thermostat for the Cultivation of Halobacterium Halobium 213
I. Gyémánt: Book Review 217
F. Szántó: Book Review 217
P. Fejes: Book Review 218
L. Seres: Book Review 219